



Cite this: *Chem. Commun.*, 2019, 55, 5139

Received 2nd February 2019,
Accepted 11th March 2019

DOI: 10.1039/c9cc00977a

rsc.li/chemcomm

5'-Morpholino modification of the sense strand of an siRNA makes it a more effective passenger†

Pawan Kumar,^{ib}^a Rubina G. Parmar,^a Christopher R. Brown,^a Jennifer L. S. Willoughby,^a Donald J. Foster,^a I. Ramesh Babu,^a Sally Schofield,^a Vasant Jadhav,^a Klaus Charisse,^a Jayaprakash K. Nair,^a Kallanthottathil G. Rajeev,^a Martin A. Maier,^a Martin Egli^{ib}^b and Muthiah Manoharan^{ib}^{*a}

The 5'-monophosphate group plays an important role in strand selection during gene silencing mediated by small-interfering RNA. We show that blocking of 5' phosphorylation of the sense strand by introducing a 5'-morpholino modification improves antisense strand selection and RNAi activity. The 5'-morpholino modification of the antisense strand triggers complete loss of activity.

Small-interfering RNAs (siRNAs) harness the natural RNA interference (RNAi) pathway to silence genes of interest and have shown tremendous potential as therapeutic agents.^{1–7} The approval of patisiran (ONPATRO[®]) in the USA and in Europe for treatment of polyneuropathy of hereditary transthyretin-mediated amyloidosis marked the translation of siRNAs into a validated class of medicines.⁸ Exogenous siRNAs are typically chemically modified, 21–23-nucleotide long, double-stranded RNAs.⁹ Once inside target cells, the RNA duplex engages with the RNA-induced silencing complex (RISC), which separates the antisense (guide) strand from the sense (passenger) strand and retains the antisense strand.¹⁰ RISC loaded with antisense strand (also called active RISC) then binds and cleaves target mRNA, thereby silencing expression of the gene.^{1–3}

Strand selection is a critical step in RNAi-mediated gene silencing, as loading of the incorrect sense strand into the RISC can lead to off-target effects through silencing of irrelevant genes.^{11,12} The strand with its 5' terminus at the thermodynamically less stable end of the duplex is selected by RISC as the antisense strand.¹³ With careful design, preferential loading of the intended antisense strand can be achieved in most cases. However, loading of the sense strand into RISC cannot be excluded, especially when the thermodynamic asymmetry between the two ends of siRNAs is not significant. It is known that the presence of the monophosphate group at the 5' end helps anchor the antisense strand in RISC, and that there is an

interaction between the 5' monophosphate of the antisense strand and MID domain of Argonaute 2 – the protein component of RISC responsible for target cleavage.^{14–17} Hence, it was hypothesized that loading of the sense strand into the RISC could be impeded by blocking 5' phosphorylation. Indeed, 5'-O-methylation (5'-OME) of one of the siRNA strands has been shown to affect strand selection.¹⁸ An unlocked nucleic acid (UNA), a monomer that features an acyclic backbone and that is not phosphorylated by natural kinases, has also been used to block the loading of the sense strand into RISC, leading to preferential selection of the desired antisense strand.^{11,12} Moreover, RISC loading and RNAi activity can partially be restored by incorporating a phosphate group at the UNA modification, further strengthening the hypothesis that the 5'-phosphate group directs RISC loading.¹⁹

In this communication, we report synthesis of 5'-morpholino-bearing nucleoside phosphoramidites and demonstrate that the presence of a morpholino moiety at the 5' end of the sense strand improves antisense strand selection and RNAi activity. We also show that the morpholino modification, when placed at the 5' end of the antisense strand, results in complete loss of RNAi activity. Among a set of 5'-end modifications tested, the morpholino modification had the largest influence on strand selection.

Initially, we evaluated five different modifications that either lack the 5'-hydroxyl group or have a sterically hindered 5'-hydroxyl group with the aim of blocking 5' phosphorylation and thus RISC loading. In order to study the impact on RNAi activity, each of these modifications was incorporated at the 5' end of the antisense or sense strand of an siRNA previously shown to silence expression of *apolipoprotein B (ApoB)*.^{4,5} The tested modifications included 5'-deoxy-5'-morpholino-2'-O-methyl uridine (**Mo**), 5'-deoxy-5'-dimethylamino-2'-O-methyl uridine (**D**), 5'-deoxy-2'-O-methyl uridine (**Me**), locked nucleic acid (**LNA**), and inverted abasic site (**ib**) (Fig. 1).

The synthesis of 5'-morpholino-2'-OME phosphoramidites (**5a–d**) was accomplished in four or five steps starting from the corresponding 3'-O-protected nucleosides **1a–d** (Scheme 1). The 5' tosylation of **1a–d** gave fully protected nucleosides **2a–d** in good yields. Heating **2a–d** with morpholine afforded 5'-morpholino

^a Alnylam Pharmaceuticals, 300 Third Street, Cambridge, Massachusetts 02142, USA. E-mail: mmanoharan@alnylam.com

^b Department of Biochemistry, School of Medicine, Vanderbilt University, Nashville, Tennessee 37232-0146, USA

† Electronic supplementary information (ESI) available. See DOI: 10.1039/c9cc00977a

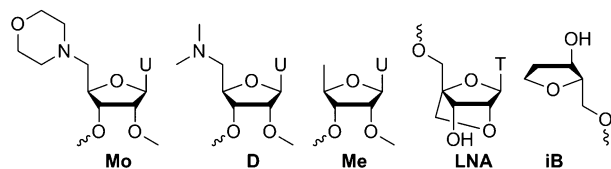
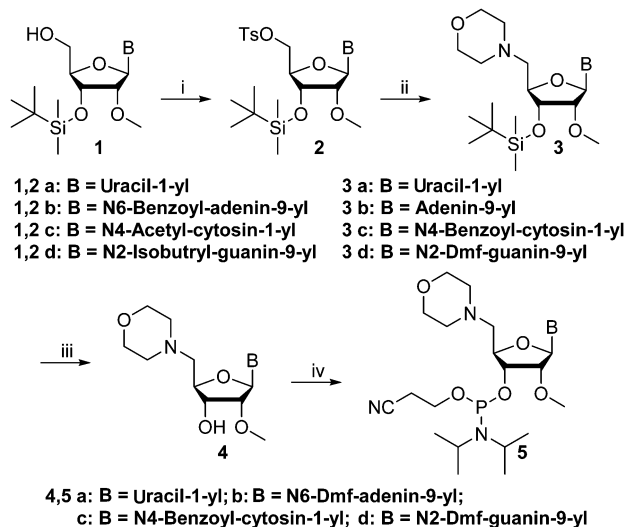


Fig. 1 Modifications tested: 5'-deoxy-5'-morpholino-2'-O-methyl uridine (**Mo**), 5'-deoxy-5'-dimethylamino-2'-O-methyl uridine (**D**), 5'-deoxy-2'-O-methyl uridine (**Me**), locked nucleic acid (**LNA**), and inverted abasic site (**iB**).

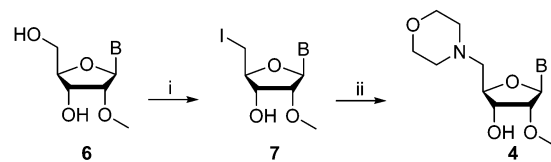
nucleosides **3a–d**. Interestingly, loss of the protecting group from the exocyclic amine of nucleobases C, A, and G was observed, probably due to the basic nature of morpholine. Therefore, protecting groups at exocyclic amines were re-installed and 3'-*O*-silyl protection was removed to yield the free alcohols **4a–d**. 3' Phosphitylation of **4a–d** then gave the desired phosphoramidites **5a–d**.

In an alternate, simplified approach, 5'-morpholino-2'-*O*-methyl U (**4a**) was obtained from 2'-*OMe* U (**6a**) in two steps (Scheme 2). This route involved 5' iodination of **6a** followed by reaction of 5'-iodo-2'-*OMe* U (**7a**) with morpholine. Importantly, in the first approach, selective 5' tosylation of unprotected 2'-*OMe* U could not be achieved. A similar 5' iodination approach was extended to purine analogs, and 5'-morpholino-2'-*OMe* A (**4b**) was successfully obtained from fully unprotected 2'-*OMe* A (**6b**, Scheme 2).

Conjugates of siRNA with the trivalent *N*-acetyl-galactosamine (GalNAc) ligand, which results in targeting of the siRNAs to hepatocytes,⁶ carrying modifications at the 5' end of the sense,



Scheme 1 Synthesis of 5'-morpholino 2'-*OMe* phosphoramidites. (i) **2a–2d**: 4-toluenesulfonyl chloride, 4-dimethylaminopyridine, CH₂Cl₂, 79%, 84%, 79%, and 56%, respectively; (ii) **3a–3b**: morpholine, 60 °C, 66%, 78%; **3c**: (A) morpholine, 60 °C, (B) *N,N*-dimethylformamidedimethyl acetal, DMF, 66%; (iii) **4a**: tetra-*n*-butylammonium fluoride (TBAF), tetrahydrofuran (THF), 86%; **4b**: (A) *N,N*-dimethylformamidedimethyl acetal, DMF, (B) TBAF, THF, 69%; **4c–4d**: TBAF, THF, 80%, 88%, respectively; (iv) **5a**: 2-cyanoethyl *N,N,N',N'*-tetraisopropyl-phosphordiamidite, 5-(ethylthio)-1-*H*-tetrazole, CH₃CN, 50%; **5b**, **5c**, **5d**: 2-cyanoethyl *N,N*-diisopropylchlorophosphordiamidite, *N,N*-diisopropylethylamine, CH₂Cl₂, 73%, 57%, 78%, respectively.



6,7 a: B = Uracil-1-yl
6,7 b: B = Adenin-9-yl

4 a: B = Uracil-1-yl
4 b: B = N6-Dmf-adenin-9-yl

Scheme 2 Simplified approach for synthesis of 5'-morpholino 2'-*OMe* phosphoramidites. (i) **2a**, **2b**: triphenylphosphine, imidazole, I₂, THF, 86%, 80%; (ii) **2a**: morpholine, THF room temperature, 62%; **2b**: (A) morpholine, THF, room temperature, (B) *N,N*-dimethylformamidedimethyl acetal, MeOH, 48%.

antisense, or both strands (Table 1) were prepared following reported procedures⁶ (see ESI[†]). To evaluate silencing, siRNAs were transfected into primary mouse hepatocytes and *Apob* mRNA was quantified by RT-qPCR (see ESI[†]). Gene silencing was normalized to levels of *Apob* in cells treated with the parent siRNA. Interestingly, siRNA conjugates with the morpholino moiety on the sense strand showed improved siRNA activity compared to the parent compound, whereas all other modifications showed activity comparable to the parent (Fig. 2). When placed at the 5' end of the antisense strand, all modifications resulted in loss of activity (Fig. 2); this is consistent with the notion that modifications that block 5' phosphorylation inhibit RISC loading. Consistent with the observation that the morpholino moiety showed the largest effect, the 5' morpholino modification on the antisense strand was the least active of all modified siRNAs tested.

The 5'-morpholino modification was selected for *in vivo* studies. siRNAs with the 5'-morpholino modification on the

Table 1 siRNAs targeting *Apob*

Entry	siRNA	siRNA duplex
1	Parent	5'-U•g•UgAcAaAUuGgGcAuCaA-GalNAc ₃ 5'-u•U•g•AuGcCcAuauUuGuCaCa•a•a
2	S5'- Mo	5'- Mo •g•UgAcAaAUuGgGcAuCaA-GalNAc ₃ 5'-u•U•g•AuGcCcAuauUuGuCaCa•a•a
3	S5'- D	5'- D •g•UgAcAaAUuGgGcAuCaA-GalNAc ₃ 5'-u•U•g•AuGcCcAuauUuGuCaCa•a•a
4	S5'- Me	5'- Me •g•UgAcAaAUuGgGcAuCaA-GalNAc ₃ 5'-u•U•g•AuGcCcAuauUuGuCaCa•a•a
5	S5'- LNA	5'- LNA •g•UgAcAaAUuGgGcAuCaA-GalNAc ₃ 5'-u•U•g•AuGcCcAuauUuGuCaCa•a•a
6	S5'- iB	5'- iB •g•UgAcAaAUuGgGcAuCaA-GalNAc ₃ 5'-u•U•g•AuGcCcAuauUuGuCaCa•a•a
7	AS5'- Mo	5'-U•g•UgAcAaAUuGgGcAuCaA-GalNAc ₃ 5'- Mo •U•g•AuGcCcAuauUuGuCaCa•a•a
8	AS5'- D	5'-U•g•UgAcAaAUuGgGcAuCaA-GalNAc ₃ 5'- D •U•g•AuGcCcAuauUuGuCaCa•a•a
9	AS5'- Me	5'-U•g•UgAcAaAUuGgGcAuCaA-GalNAc ₃ 5'- Me •U•g•AuGcCcAuauUuGuCaCa•a•a
10	AS5'- LNA	5'-U•g•UgAcAaAUuGgGcAuCaA-GalNAc ₃ 5'- LNA •U•g•AuGcCcAuauUuGuCaCa•a•a
11	AS5'- iB	5'-U•g•UgAcAaAUuGgGcAuCaA-GalNAc ₃ 5'- iB •U•g•AuGcCcAuauUuGuCaCa•a•a
12	S/AS5'- Mo	5'- Mo •g•UgAcAaAUuGgGcAuCaA-GalNAc ₃ 5'- Mo •U•g•AuGcCcAuauUuGuCaCa•a•a

Abbreviations and symbols: S, sense strand; AS, antisense strand; uppercase, 2'-F; lowercase, 2'-*OMe*; •, phosphorothioate; GalNAc₃, hydroxypropyl trivalent *N*-acetyl-galactosamine ligand. For the structures of **Mo**, **D**, **Me**, **LNA**, and **iB** see Fig. 1.

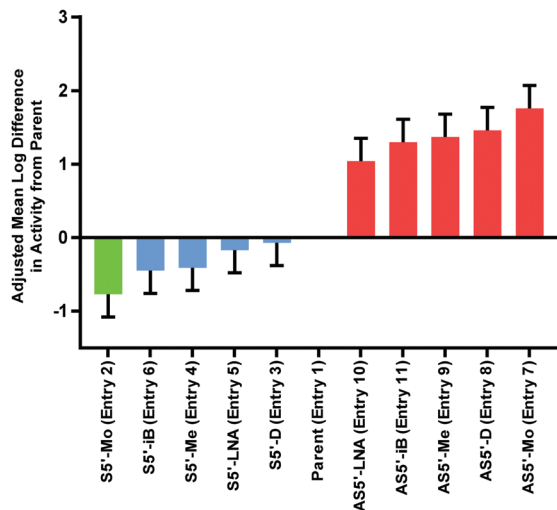


Fig. 2 The 5' morpholino on the sense strand enhances siRNA activity. *In vitro* RNAi activity of siRNA–GalNAc conjugates modified at the 5' end of the sense strand (S, green and blue) or antisense strand (AS, red) as indicated. Entry numbers refer to Table 1. Plotted is mean log difference in activity relative to the parent siRNA.

sense strand, the antisense strand, or on both strands were compared to the siRNA without a 5' modification. Mice were treated subcutaneously with 3 mg kg⁻¹ of siRNA, and cohorts were sacrificed on days 3, 7, and 15 for analysis of expression of *Apob* in liver (see ESI†). The siRNA with the 5' morpholino on the sense strand had higher activity than the parent on day 3 (Fig. 3). These data suggest that blocking sense strand loading improves loading of antisense strand into the active RISC. The effect was less pronounced on days 7 and 15. siRNAs with the 5'-morpholino modification on the antisense strand or both strands were inactive (Fig. 3), consistent with the hypothesis that the 5' morpholino blocks phosphorylation and impedes RISC loading.

To confirm that the loss of activity resulting from modification of the 5' end of the antisense strand with morpholino is due to impeded RISC loading, the levels of each siRNA strand were measured in liver lysates and in RISC precipitated from liver lysates (see ESI†). The amount of siRNA in liver was not affected by the presence of 5'-morpholino modification on day 3 (Fig. 4A; for data

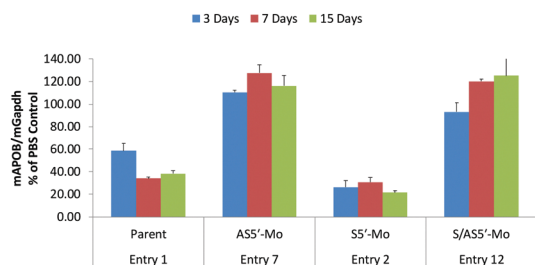


Fig. 3 The 5'-morpholino modification directs strand selection *in vivo*. Mice ($n = 3$ per group) were treated with a single dose (3 mg kg⁻¹) of parent, AS5'-Mo, S5'-Mo, or S/AS5'-Mo siRNA targeting *Apob*. Cohorts of mice were sacrificed at 3, 7, and 15 days postdose, and livers were processed for mRNA quantification using qPCR. *Apob* mRNA levels were normalized to *Gapdh* mRNA. Data are expressed as percent of *Apob* in the PBS-treated control animals.

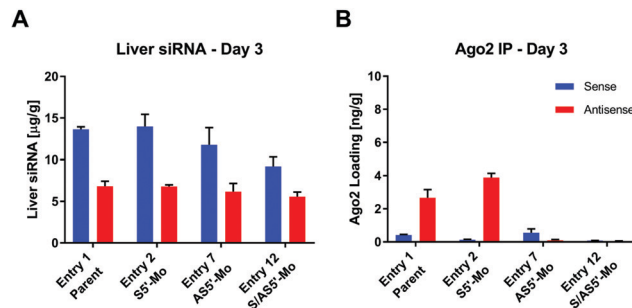


Fig. 4 5'-Morpholino modification of the sense strand increases RISC loading of paired antisense strand. Mice ($n = 3$ per group) were treated with a single dose of 3 mg kg⁻¹ parent, AS5'-Mo, S5'-Mo, or S/AS5'-Mo siRNA targeting *Apob*. Cohorts of mice were sacrificed at 3, 7, and 15 days postdose, and liver lysates were generated. (A) Liver levels of the antisense and sense strands of siRNA–GalNAc conjugates quantification using RT–qPCR. (B) Ago2 was immunoprecipitated and Ago2-bound antisense and sense strand levels were quantification using RT–qPCR.

from days 7 and 15 see Fig. S1, ESI†). However, no Ago2 loading of the antisense strand with the 5'-morpholino modification was observed (Fig. 4B). This demonstrates that the lack of activity of the siRNA with a 5'-modified antisense strand is due to its inability to load or remain loaded in the RISC. Furthermore, on day 3, for siRNA modified on the sense strand we observed slightly higher levels of antisense strand in the RISC than observed for the parent siRNA, consistent with improved RNAi activity. This higher level of loaded antisense strand was also seen on day 15 (Fig. S1, ESI†).

To test whether the morpholino modification of the sense strand would improve activity of an siRNA targeting another gene, modified siRNAs targeting the *FIX* gene²⁰ were synthesized (Table S2, ESI†). Mice were treated with 1 mg kg⁻¹ of siRNA subcutaneously, and circulating FIX levels were assayed on days 7, 14, and 21 post dose (Fig. S2, ESI†). siRNA conjugates with the 5'-morpholino modification on the antisense strand showed complete loss of activity. siRNA conjugates with a 5'-morpholino moiety on the sense strand showed activity comparable to that of the parent compound. These results suggest generalizability of the 5'-morpholino modification.

Next, we performed molecular modeling studies. The crystal structure of the human Ago2 MID domain in complex with UMP²¹ (PDB ID 3LUJ) was used as a template (Fig. 5A). The phosphate group was removed and replaced by a morpholino moiety using the program UCSF Chimera.²² The initial model was refined using the Amber 14ff force field in combination with Gasteiger potentials as implemented in UCSF Chimera. The final model demonstrates that the morpholino modification fits well inside the MID domain binding site as indicated by only minor adjustments of adjacent amino acid side chains (Fig. 5B). However, all of the interactions with the phosphate group observed in the structure with UMP are lost except for a single hydrogen bond between Lys-570 and the morpholino ring oxygen (N–H...O distance of 2.35 Å). As the morpholino group is positively charged and the other oxygen is not a potent acceptor, the stabilizing effect of this hydrogen bond is presumably negligible. Furthermore, the cationic morpholino may generate repulsive interactions with Lys-570 and Lys-533 through electronic field effects.

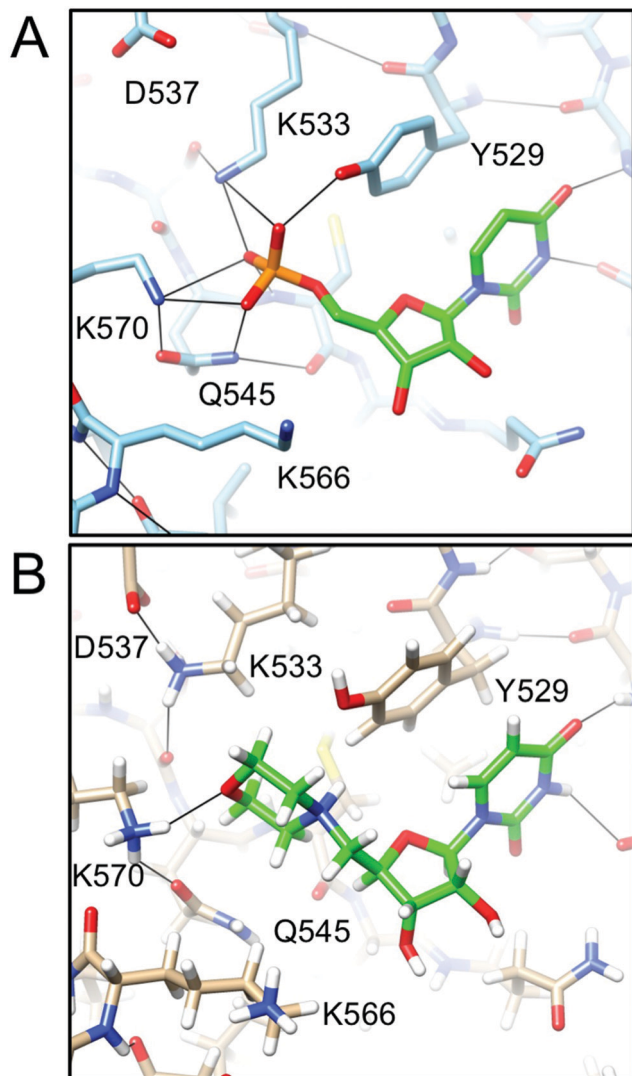


Fig. 5 Illustrations of the binding modes of (A) UMP and (B) 5'-morpholino-U to Ago2 MID. Substrate carbon, oxygen, nitrogen, phosphorus, and hydrogen (panel B only) atoms are green, red, blue, orange, and white, respectively. Hydrogen bonds are thin solid lines in black, and selected Ago2 residues are labeled.

In summary, we showed that by blocking phosphorylation using a 5'-morpholino modification, loading and/or retention of the modified strand in the RISC was reduced. Importantly, RNAi activity and levels of the antisense strand loaded into RISC were improved by introducing a 5'-morpholino modification on the sense strand. Modification of the 5' end of the sense strand decreased its selection, making it a more efficient passenger. Our investigation confirms the earlier observations that the 5'-phosphate group plays an important role in RISC loading.^{15–18,23,24} Recently, various chemical modifications have been evaluated with the aim of mitigating potential off-target effects associated with siRNAs. These include base modifications,²⁵ backbone modifications,²⁶ and thermally destabilizing modifications such as UNA¹² and GNA.²⁷ The 5'-morpholino modification reported here is an alternative

and effective strategy to nullify the off-target effects originating from loading of the sense strand into RISC complex.

We acknowledge the teachings from the past, “Why Nature Chose Phosphates²⁸” (Professor Frank H. Westheimer) and “Biomimetic Chemistry²⁹” (Professor Ronald Breslow) which inspired some of the concepts described in this communication.

Conflicts of interest

All authors except RGP, KGR, and ME are current employees of Anlylam Pharmaceuticals.

References

- 1 S. M. Elbashir, J. Harborth, W. Lendeckel, A. Yalcin, K. Weber and T. Tuschl, *Nature*, 2001, **411**, 494.
- 2 M. Manoharan, *Curr. Opin. Chem. Biol.*, 2004, **8**, 570–579.
- 3 D. Bumcrot, M. Manoharan, V. Koteliensky and D. W. Y. Sah, *Nat. Chem. Biol.*, 2006, **2**, 711.
- 4 J. Soutschek, A. Akinc, B. Bramlage, K. Charisse, R. Constien and M. Donoghue, *et al.*, *Nature*, 2004, **432**, 173.
- 5 T. S. Zimmermann, A. C. H. Lee, A. Akinc, B. Bramlage, D. Bumcrot and M. N. Fedoruk, *et al.*, *Nature*, 2006, **441**, 111.
- 6 J. K. Nair, J. L. S. Willoughby, A. Chan, K. Charisse, M. R. Alam and Q. Wang, *et al.*, *J. Am. Chem. Soc.*, 2014, **136**, 16958–16961.
- 7 K. Fitzgerald, S. White, A. Borodovsky, B. R. Bettencourt, A. Strahs and V. Clausen, *et al.*, *N. Engl. J. Med.*, 2017, **376**, 41–51.
- 8 D. Adams, A. Gonzalez-Duarte, W. D. O’Riordan, C.-C. Yang, M. Ueda and A. V. Kristen, *et al.*, *N. Engl. J. Med.*, 2018, **379**, 11–21.
- 9 S. M. Elbashir, J. Martinez, A. Patkaniowska, W. Lendeckel and T. Tuschl, *EMBO J.*, 2001, **20**, 6877–6888.
- 10 G. J. Hannon, *Nature*, 2002, **418**, 244.
- 11 N. M. Snead, J. R. Escamilla-Powers, J. J. Rossi and A. P. McCaffrey, *Mol. Ther. – Nucleic Acids*, 2013, **2**, e103.
- 12 N. Vaish, F. Chen, S. Seth, K. Fosnaugh, Y. Liu and R. Adami, *et al.*, *Nucleic Acids Res.*, 2011, **39**, 1823–1832.
- 13 D. S. Schwarz, G. Hutvagner, T. Du, Z. Xu, N. Aronin and P. D. Zamore, *Cell*, 2003, **115**, 199–208.
- 14 E. Elkayam, C.-D. Kuhn, A. Tocilj, A. D. Haase, E. M. Greene, G. J. Hannon and L. Joshua-Tor, *Cell*, 2012, **150**, 100–110.
- 15 N. T. Schirle and I. J. MacRae, *Science*, 2012, **336**, 1037.
- 16 E. Elkayam, R. Parmar, C. R. Brown, J. L. Willoughby, C. S. Theile, M. Manoharan and L. Joshua-Tor, *Nucleic Acids Res.*, 2017, **45**, 3528–3536.
- 17 R. G. Parmar, C. R. Brown, S. Matsuda, J. L. S. Willoughby, C. S. Theile and K. Charisse, *et al.*, *J. Med. Chem.*, 2018, **61**, 734–744.
- 18 P. Y. Chen, L. Weinmann, D. Gaidatzis, Y. Pei, M. Zavolan, T. Tuschl and G. Meister, *RNA*, 2007, **14**, 263–274.
- 19 D. M. Kenski, A. J. Cooper, J. J. Li, A. T. Willingham, H. J. Haringsma and T. A. Young, *et al.*, *Nucleic Acids Res.*, 2010, **38**, 660–671.
- 20 Z. Chen, B. Luo, T.-Q. Cai, A. Thankappan, Y. Xu and W. Wu, *et al.*, *Mol. Ther. – Nucleic Acids*, 2015, **4**, e224.
- 21 F. Frank, N. Sonenberg and B. Nagar, *Nature*, 2010, **465**, 818.
- 22 E. F. Pettersen, T. D. Goddard, C. C. Huang, G. S. Couch, D. M. Greenblatt, E. C. Meng and T. E. Ferrin, *J. Comput. Chem.*, 2004, **25**, 1605–1612.
- 23 S. M. Elbashir, W. Lendeckel and T. Tuschl, *Genes Dev.*, 2001, **15**, 188–200.
- 24 S. Weitzer and J. Martinez, *Nature*, 2007, **447**, 222.
- 25 S. R. Suter, A. Ball-Jones, M. M. Mumbleau, R. Valenzuela, J. Ibarra-Soza and H. Owens, *et al.*, *Org. Biomol. Chem.*, 2017, **15**, 10029–10036.
- 26 T. Hardcastle, I. Novosjolova, V. Kotikam, S. K. Cheruiyot, D. Mutisya and S. D. Kennedy, *et al.*, *ACS Chem. Biol.*, 2018, **13**, 533–536.
- 27 M. M. Janas, M. K. Schlegel, C. E. Harbison, V. O. Yilmaz, Y. Jiang and R. Parmar, *et al.*, *Nat. Commun.*, 2018, **9**, 723.
- 28 F. H. Westheimer, *Science*, 1987, **235**, 1173–1178.
- 29 R. Breslow, *Chem. Soc. Rev.*, 1972, **1**, 553–580.

5'-Morpholino modification of the sense strand of an siRNA makes it a more effective passenger

Pawan Kumar,^a Rubina G. Parmar,^a Christopher R. Brown,^a Jennifer L. S. Willoughby,^a Donald J. Foster,^a Ramesh I. Babu,^a Sally Schofield,^a Vasant Jadhav,^a Klaus Charisse,^a Jayaprakash K. Nair,^a Kallanthottathil G. Rajeev,^a Martin A. Maier,^a Martin Egli,^b and Muthiah Manoharan*^a

^aAlnylam Pharmaceuticals, 300 Third street, Cambridge, Massachusetts 02142, USA.

^bDepartment of Biochemistry, School of Medicine, Vanderbilt University, Nashville, TN 37232-0146, USA.

*To whom correspondence should be sent: Tel: 617-551-8319; email: mmanoharan@alnylam.com

Electronic Supplementary Information

Contents

1. Experimental Details:	3
1.1 General synthetic details	3
1.2 Synthesis of nucleosides and phosphoramidites	3
1.3 Oligonucleotide synthesis	17
1.4 <i>In vitro</i> RNAi activity	19
1.5 Quantification of whole liver and Ago2-associated siRNA levels	19
1.6 <i>In vivo</i> RNAi activity targeting <i>FIX</i> gene	20
1.7 Representative NMR spectra	22
1.8 Representative MS spec of Oligonucleotides	42

1. Experimental Details:

1.1 General synthetic details

Commercially available starting materials, reagents, and solvents were used as received. All moisture-sensitive reactions were carried under anhydrous conditions under argon atmosphere. Flash chromatography was performed on a Teledyne ISCO Combi Flash system using pre-packed ReadySep Teledyne ISCO silica gel columns. TLC was performed on Merck silica-coated plates 60 F₂₅₄. Compounds were visualized under UV light (254 nm) or after spraying with the *p*-anisaldehyde staining solution followed by heating. ESI-HRMS spectra were recorded on Waters QToF API US spectrometer using the direct flow injection in the positive mode (capillary = 3000 kV, cone = 35, source temperature = 120 °C, and desolvation temperature = 350 °C). ¹H and ¹³C NMR spectra were recorded at room temperature on Varian spectrometers, and chemical shifts in ppm are referenced to the residual solvent peaks. Coupling constants are given in Hertz. Signal splitting patterns are described as singlet (s), doublet (d), triplet (t), quartet (q), broad signal (br), or multiplet (m). ³¹P NMR spectra were recorded under proton-decoupled mode; chemical shifts are referenced to external H₃PO₄ (80%).

1.2 Synthesis of nucleosides and phosphoramidites

Synthesis of nucleoside 1a-1d

Nucleoside **1a-1d** were prepared following literature procedure.¹

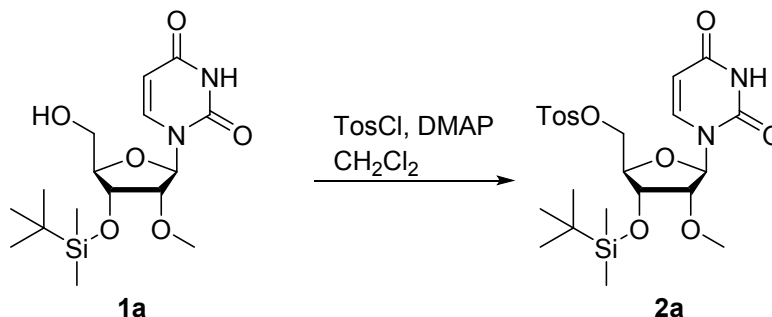
1a: ¹H (400 MHz, d₆-DMSO) δ 11.35 (s, 1H), 7.91 (d, *J* = 8.1 Hz, 1H), 5.82 (d, *J* = 4.8 Hz, 1H), 5.65 (d, *J* = 8.1 Hz, 1H), 5.17 (t, *J* = 4.9 Hz, 1H), 4.28 (t, *J* = 4.7 Hz, 1H), 3.83 (t, *J* = 4.9 Hz, 2H), 3.65 (dd, *J* = 15.5, 4.9 Hz, 1H), 3.58 – 3.46 (m, 1H), 3.33 (s, 3H), 0.87 (s, 9H), 0.08 (s, 6H). ¹³C (126 MHz, d₆-DMSO) δ 163.03, 150.47, 140.30, 101.86, 86.13, 85.00, 82.17, 69.68, 60.00, 57.58, 25.62, 17.78, -4.85, -4.96.

1b: ¹H (400 MHz, d₆-DMSO) δ 11.22 (s, 1H), 8.76 (s, 2H), 8.04 (d, *J* = 7.3 Hz, 2H), 7.64 (t, *J* = 7.5 Hz, 1H), 7.54 (t, *J* = 7.6 Hz, 2H), 6.14 (d, *J* = 5.9 Hz, 1H), 5.20 (t, *J* = 5.5 Hz, 1H), 4.59 – 4.57 (m, 1H), 4.53 (t, *J* = 5.3 Hz, 1H), 3.98 (q, *J* = 4.0 Hz, 1H), 3.76 – 3.66 (m, 1H), 3.63 – 3.53 (m, 1H), 3.32 (s, 3H), 0.92 (s, 9H), 0.13 (s, 6H). ¹³C (126 MHz, d₆-DMSO) δ 165.58, 152.03, 151.70, 150.48, 143.05, 133.26, 132.43, 128.46, 128.43, 125.84, 86.37, 85.48, 81.91, 70.22, 60.76, 57.64, 25.65, 17.82, -4.84, -4.85.

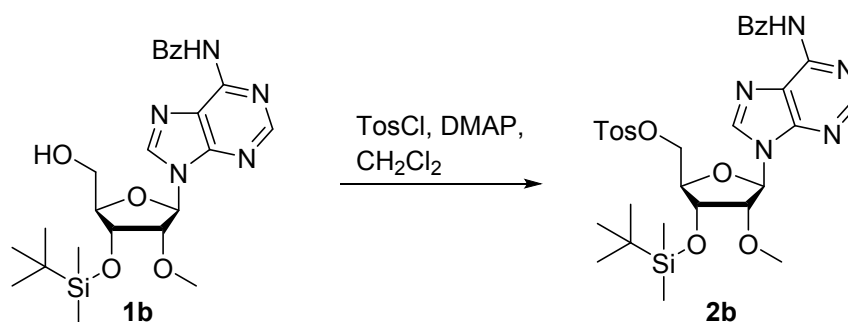
1c: ¹H (400 MHz, d₆-DMSO) δ 10.91 (s, 1H), 8.44 (d, *J* = 7.5 Hz, 1H), 7.19 (d, *J* = 7.5 Hz, 1H), 5.82 (d, *J* = 2.4 Hz, 1H), 5.23 (t, *J* = 4.7 Hz, 1H), 4.23 (dd, *J* = 7.0, 4.8 Hz, 1H), 3.92 – 3.85 (m, 1H), 3.81 – 3.68 (m, 1H), 3.60 – 3.50 (m, 1H), 3.43 (s, 3H), 2.09 (s, 3H), 0.85 (s, 9H), 0.05 (s, 6H). ¹³C (126 MHz, d₆-DMSO) 170.98, 162.39, 154.42, 145.02, 95.25, 88.05, 84.06, 83.11, 68.68, 59.00, 57.77, 25.59, 24.32, 17.76, -4.86, -5.09.

1d: ^1H (400 MHz, d_6 -DMSO) δ 12.10 (s, 1H), 11.60 (s, 1H), 8.32 (s, 1H), 5.86 (d, $J = 6.7$ Hz, 1H), 5.16 (t, $J = 5.3$ Hz, 1H), 4.46 (dd, $J = 4.6, 2.4$ Hz, 1H), 4.32 (dd, $J = 6.7, 4.6$ Hz, 1H), 3.93 – 3.90 (m, 1H), 3.64 – 3.58 (m, 1H), 3.57 – 3.50 (m, 1H), 3.29 (s, 3H), 2.76 (p, $J = 6.8$ Hz, 1H), 1.11 (d, $J = 6.8$ Hz, 6H), 0.89 (s, 9H), 0.12 (s, 3H), 0.11 (s, 3H). ^{13}C (126 MHz, d_6 -DMSO) 180.12, 154.74, 148.82, 148.26, 137.33, 120.10, 86.65, 84.29, 82.36, 70.39, 60.79, 57.72, 34.70, 25.64, 18.84, 17.82, -4.88, -4.87.

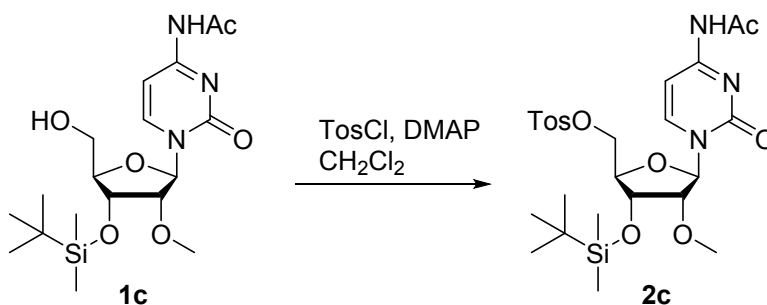
Synthesis of nucleoside **2a**



Alcohol **1a** (7.45 g, 20 mmol) and 4-dimethylaminopyridine (DMAP, 4.89 g, 40 mmol) were dissolved in dry CH_2Cl_2 . 4-Methylbenzenesulfonyl chloride (TosCl, 5.72 g, 30 mmol) was added at 0 °C (ice bath), and the reaction mixture was stirred at 0 °C for 1 h and then at room temperature for 2 h. The reaction was quenched by adding saturated aqueous NaHCO_3 (150 mL) and extracted with CH_2Cl_2 (2 \times 100 mL). The combined organic phases were dried (MgSO_4), and the crude product was purified by flash chromatography using a gradient of 0 – 70 % EtOAc in hexanes to afford nucleoside **2a** (8.40 g, 79%) as a white form. MS (ESI⁺) m/z calcd for $\text{C}_{23}\text{H}_{35}\text{N}_2\text{O}_8\text{SSi}$ [$\text{M} + \text{H}$]⁺ 527.1878, found 527.1883. ^1H (400 MHz, d_6 -DMSO) δ 11.40 (d, $J = 2.2$ Hz, 1H), 7.88 – 7.73 (m, 2H), 7.52 (d, $J = 8.1$ Hz, 1H), 7.48 (d, $J = 8.0$ Hz, 2H), 5.73 (d, $J = 4.3$ Hz, 1H), 5.60 (dd, $J = 8.1, 2.2$ Hz, 1H), 4.21 (dd, $J = 8.9, 4.5$ Hz, 2H), 4.15 (d, $J = 5.4$ Hz, 1H), 3.92 – 3.90 (m, $J = 5.5, 3.5$ Hz, 1H), 3.86 (t, $J = 4.8$ Hz, 1H), 3.30 (s, 3H), 2.40 (s, 3H), 0.81 (s, 9H), 0.03 (s, 3H), 0.01 (s, 3H). ^{13}C (126 MHz, d_6 -DMSO) δ 162.97, 150.27, 145.31, 140.47, 131.82, 130.24, 127.69, 102.04, 87.49, 80.90, 80.77, 69.49, 68.88, 57.63, 25.51, 21.09, 17.66, -4.89, -5.25.

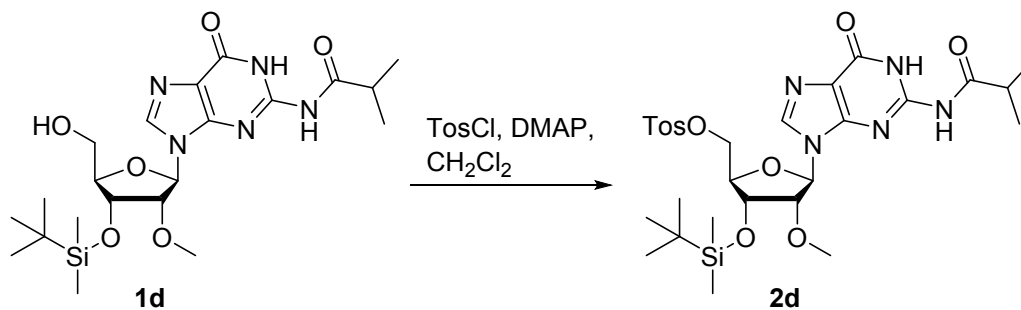
Synthesis of nucleoside 2b

Alcohol **1b** (1.00 g, 2.00 mmol) and 4-dimethylaminopyridine (DMAP, 0.49 g, 3.00 mmol) were dissolved in dry CH_2Cl_2 (20 mL), and the reaction mixture was cooled to 0–4 °C (ice bath). 4-Toluenesulfonyl chloride (TosCl, 0.48 g, 2.50 mmol) was added, and reaction mixture was stirred at 0 °C (ice bath) for 1 h and then at room temperature for 3 h. The reaction was diluted with CH_2Cl_2 (100 mL), washed with saturated aqueous NaHCO_3 (100 mL), dried, and concentrated. The residue was purified by column chromatography using a gradient of 0 – 4% MeOH in CH_2Cl_2 to obtain **2b** (1.10 g, 84%) as a white foam. MS (ESI⁺) m/z calcd for $\text{C}_{31}\text{H}_{40}\text{N}_5\text{O}_7\text{SSi}$ $[\text{M} + \text{H}]^+$ 654.2412, found 654.2423. ^1H (400 MHz, d_6 -DMSO) δ 11.24 (s, 1H), 8.69 (s, 1H), 8.61 (s, 1H), 8.11 – 7.99 (m, 2H), 7.73 – 7.68 (m, 2H), 7.68 – 7.62 (m, 1H), 7.56 (dd, $J = 8.3, 6.8$ Hz, 2H), 7.42 – 7.29 (m, 2H), 6.10 (d, $J = 5.2$ Hz, 1H), 4.61 (t, $J = 4.4$ Hz, 1H), 4.55 (t, $J = 5.0$ Hz, 1H), 4.37 – 4.28 (m, 2H), 4.09 – 4.06 (m, 1H), 3.29 (s, 3H), 2.35 (s, 3H), 0.87 (s, 9H), 0.10 (s, 3H), 0.08 (s, 3H). ^{13}C (126 MHz, d_6 -DMSO) δ 165.59, 151.73, 151.60, 150.53, 145.09, 143.34, 133.25, 132.46, 131.85, 129.99, 128.47, 128.44, 127.49, 125.90, 85.93, 81.98, 80.90, 69.93, 69.23, 57.71, 25.54, 20.99, 17.70, -4.92, -5.12.

Synthesis of nucleoside 2c

Alcohol **1c** (2.50 g, 6.04 mmol) and 4-dimethylaminopyridine (DMAP, 1.47 g, 12.03 mmol) were taken in dry CH₂Cl₂ (50 mL) and reaction mixture was cooled to 0–4°C (ice bath). 4-Toluenesulfonyl chloride (TosCl, 1.44 g, 7.55 mmol) was added and reaction mixture was stirred in ice bath for 3h. The reaction was diluted with CH₂Cl₂ (100 mL), washed with saturated aqueous NaHCO₃ (2 × 30 mL), dried, and concentrated. The residue was purified by column chromatography using a gradient of 0 – 5% MeOH in CH₂Cl₂ to obtain **2c** (2.71 g, 79%) as a white foam. MS (ESI⁺) *m/z* calcd for C₂₅H₃₈N₃O₈SSi [M + H]⁺ 568.2143, found 568.2144. ¹H (400 MHz, d₆-DMSO) δ 10.94 (s, 1H), 7.85 (d, *J* = 7.5 Hz, 1H), 7.81 (d, *J* = 8.3 Hz, 2H), 7.49 (d, *J* = 8.1 Hz, 2H), 7.12 (d, *J* = 7.5 Hz, 1H), 5.78 (d, *J* = 2.2 Hz, 1H), 4.30 (dd, *J* = 11.4, 2.8 Hz, 1H), 4.24 (dd, *J* = 11.4, 4.9 Hz, 1H), 4.09 (dd, *J* = 7.6, 4.9 Hz, 1H), 4.05 – 3.98 (m, 1H), 3.80 (dd, *J* = 4.9, 2.3 Hz, 1H), 3.40 (s, 3H), 2.41 (s, 3H), 2.10 (s, 3H), 0.79 (s, 9H), 0.02 (s, 3H), -0.01 (s, 3H). ¹³C (101 MHz, d₆-DMSO) δ 171.04, 162.45, 154.18, 145.40, 144.50, 131.73, 130.28, 127.66, 95.43, 89.09, 81.95, 80.29, 69.12, 68.37, 57.78, 25.46, 24.34, 21.09, 17.59, -4.88, -5.39.

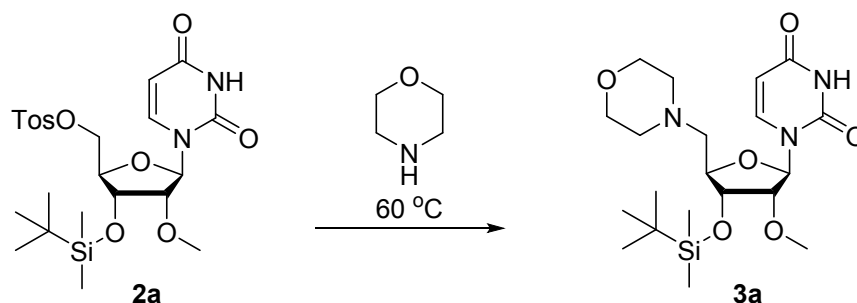
Synthesis of nucleoside **2d**



Alcohol **1d** (4.81 g, 10 mmol) and 4-dimethylaminopyridine (DMAP, 2.45 g, 20 mmol) were dissolved in dry CH₂Cl₂ (40 mL). 4-Toluenesulfonyl chloride (TosCl, 2.86 g, 15 mmol) was added at 0°C (ice bath) and the reaction mixture was stirred at 0 °C for 1 h and then at room temperature for 2 h. The reaction was quenched by adding saturated aqueous NaHCO₃ (100 mL) and extracted with CH₂Cl₂ (2 × 60 mL). The combined organic phases were dried (MgSO₄), and the crude product was purified by column chromatography using a gradient of 0 – 4% MeOH in CH₂Cl₂ to afford nucleoside **2d** (3.60 g, 56%) as a white form. MS (ESI⁺) *m/z* calcd for C₂₈H₄₂N₅O₈SSi [M + H]⁺ 636.2518, found 636.2521. ¹H (400 MHz, d₆-DMSO) δ 12.08 (s, 1H), 11.53 (s, 1H), 8.17 (s, 1H), 7.81 – 7.70 (m, 2H), 7.40 (d, *J* = 8.1 Hz, 2H), 5.83 (d, *J* = 5.3 Hz, 1H), 4.37 – 4.30 (m, 2H), 4.27 – 4.22 (m, 2H), 4.03 – 4.00 (m, 1H), 3.27 (s, 3H), 2.77 – 2.73 (m, 1H), 2.38 (s, 3H), 1.11 (d, *J* = 6.8 Hz, 6H), 0.85 (s, 9H), 0.07 (s, 3H), 0.06 (s, 3H). ¹³C (126 MHz, d₆-DMSO) δ

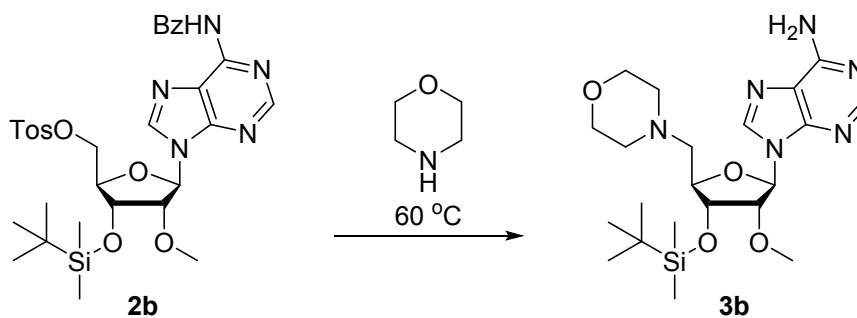
180.04, 154.75, 148.71, 148.24, 145.19, 137.33, 131.93, 130.10, 127.57, 120.19, 84.52, 82.49, 81.26, 69.92, 69.49, 57.83, 34.77, 25.56, 21.06, 18.85, 18.83, 17.72, -4.96, -5.12.

Synthesis of nucleoside **3a**



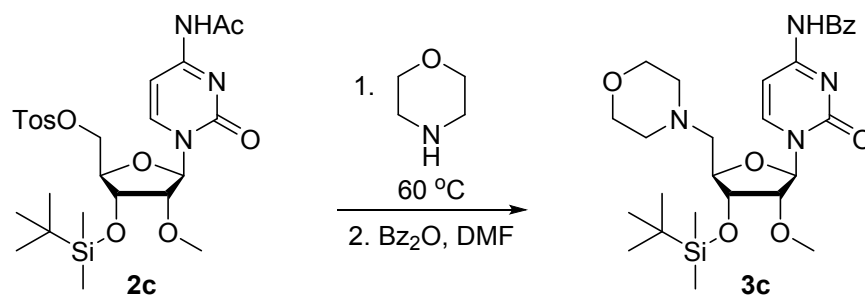
Nucleoside **2a** (2.0 g, 3.79 mmol) was dissolved in morpholine (25 mL), and the reaction mixture was stirred at 60 °C for 18 h. Solvent was removed at reduced pressure, and the residue was dissolved in CH₂Cl₂ (100 mL) and washed with H₂O (50 mL). The aqueous phase was back extracted with CH₂Cl₂ (2 × 30 mL), and the combined organic phases were dried (MgSO₄) and concentrated, and the crude was purified by column chromatography using a gradient of 0 – 5 % MeOH in CH₂Cl₂ to afford nucleoside **3a** (1.1 g, 66%) as white powder. MS (ESI⁺) *m/z* calcd for C₂₀H₃₆N₃O₆Si [M + H]⁺ 442.2368, found 442.2378. ¹H (400 MHz, d₆-DMSO) δ 11.37 (s, 1H), 7.69 (d, *J* = 8.1 Hz, 1H), 5.78 (d, *J* = 4.5 Hz, 1H), 5.67 (d, *J* = 8.0 Hz, 1H), 4.15 (t, *J* = 5.2 Hz, 1H), 3.90 – 3.85 (m, 2H), 3.55 (t, *J* = 4.6 Hz, 4H), 3.32 (s, 3H), 2.59 (dd, *J* = 13.5, 5.1 Hz, 1H), 2.47 – 2.42 (m, 5H), 0.87 (s, 9H), 0.09 (s, 6H). ¹³C (101 MHz, d₆-DMSO) δ 162.96, 150.35, 140.90, 102.11, 87.07, 81.46, 80.92, 71.66, 66.14, 59.73, 57.42, 54.01, 25.61, 17.76, -4.70, -4.99.

Synthesis of nucleoside **3b**



Nucleoside **2b** (2.4 g, 3.6 mmol) was dissolved in morpholine (20 mL), and the reaction mixture was stirred at 60 °C for 16 h. Solvents were removed at reduced pressure, and the residue was dissolved in CH₂Cl₂ (50 mL) and washed with saturated aqueous NaHCO₃ (50 mL). The aqueous phase was back extracted with CH₂Cl₂ (2 × 30 mL). The combined organic phases were concentrated, and the residue was purified by column chromatography using a gradient of 0 – 7% MeOH in CH₂Cl₂ to yield nucleoside **3b** (1.35 g, 78%) as a white foam. MS (ESI⁺) *m/z* calcd for C₂₁H₃₇N₆O₄Si [M + H]⁺ 465.2640, found 465.2630. ¹H NMR (400 MHz, CDCl₃) δ 8.33 (s, 1H), 7.94 (s, 1H), 5.99 (d, *J* = 3.4 Hz, 1H), 5.79 (s, 2H), 4.50 (dd, *J* = 6.2, 5.0 Hz, 1H), 4.37 (dd, *J* = 5.1, 3.4 Hz, 1H), 4.24 – 4.15 (m, 1H), 3.70 (t, *J* = 4.7 Hz, 4H), 3.46 (s, 3H), 2.69 (dd, *J* = 5.5, 3.6 Hz, 2H), 2.63 – 2.45 (m, 4H); 0.94 (s, 9H), 0.14 (s, 3H), 0.13 (s, 3H). δ_c (101 MHz, CDCl₃) 155.74, 153.18, 149.69, 140.18, 120.75, 87.98, 82.58, 81.99, 72.77, 67.05, 60.89, 58.67, 54.75, 25.97, 18.38, -4.28, -4.56.

Synthesis of nucleoside **3c**



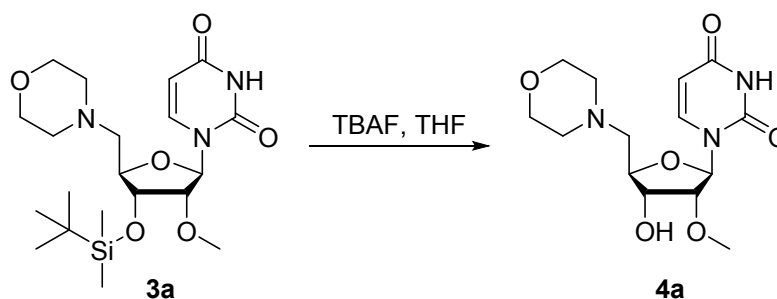
Nucleoside **2c** (3.7 g, 6.51 mmol) was dissolved in morpholine (20 mL). The resulting solution was heated at 60 °C for 24 h. Solvents were removed, and the crude was purified by column chromatography using a gradient of 0–12% MeOH in CH₂Cl₂. The isolated product (3.5 g) was dissolved DMF (15 mL). To this solution was added benzoic anhydride (1.61 g, 7.11 mmol), and the reaction mixture was stirred at room temperature for 16 h. Solvent was removed, and the residue was dissolved in EtOAc (100 mL) and washed with H₂O (2 × 50 mL). The combined aqueous phases were back extracted with EtOAc (50 mL), and the combined organic phases were dried (MgSO₄) and concentrated at reduced pressure. The residue was purified by column chromatography using a gradient of 0 – 5% MeOH in CH₂Cl₂ to afford nucleoside **3c** (2.35 g, 66% over 2 steps) as white foam. MS (ESI⁺) *m/z* calcd for C₂₇H₄₁N₄O₆Si [M + H]⁺ 545.2790, found 545.2791. ¹H (400 MHz, d₆-DMSO) δ 11.33 (s, 1H), 8.24 (d, *J* = 7.5 Hz, 1H), 8.03 – 7.97 (m, 2H), 7.65 – 7.58 (m, 1H), 7.55 – 7.47 (m, 2H), 7.40 (d, *J* = 7.5 Hz, 1H), 5.88 (d, *J* = 2.8 Hz, 1H), 4.08 (dd, *J* = 7.1, 4.9 Hz, 1H), 3.98 (dt, *J* = 6.9, 5.1 Hz, 1H), 3.83 (dd, *J* = 5.0, 2.8 Hz, 1H), 3.58 (t, *J* = 4.6 Hz, 4H), 3.42 (s, 3H), 2.63 (d, *J* = 5.1 Hz, 2H), 2.52 – 2.43 (m, 5H), 0.87 (s, 9H), 0.08 (s, 6H). ¹³C (101 MHz, d₆-DMSO) δ 167.55, 163.09,

154.18, 145.29, 133.11, 132.71, 129.20, 128.43, 96.54, 88.72, 82.17, 81.29, 71.47, 66.17, 59.46, 57.57, 54.07, 25.59, 17.72, -4.65, -5.08.

Synthesis of nucleoside **3d**

Nucleoside **2d** (1.4 g, 2.20 mmol) was dissolved in morpholine (20 mL). The resulting solution was heated at 60 °C for 40 h. Solvent was removed, and the crude was dissolved in CHCl₃ (100 mL) and washed with H₂O (50 mL). The aqueous phase was back extracted with CHCl₃ (50 mL), and the combined organic phases were dried (MgSO₄) and concentrated at reduced pressure. The residue was dissolved in MeOH (15 mL) and to this was added dimethylformamide dimethyl acetal (DMF-DMA, 380 mg, 3.2 mmol). The resulting reaction mixture was stirred at room temperature for 18 h. The solvents were removed, and the crude was purified by column chromatography using a gradient of 0 – 6% MeOH in CH₂Cl₂ to afford nucleoside **3d** (0.78 g, 66%) as a white foam. MS (ESI⁺) *m/z* calcd for C₂₄H₄₂N₇O₅Si [M + H]⁺ 536.3011, found 536.2994. ¹H (400 MHz, d₆-DMSO) δ 11.37 (s, 1H), 8.51 (s, 1H), 8.06 (s, 1H), 5.87 – 5.86 (m, 1H), 4.41 (d, *J* = 3.6 Hz, 2H), 3.96 (td, *J* = 6.1, 2.6 Hz, 1H), 3.53 (t, *J* = 4.6 Hz, 4H), 3.28 (s, 3H), 3.14 (s, 3H), 3.03 (s, 3H), 2.64 (dd, *J* = 13.3, 5.9 Hz, 1H), 2.54 – 2.49 (m, 1H), 2.46 – 2.34 (m, 4H), 0.90 (s, 9H), 0.12 (s, 6H). ¹³C (101 MHz, d₆-DMSO) δ 157.76, 157.50, 157.23, 149.72, 137.28, 120.02, 85.23, 82.41, 81.05, 72.18, 66.15, 60.14, 57.54, 53.91, 40.69, 34.63, 25.66, 17.84, -4.68, -4.86.

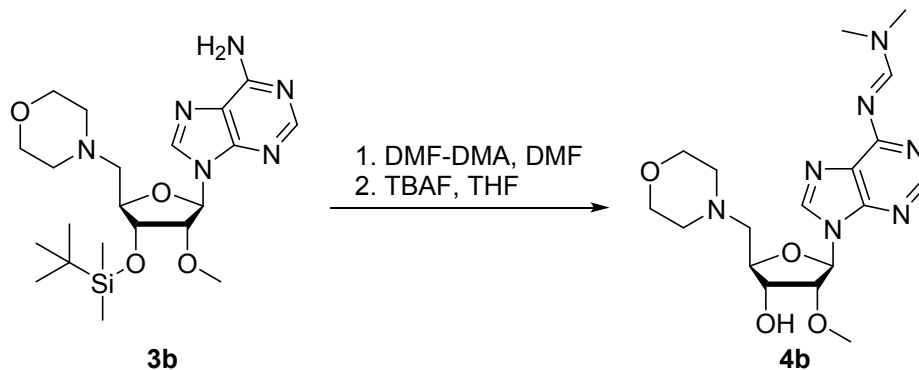
Synthesis of nucleoside **4a**



Nucleoside **3a** (500 mg, 1.13 mmol) was dissolved in THF (5 mL). To this was added tetra-*n*-butylammonium fluoride (TBAF, 1 M in THF, 1.5 mL, 1.5 mmol). The reaction mixture was stirred at room temperature for 1 h. Solvents were removed, and the residue was purified by column chromatography using a gradient of 0-5% MeOH in EtOAc to obtain alcohol **4a** (320 mg, 86%) as white amorphous powder. MS (ESI⁺) *m/z* calcd for C₁₄H₂₂N₃O₆ [M + H]⁺ 328.1503, found 328.1501. ¹H NMR (500 MHz, d₆-DMSO) δ

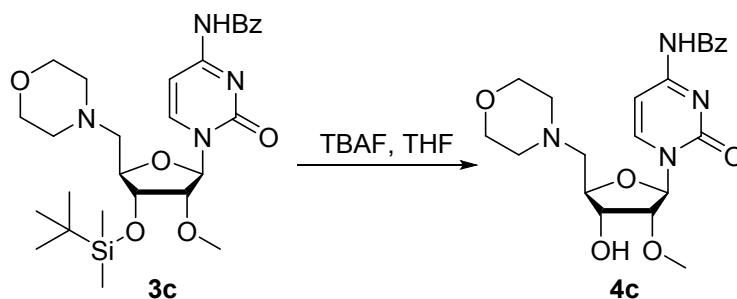
11.35 (d, $J = 2.2$ Hz, 1H), 7.71 (d, $J = 8.1$ Hz, 1H), 5.76 (d, $J = 4.0$ Hz, 1H), 5.65 (dd, $J = 8.0, 2.1$ Hz, 1H), 5.18 (d, $J = 6.5$ Hz, 1H), 3.94 (q, $J = 6.0$ Hz, 1H), 3.88 (td, $J = 6.4, 3.9$ Hz, 1H), 3.79 (dd, $J = 5.2, 4.1$ Hz, 1H), 3.55 (t, $J = 4.7$ Hz, 4H), 3.36 (s, 3H), 2.63 (dd, $J = 13.6, 3.9$ Hz, 1H), 2.56 – 2.36 (m, 5H). δ_c (101 MHz, d6-DMSO) 163.00, 150.31, 140.79, 101.96, 87.07, 81.63, 81.48, 70.23, 66.14, 59.88, 57.63, 53.99.

Synthesis of nucleoside **4b**



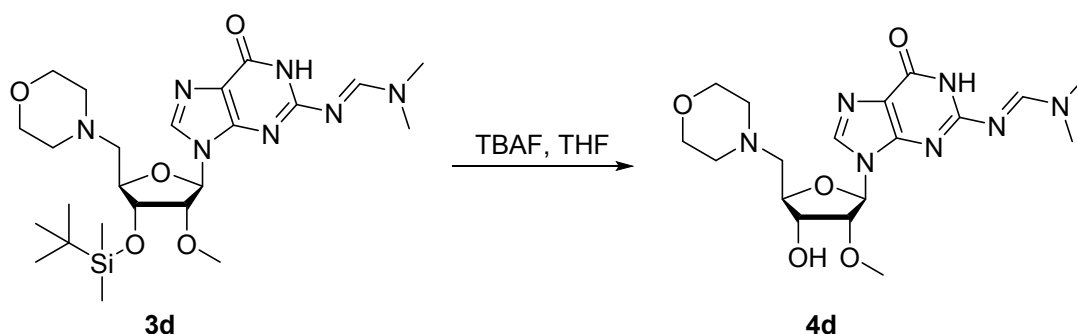
To a solution of nucleoside **3b** (1.3 g, 2.79 mmol) in DMF (10 mL) was added dimethylformamide dimethyl acetal (DMF-DMA, 0.75 mL, 5.60 mmol). The reaction mixture was stirred at 50 °C for 5 h. The solvent was removed at reduced pressure, and the crude was dissolved in THF (6 mL). TBAF (1M in THF, 3.3 mL, 3.3 mmol) was added, and the reaction mixture was stirred at room temperature for 2 h. The solvent was removed at reduced pressure, and the residue was purified by column chromatography using a gradient of 0 – 7% MeOH in CH₂Cl₂ to yield **4b** (0.81 g, 69%) as a white foam. MS (ESI⁺) m/z calcd for C₁₈H₂₈N₇O₄ [M + H]⁺ 406.2197, found 406.2209. ¹H NMR (400 MHz, d6-DMSO) δ 8.90 (s, 1H), 8.47 (s, 1H), 8.42 (s, 1H), 6.02 (d, $J = 5.0$ Hz, 1H), 5.29 (d, $J = 6.0$ Hz, 1H), 4.41 (t, $J = 5.0$ Hz, 1H), 4.31 (q, $J = 5.2$ Hz, 1H), 4.04 – 4.00 (m, 1H), 3.52 (t, $J = 4.4$ Hz, 4H), 3.34 (s, 3H), 3.19 (s, 3H), 3.12 (s, 3H), 2.67 (dd, $J = 13.4, 4.3$ Hz, 1H), 2.54 (dd, $J = 13.4, 7.0$ Hz, 1H), 2.44 – 2.33 (m, 4H). ¹³C (126 MHz, d6-DMSO) δ 159.27, 157.97, 152.00, 151.19, 141.46, 125.68, 85.60, 82.28, 81.50, 70.51, 66.11, 60.39, 57.62, 53.85, 40.63, 34.53.

Synthesis of nucleoside **4c**



Protected nucleoside **3c** (2.35 g, 1.13 mmol) was dissolved in THF (10 mL). To this was added tetra-*n*-butylammonium fluoride (TBAF, 1M in THF, 6.5 mL, 6.5 mmol). The reaction mixture was stirred at room temperature for 1 h. Solvents were removed, and the residue was purified by column chromatography using a gradient of 0–8% MeOH in EtOAc to obtain alcohol **4c** (1.48 g, 80%) as a white foam. MS (ESI⁺) *m/z* calcd for C₂₁H₂₇N₄O₆ [M + H]⁺ 431.1925, found 431.1936. ¹H NMR (500 MHz, d₆-DMSO) δ 11.30 (s, 1H), 8.30 (d, *J* = 7.6 Hz, 1H), 8.04 – 7.94 (m, 2H), 7.62 (t, *J* = 7.4 Hz, 1H), 7.51 (t, *J* = 7.7 Hz, 2H), 7.39 (d, *J* = 7.5 Hz, 1H), 5.84 (d, *J* = 2.0 Hz, 1H), 5.18 (d, *J* = 7.0 Hz, 1H), 3.99 – 3.95 (m, 1H), 3.90 – 3.86 (m, 1H), 3.73 (dd, *J* = 5.0, 2.1 Hz, 1H), 3.58 (t, *J* = 4.7 Hz, 4H), 3.47 (s, 3H), 2.71 (dd, *J* = 13.8, 3.1 Hz, 1H), 2.63 (dd, *J* = 14.0, 6.5 Hz, 1H), 2.56 – 2.41 (m, 4H), δ_c (101 MHz, d₆-DMSO) 167.50, 163.07, 154.13, 145.19, 133.13, 132.70, 129.21, 128.43, 128.40, 96.36, 88.74, 82.81, 81.31, 70.09, 66.24, 59.36, 57.86, 54.12.

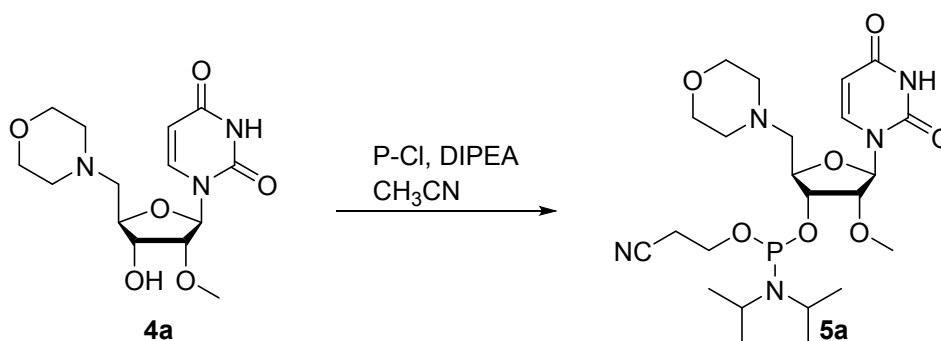
Synthesis of nucleoside 4d



To a solution of **3** (0.63 g, 1.25 mmol) in THF (5 mL) was added tetra-*n*-butylammonium fluoride (TBAF, 1M in THF, 1.5 mL, 1.5 mmol). The reaction mixture was stirred at room temperature for 2 h. The solvent was removed at reduced pressure, and the residue was purified by column chromatography using a gradient of 0 – 8% MeOH in CH₂Cl₂ to yield **4d** (0.46 g, 88%) as a white foam. MS (ESI⁺) *m/z* calcd for C₁₈H₂₈N₇O₅ [M + H]⁺ 422.2146, found 422.2154. ¹H NMR (400 MHz, d₆-DMSO) δ 11.35 (s, 1H), 8.54 (s, 1H), 8.03 (s, 1H), 5.87 (d, *J* = 5.1 Hz, 1H), 5.28 (d, *J* = 5.4 Hz, 1H), 4.24 (dt, *J* = 12.5, 5.0 Hz, 2H), 4.00 – 3.96

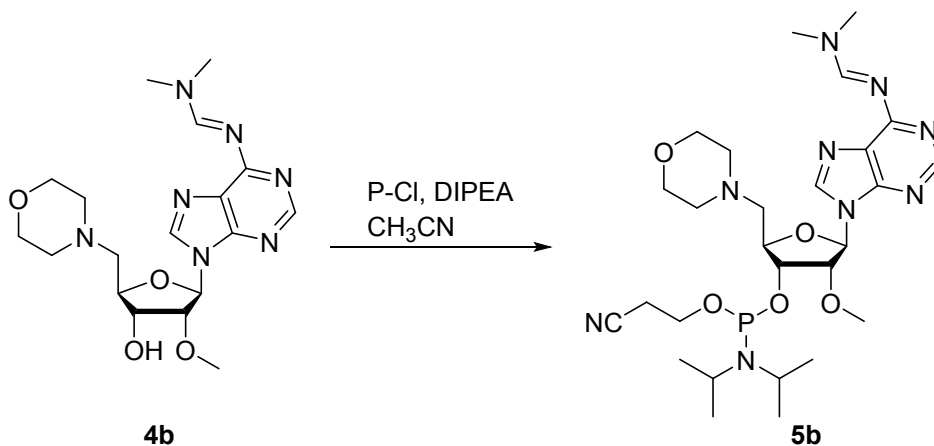
(m, 1H), 3.53 (t, $J = 4.6$ Hz, 4H), 3.34 (s, 3H), 3.15 (s, 3H), 3.03 (s, 3H), 2.65 (dd, $J = 13.3, 4.7$ Hz, 1H), 2.55 – 2.50 (m, 1H), 2.40 (dt, $J = 9.2, 4.9$ Hz, 4H). ^{13}C NMR (126 MHz, $\text{d}_6\text{-DMSO}$) δ 157.87, 157.52, 157.28, 149.79, 136.79, 119.76, 84.84, 82.34, 81.87, 70.52, 66.12, 60.54, 57.55, 53.85, 40.70, 34.67.

Synthesis of nucleoside 5a



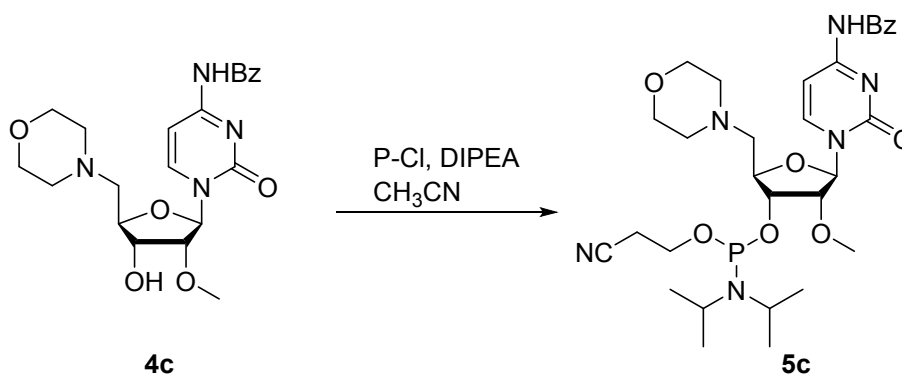
To a solution of **4a** (6.2 gm, 18 mmol) in dry CH_3CN (60 mL) was added ethyl thiotetrazole (2.4 g, 18 mmol). 2-Cyanoethyl N, N, N', N' -tetraisopropylphosphordiamidite (6.8 gm, 22 mmol,) was added slowly to the reaction mixture and stirred at room temperature for 3 h. The reaction mixture was filtered and purified by column chromatography using a gradient of EtOAc in hexanes containing 0.2% triethylamine to yield **5a** (5.0 g, 50%). MS (ESI⁺) m/z calcd for $\text{C}_{23}\text{H}_{39}\text{N}_5\text{O}_7\text{P}$ [$\text{M} + \text{H}$]⁺ 528.2582, found 528.2592. ^{31}P NMR (202 MHz, CD_3CN) δ 151.04, 150.76.

Synthesis of nucleoside 5b

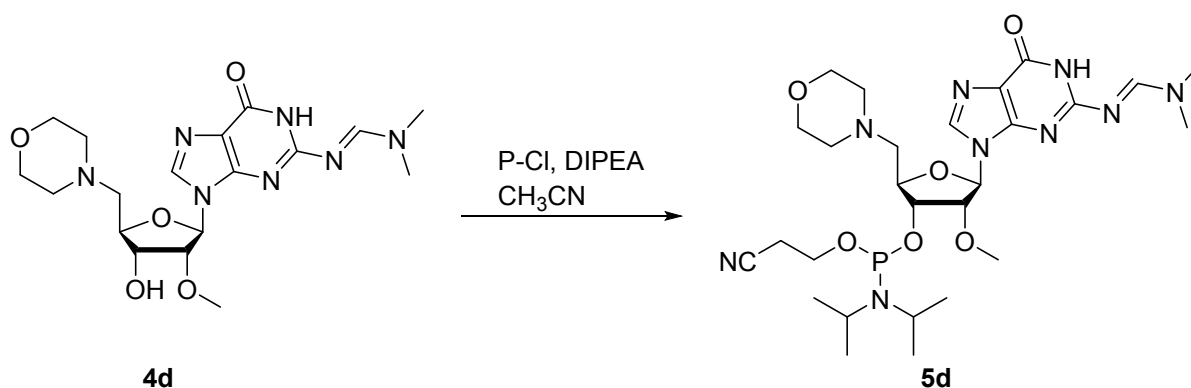


Nucleoside **4b** (0.82 g, 1.35 mmol) was co-evaporated with dry CH₃CN and re-dissolved in dry CH₃CN (6 mL). N, N-diisopropylethylamine (DIPEA, 1.0 g, 7.73 mmol) and 2-cyanoethyl N,N-diisopropylchlorophosphoramidite (P-Cl, 0.95 g, 4.03 mmol) were added, and the reaction mixture was stirred at room temperature for 2 h. The reaction mixture was diluted with CH₂Cl₂ (50 mL) and washed with saturated aqueous NaHCO₃ (20 mL) followed by brine (20 mL). The combined aqueous phase was back extracted with CH₂Cl₂ (20 mL), and the combined organic phase was dried (MgSO₄) and concentrated under reduced pressure. The residue was purified by column chromatography using a gradient of 0 – 3% MeOH in CH₂Cl₂ (containing 0.2% Et₃N) to obtain phosphoramidite **5b** (0.90 g, 73%) as a white foam. MS (ESI⁺) m/z calcd for C₂₇H₄₅N₉O₅P [M + H]⁺ 606.3276, found 606.3286. ³¹P (202 MHz, CD₃CN) δ 151.04, 150.70

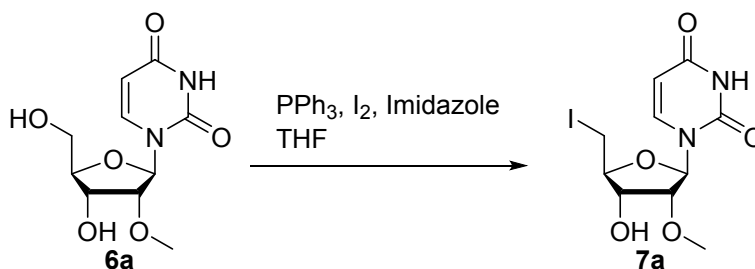
Synthesis of nucleoside **5c**



Nucleoside **4c** (0.50 g, 1.16 mmol) was co-evaporated with dry CH₃CN (5mL) and re-dissolved in dry CH₃CN (5mL). N, N -diisopropylethylamine (DIPEA, 0.60 g, 4.64 mmol) and 2-cyanoethyl N,N-diisopropylchlorophosphoramidite (P-Cl, 0.55 g, 2.32 mmol) were added, and the reaction mixture was stirred at room temperature for 2 h. The solvents were evaporated under reduced pressure, and the crude was purified by column chromatography using a gradient of 0 – 2% MeOH in CH₂Cl₂ (containing 0.2% Et₃N) to obtain phosphoramidite **5c** (0.40 g, 57%) as a white foam. MS (ESI⁺) m/z calcd for C₃₀H₄₄N₆O₇P [M + H]⁺ 631.3004, found 631.3034. ³¹P (202 MHz, CD₃CN) δ 151.25, 150.89.

Synthesis of nucleoside 5d

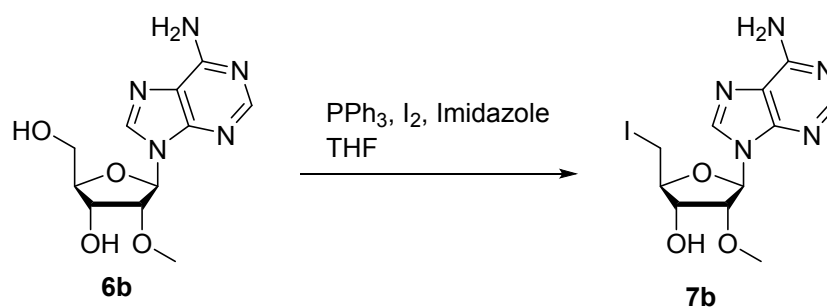
Nucleoside **4d** (0.40 g, 0.95 mmol) was co-evaporated with dry CH_3CN and re-dissolved in dry CH_3CN (5 mL). *N,N*-diisopropylethylamine (DIPEA, 0.60 g, 4.64 mmol) and 2-cyanoethyl *N,N*-diisopropylchlorophosphoramidite (P-Cl, 0.66 g, 2.78 mmol) were added, and the reaction mixture was stirred at room temperature for 2 h. The reaction mixture was diluted with CH_2Cl_2 (50 mL) and washed with saturated aqueous NaHCO_3 (20 mL) followed by brine (20 mL). The combined aqueous phase was back extracted with CH_2Cl_2 (20 mL), and the combined organic phases were dried (MgSO_4) and concentrated under reduced pressure. The residue was purified by column chromatography using a gradient of 0 – 3% MeOH in CH_2Cl_2 (containing 0.2% Et_3N) to obtain phosphoramidite **5d** (460 mg, 77%). MS (ESI⁺) m/z calcd for $\text{C}_{27}\text{H}_{45}\text{N}_9\text{O}_6\text{P}$ [$\text{M} + \text{H}$]⁺ 622.3225, found 622.3240. ³¹P (202 MHz, CD_3CN) δ 151.24, 150.89.

Synthesis of nucleoside 7a

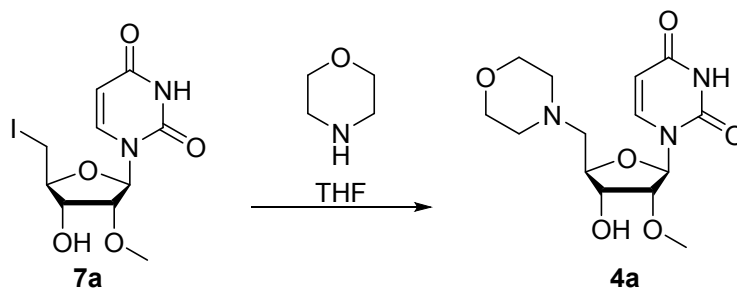
2'-*O*-Methyluridine (**6a**, 2.58 g, 10 mmol), imidazole (1.36 g, 20 mmol), and triphenylphosphine (3.93 g, 15 mmol) were suspended in dry THF (50 mL). To this was added a solution of iodine (3.16 g, 12.5 mmol)

in THF (20 mL) dropwise at 0 °C. The reaction mixture was slowly warmed to room temperature and stirred for another 3 h. The solvent was removed at reduced pressure, and the residue was purified by column chromatography using a gradient of 0 – 7% MeOH in CH₂Cl₂ to afford the desired nucleoside **7a** (3.26 g, 86%) as a pale-yellow foam. MS (ESI⁺) *m/z* calcd for C₁₀H₁₄IN₂O₅ [M + H]⁺ 368.9942, found 368.9951. ¹H NMR (400 MHz, d₆-DMSO) δ 11.40 (d, *J* = 2.1 Hz, 1H), 7.67 (d, *J* = 8.1 Hz, 1H), 5.85 (d, *J* = 5.4 Hz, 1H), 5.68 (dd, *J* = 8.1 Hz, 2.2 Hz, 1H), 5.44 (d, *J* = 6.0 Hz, 1H), 4.04 – 4.00 (m, 1H), 3.97 (t, *J* = 5.4 Hz, 1H), 3.88 – 3.79 (m, 1H), 3.54 (dd, *J* = 10.6 Hz, 5.4 Hz, 1H), 3.39 (dd, *J* = 10.6 Hz, 6.8 Hz, 1H), 3.33 (s, 3H). ¹³C NMR (101 MHz, d₆-DMSO) δ 162.87, 150.41, 140.86, 102.31, 86.70, 83.31, 81.22, 71.44, 57.60, 7.23.

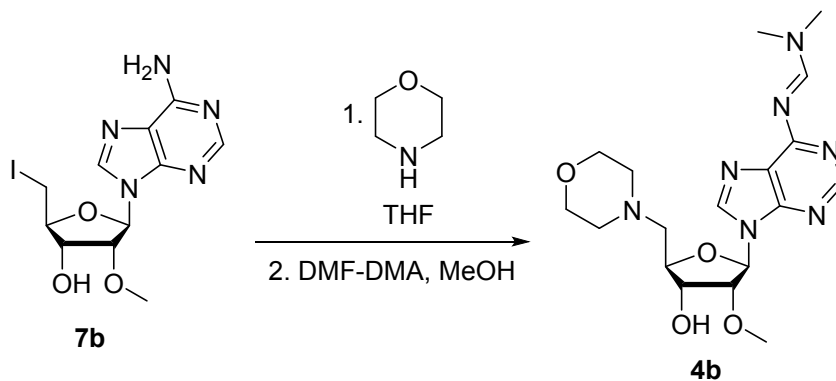
Synthesis of nucleoside **7b**



Nucleoside **6b** (1.44 g, 5.0 mmol), imidazole (0.70 g, 10.0 mmol) and triphenylphosphine (2.00 g, 7.5 mmol) were suspended in dry THF (30 mL). To this was added a solution of iodine (1.60 g, 6.3 mmol) in THF (10 mL) dropwise at 0 °C. The reaction mixture was slowly warmed to room temperature and stirred for another 3 h. The solvent was removed at reduced pressure, and the residue was purified by column chromatography using a gradient of 0 – 8% MeOH in CH₂Cl₂ to afford the nucleoside **7b** (1.60 g, 82%) as an amorphous solid. MS (ESI⁺) *m/z* calcd for C₁₁H₁₅IN₅O₃ [M + H]⁺ 392.0214, found 392.0222. ¹H NMR (400 MHz, d₆-DMSO) δ 8.37 (s, 1H), 8.15 (s, 1H), 7.32 (s, 2H), 6.02 (d, *J* = 5.9 Hz, 1H), 5.54 (d, *J* = 5.5 Hz, 1H), 4.59 (t, *J* = 5.4 Hz, 1H), 4.38 – 4.34 (m, 1H), 4.02 – 3.98 (m, 1H), 3.60 (dd, *J* = 10.5, 5.9 Hz, 1H), 3.47 (dd, *J* = 10.4, 7.0 Hz, 1H), 3.31 (s, 3H, OCH₃). ¹³C NMR (126 MHz, d₆-DMSO) 156.12, 152.78, 149.27, 139.80, 119.11, 85.58, 84.42, 81.45, 71.45, 57.63, 7.52. Note: The compound was found to be unstable in solution. NMR samples were prepared at the time of the experiment.

Alternative synthesis of nucleoside 4a

5'-Iodo-2'-*O*-methyluridine **7a** (1.0 g, 2.71 mmol) was dissolved in THF (5 mL). Morpholine (5 mL) was added, and the reaction mixture was stirred at room temperature for 16 h. A white solid precipitated during this period. The solid was removed by filtration and washed with CH₂Cl₂ (50 mL). The filtrate was purified by column chromatography using a gradient of 0 – 8% MeOH in CH₂Cl₂ to afford the nucleoside **4a** (0.55 g, 62%) as a white powder.

Alternative synthesis of nucleoside 4b

Nucleoside **7b** (1.0 g, 2.55 mmol) was dissolved in THF (5 mL) and morpholine (5 mL). The reaction mixture was then stirred for 2 days at room temperature. A white solid precipitated. The solid was removed by filtration, washed with CH₂Cl₂ (50 mL), and purified by column chromatography using a gradient of 0 – 8% MeOH in CH₂Cl₂ to obtain white solid (0.7 g). The solid was dissolved in dry MeOH (6 mL) and to this solution was added dimethylformamide dimethyl acetal (DMF-DMA, 0.80 g, 6.7 mmol). The resulting

solution was stirred for 16 h at room temperature. The solvents were removed, and the crude was purified by column chromatography using a gradient of 0 – 7% MeOH in CH₂Cl₂ to afford nucleoside **4b** (550 mg, 48% over 2 steps) as a white solid material.

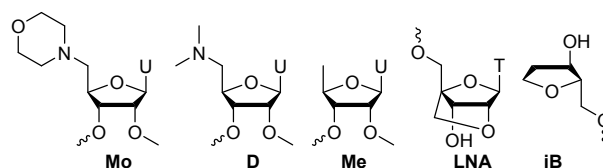
1.3 Oligonucleotide synthesis

Oligonucleotides were synthesized on a Mermade 192 synthesizer using universal or custom supports following protocol described by Schlegel et al.² A solution of 0.25 M 5-(*S*-ethylthio)-1*H*tetrazole in acetonitrile was used as the activator. The phosphoramidite solutions were 0.10 M in anhydrous acetonitrile or 9:1 acetonitrile:DMF (2'-OMe-C, 2'-OMe-A and 2'-OMe-G). The oxidizing reagent was 0.02 M I₂ in THF/pyridine/H₂O. *N,N*-Dimethyl-*N'*-(3-thioxo-3*H*-1,2,4-dithiazol-5-yl)methanimidamide (DDTT), 0.1 M in pyridine, was used as the sulfurizing reagent. The detritylation reagent was 3% dichloroacetic acid (DCA) in CH₂Cl₂. After trityl-off synthesis, oligonucleotides were removed from solid support by incubating the columns with 40% aqueous methylamine (150 μL for 30 min). A very light vacuum was applied to drain the solution into a plate, and procedure was repeated. The plate containing combined solution was shaken for 1h at room temperature whereupon a cold mixture of acetonitrile:EtOH (1.2 mL) was added, and the plate was left at –20 °C for 16h. This resulted in precipitation of oligonucleotides which were then recovered by centrifuging the plate at 3000 rpm at 4 °C for 45 minutes. The supernatant was removed and the pellets were dissolved in 20 mM aqueous NaOAc. The oligonucleotides were then desalted using GE Hi-trap desalting column using water as eluent. The oligonucleotides were identified by using HPLC-MS and were obtained in purity of ≥80%. Hybridization to generate siRNA duplexes was performed by mixing equimolar amounts of complementary strands in 1×PBS buffer, pH 7.4, and by heating in an over at 100 °C for 45 min followed by slow cooling to room temperature.

Table S1: Mass spec analysis of modified oligonucleotides

Entry	siRNA	siRNA duplex	Mass	
			calculated	found
1	Parent	5'-U•g•UgAcAaAUuGgGcAuCaA-GalNAc ₃ 5'-u•U•gAuGcCcAuauUuGuCaCa•a•a	8715.3 7531.9	8714.0 7530.7
2	S5'-Mo	5'-Mo•g•UgAcAaAUuGgGcAuCaA-GalNAc ₃ 5'-u•U•gAuGcCcAuauUuGuCaCa•a•a	8797.5 7531.9	8794.9 7530.6

3	S5'-D	5'-D•g•UgAcAaAUuGgGcAuCaA-GalNAc ₃ 5'-u•U•gAuGcCcAuauUuGuCaCa•a•a	8755.4 7531.9	8752.6 7531.0
4	S5'-Me	5'-Me•g•UgAcAaAUuGgGcAuCaA-GalNAc ₃ 5'-u•U•gAuGcCcAuauUuGuCaCa•a•a	8712.4 7531.9	8709.8 7530.5
5	S5'-LNA	5'-LNA•g•UgAcAaAUuGgGcAuCaA-GalNAc ₃ 5'-u•U•gAuGcCcAuauUuGuCaCa•a•a	8739.4 7531.9	8737.9 7530.9
6	S5'-iB	5'-iBU•g•UgAcAaAUuGgGcAuCaA-GalNAc ₃ 5'-u•U•gAuGcCcAuauUuGuCaCa•a•a	8895.4 7531.9	8893.6 7530.7
7	AS5'-Mo	5'-U•g•UgAcAaAUuGgGcAuCaA-GalNAc ₃ 5'-Mo•U•gAuGcCcAuauUuGuCaCa•a•a	8715.3 7602.0	8713.9 7599.2
8	AS5'-D	5'-U•g•UgAcAaAUuGgGcAuCaA-GalNAc ₃ 5'-D•U•gAuGcCcAuauUuGuCaCa•a•a	8715.3 7560.0	8714.0 7557.9
9	AS5'-Me	5'-U•g•UgAcAaAUuGgGcAuCaA-GalNAc ₃ 5'-Me•U•gAuGcCcAuauUuGuCaCa•a•a	8715.3 7516.9	8713.9 7514.3
10	AS5'-LNA	5'-U•g•UgAcAaAUuGgGcAuCaA-GalNAc ₃ 5'-LNA•U•gAuGcCcAuauUuGuCaCa•a•a	8715.3 7543.9	8713.8 7542.6
11	AS5'-iB	5'-U•g•UgAcAaAUuGgGcAuCaA-GalNAc ₃ 5'-iBU•U•gAuGcCcAuauUuGuCaCa•a•a	8715.3 7711.9	8713.8 7709.8
12	S/As-5'-Mo	5'-Mo•g•UgAcAaAUuGgGcAuCaA-GalNAc ₃ 5'-Mo•U•gAuGcCcAuauUuGuCaCa•a•a	8795.5 7602.0	8794.9 7599.2



Structure of modifications: 5'-deoxy-5'-morpholino-2'-O-methyl uridine (**Mo**), 5'-deoxy-5'-dimethylamino-2'-O-methyl uridine (**D**), 5'-deoxy-2'-O-methyl uridine (**Me**), locked nucleic acid (**LNA**), and inverted abasic site (**iB**).

1.4 *In vitro* RNAi activity

To 5 μL of siRNA in each well of a 384-well collagen-coated plate were added 4.9 μL of Opti-MEM and 0.1 μL of Lipofectamine RNAiMax (Invitrogen). The final siRNA concentrations were 0.1 or 10 nM. Plates were incubated at room temperature for 15 min, and 40 μL of William's E Medium (Life Technologies) containing $\sim 5 \times 10^3$ primary mouse hepatocytes cells were added. Each condition was assessed in quadruplicate. Cells were incubated for 24 h prior to RNA purification. RNA was isolated with DynaBeads (ThermoFisher), and reverse transcribed into cDNA according to manufacturer's protocol (Applied Biosystems). Multiplex qPCR reactions were performed in duplicate using a gene-specific TaqMan assay for *apob* (ThermoFisher Scientific, #Mm01545156_m1) and mouse *Gapdh* (#4352339E) as an endogenous

control. Real-Time PCR was performed on a Roche LightCycler 480 using LightCycler 480 Probes Master Mix (Roche). Data were analyzed using the $\Delta\Delta C_t$ method, normalizing *apob* expression to *Gapdh*, followed by normalization to the average of the control siRNA-transfected wells. Data were expressed as mean log difference from cells treated with the parent siRNA. Various designs were compared to parent design by multiple linear regression using the software package R.

1.5 Quantification of whole liver and Ago2-associated siRNA levels

Mice ($n=3$ per group) were sacrificed on days 3, 7, and 15 post-dose, and livers were snap-frozen in liquid nitrogen and ground into powder for downstream analysis. Total siRNA liver levels and Ago2-bound siRNA were measured by SL-qPCR based on previously published methods.¹ For SL-qPCR of *apob*-targeting siRNAs, the following probes and primers were used: sense stem loop primer 5'-GTCGTATCCAGTGCAGGGTCCGAGGTATTCGCACTGGATACGACTGATGCCCAT-3', sense forward primer 5'-gccgcgctGTGACAAATATG-3', sense probe 5'-CTGATACGACTGATGCC-3', antisense stem loop primer 5'-GTCGTATCCAGTGCAGGGTCCGAGGTATTCGCACTGGATACGACTTTGTGACAA-3', antisense forward primer 5'-gccgcgctTGATGCCCAT-3', antisense probe 5'-CTGATACGACTTTGTGAC-3', and universal reverse primer 5'-GTGCAGGGTCCGAGGT-3'.

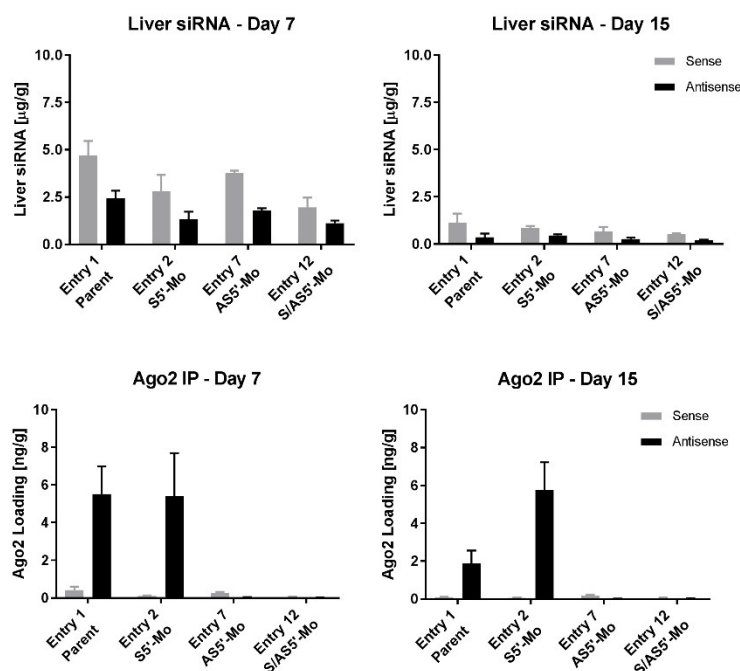


Figure S1. Mice (n=3 per group) were treated with a single dose of 3 mg/kg parent, AS5'-Mo, S5'-Mo, or S/AS5'-Mo siRNAs targeting *apob*. Cohorts of mice were sacrificed at 3, 7, and 15 days post-dose, and liver lysates were generated. (A) Liver levels of the antisense and passenger strand of siRNAs were quantified by RT-qPCR. (B) Ago2 was immunoprecipitated, and Ago2-bound antisense (antisense) and passenger (sense) strand levels were quantified by RT-qPCR.

1.6 *In vivo* RNAi activity targeting *FIX* gene

Table S2. siRNAs targeting *FIX* gene

Entry	siRNA	siRNA duplex
1	Parent	5'-u•g•gaagCfaGfUfAfuguugaugga-GalNAC ₃ 5'- u•Cf•cauCfaAfCfauacUfgCfuucca•a•a
2	S5'-Mo	5'- Mo u•g•gaagCfaGfUfAfuguugaugga- GalNAC ₃ 5'- u•Cf•cauCfaAfCfauacUfgCfuucca•a•a
3	AS5'-Mo	5'-u•g•gaagCfaGfUfAfuguugaugga-GalNAC ₃ 5'- Mo u•Cf•cauCfaAfCfauacUfgCfuucca•a•a

Abbreviations and symbols: S, sense strand; AS, antisense strand; Mo, morpholino; uppercase, 2'-F; lowercase, 2'-OMe; •, phosphorothioate; GalNAC₃, hydroxypropyl trivalent N-acetyl-galactosamine ligand.

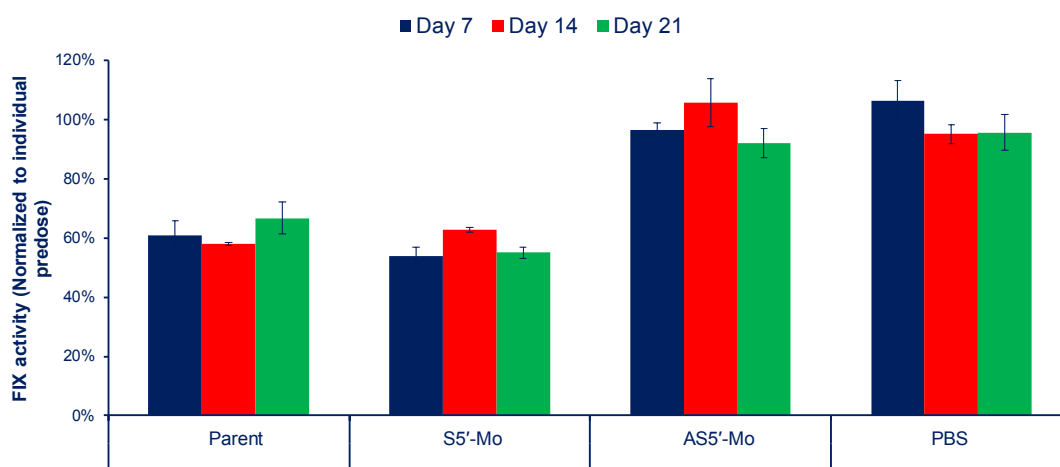
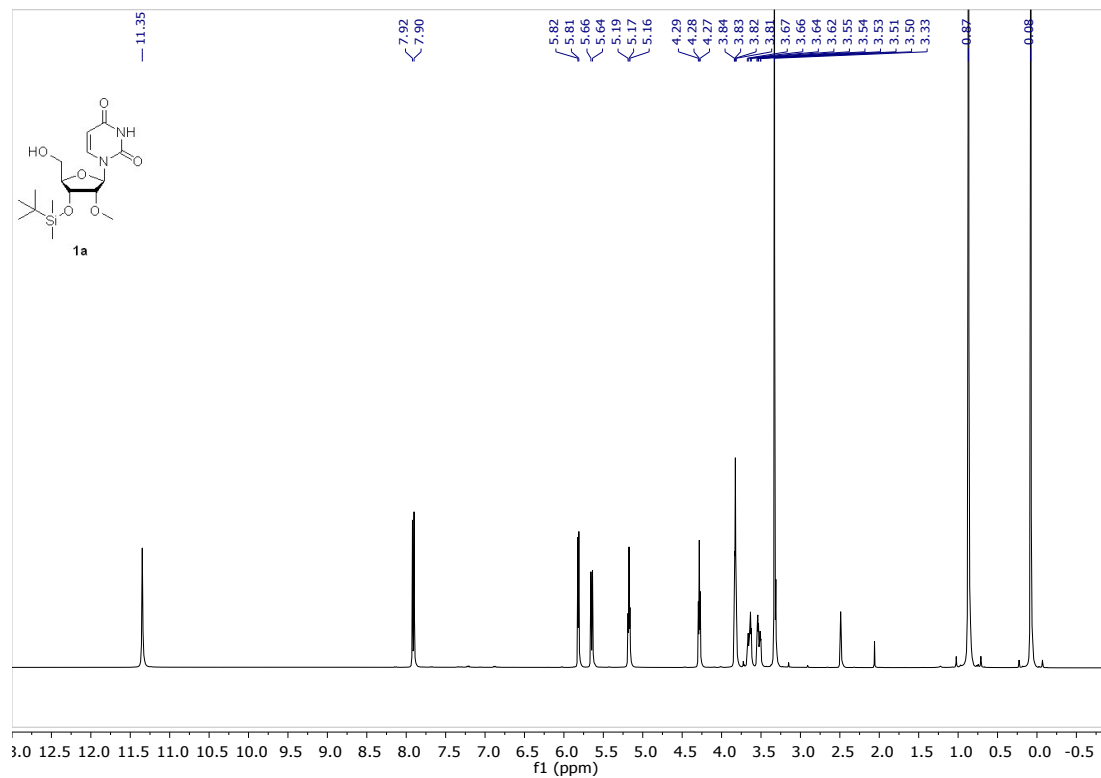
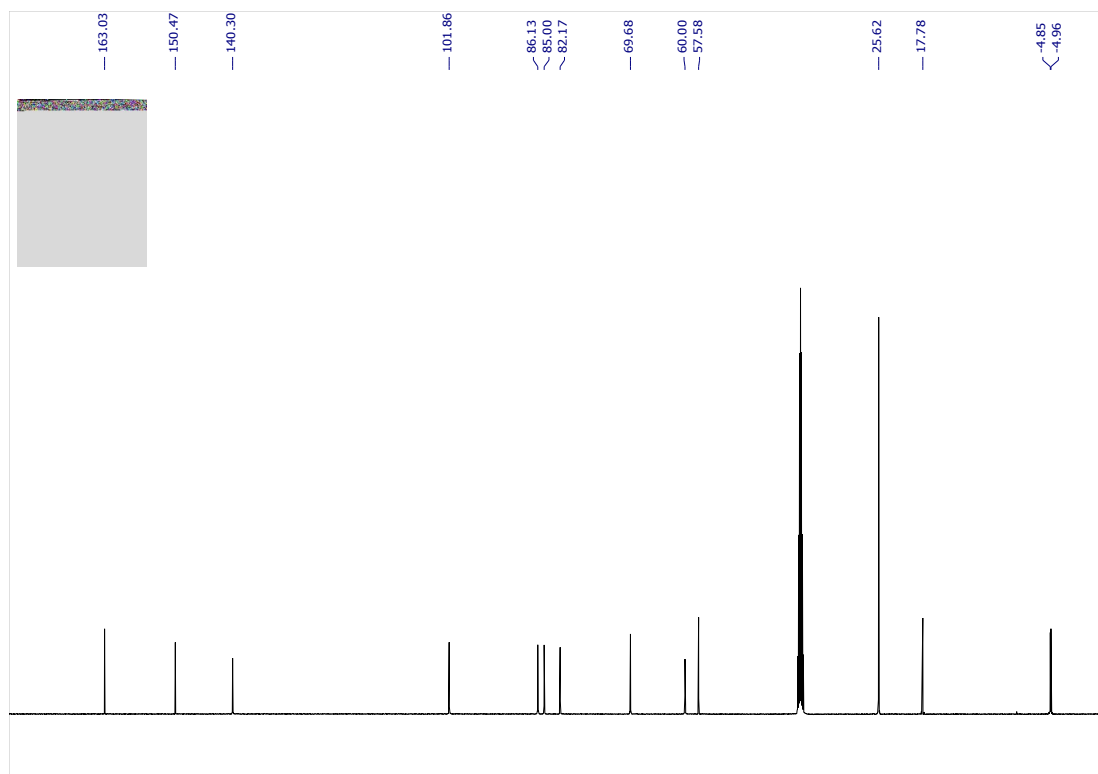
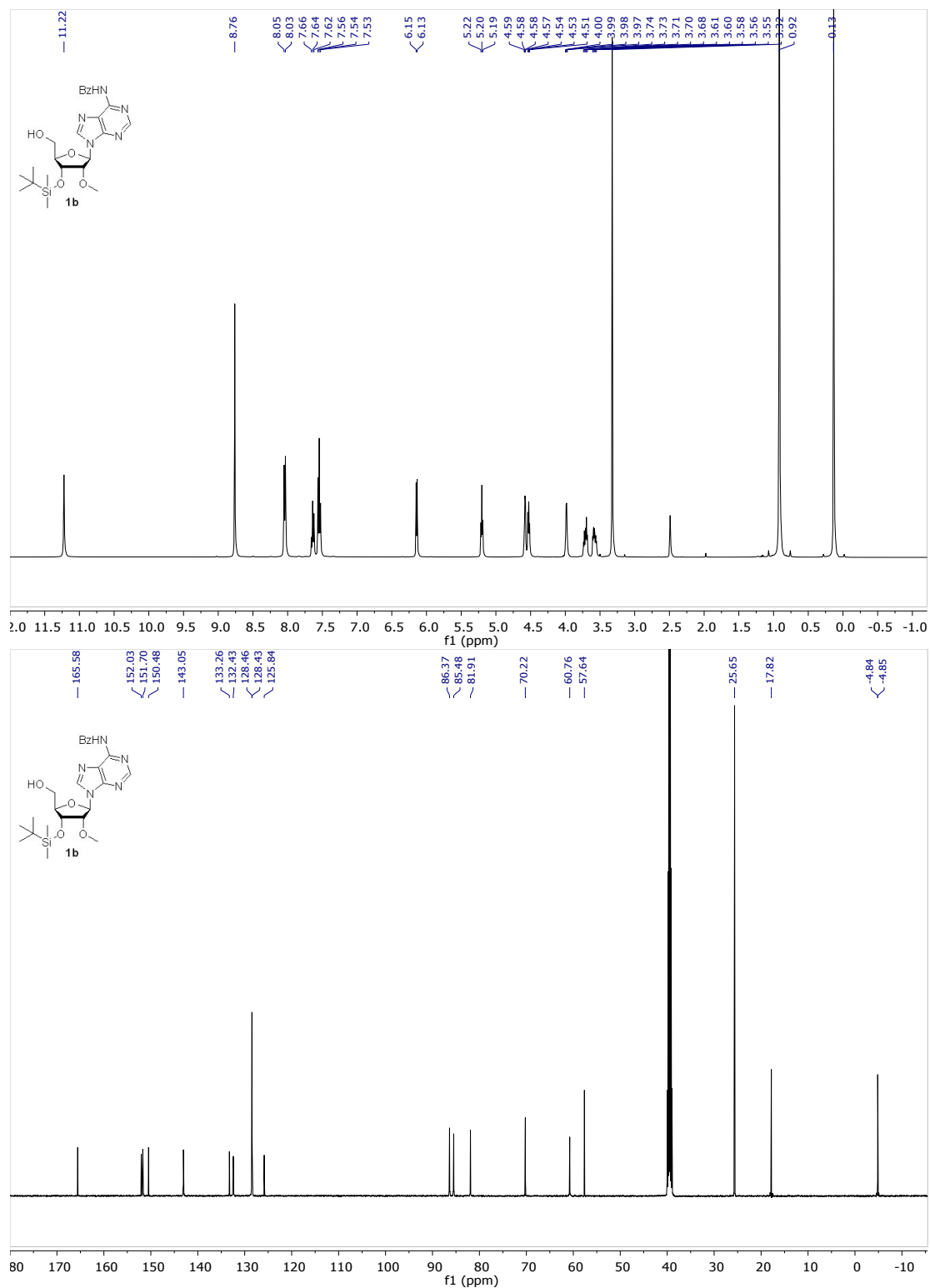


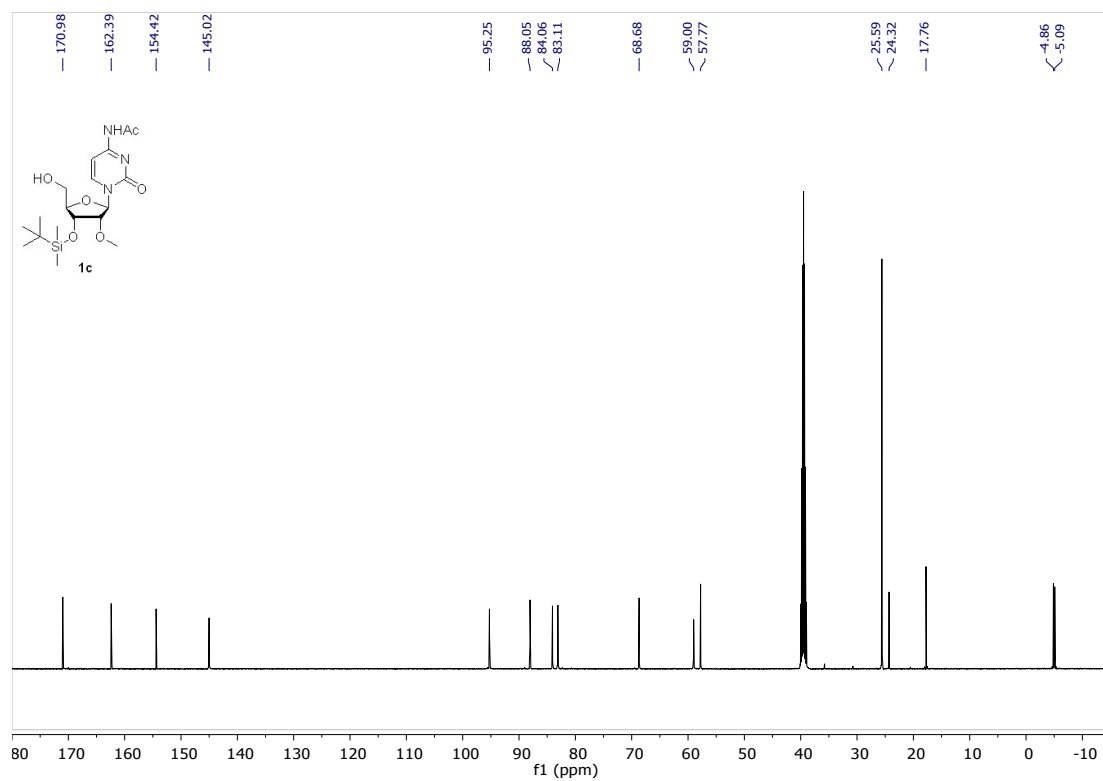
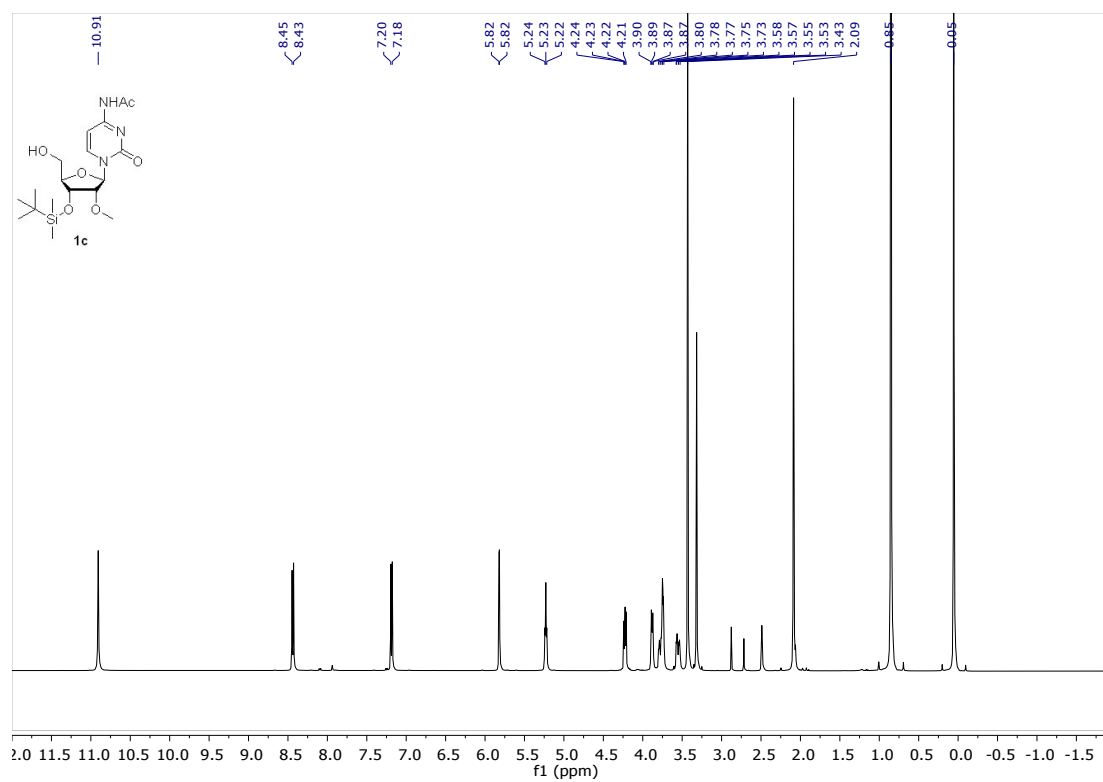
Figure S2: Serum FIX levels in mice on days 7 (blue), 14 (red), and 21 (green) following a single subcutaneous 1 mg/kg dose of indicated siRNAs (Table S2). FIX levels were normalized to the individual pre-dose values. The experiments were conducted as described in literature.³

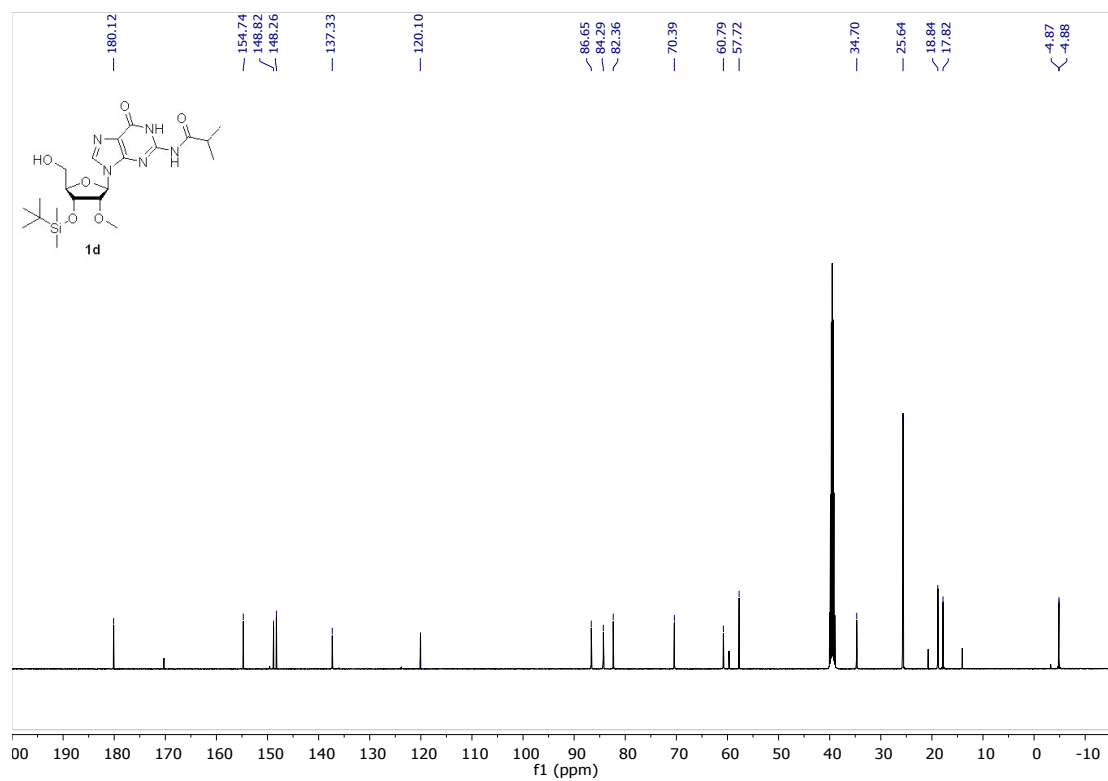
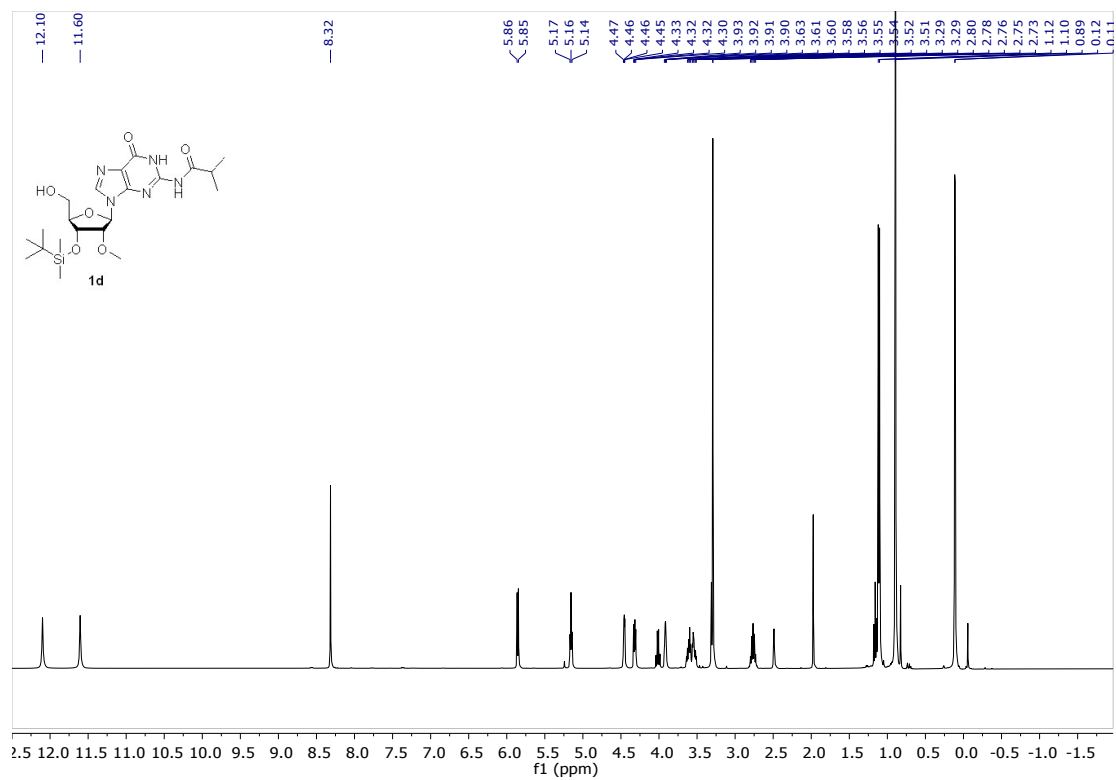
1.7 Representative NMR spectra

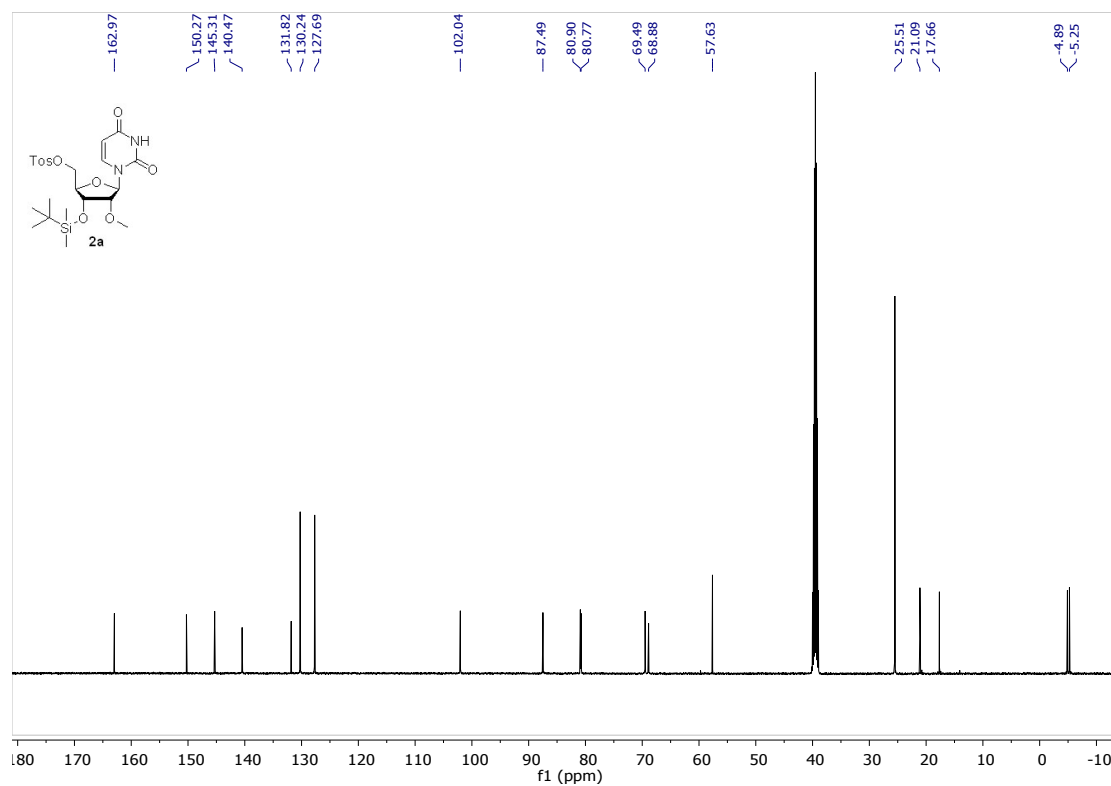
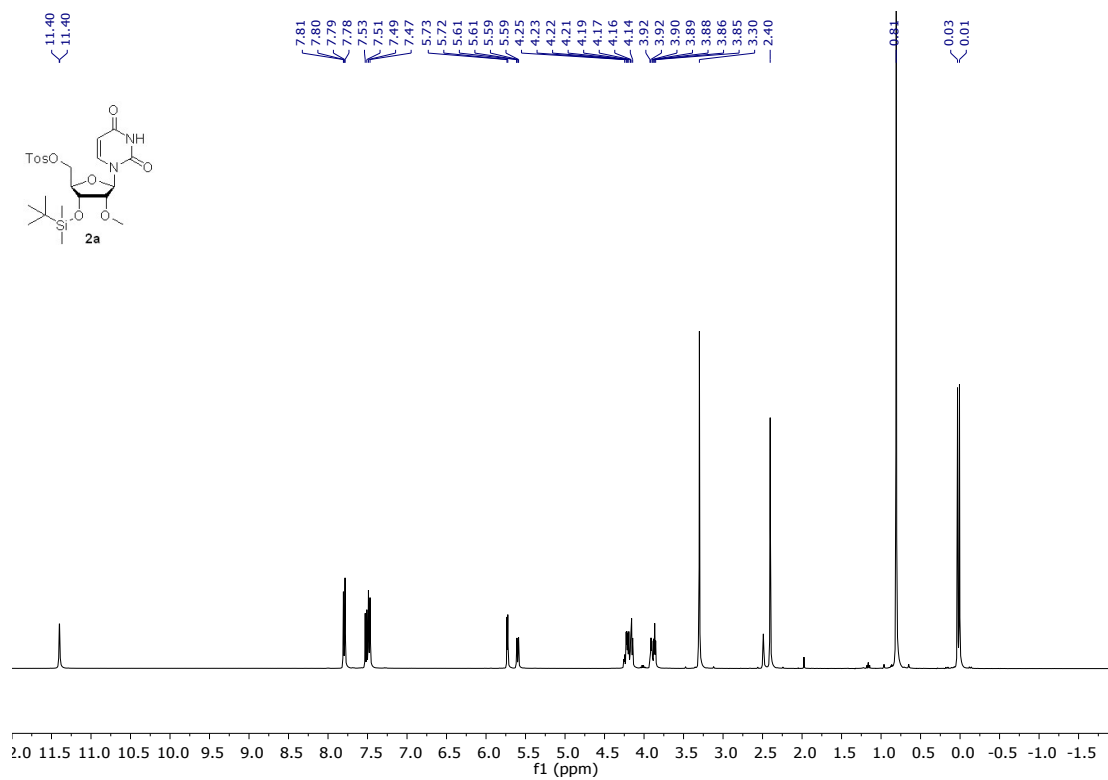


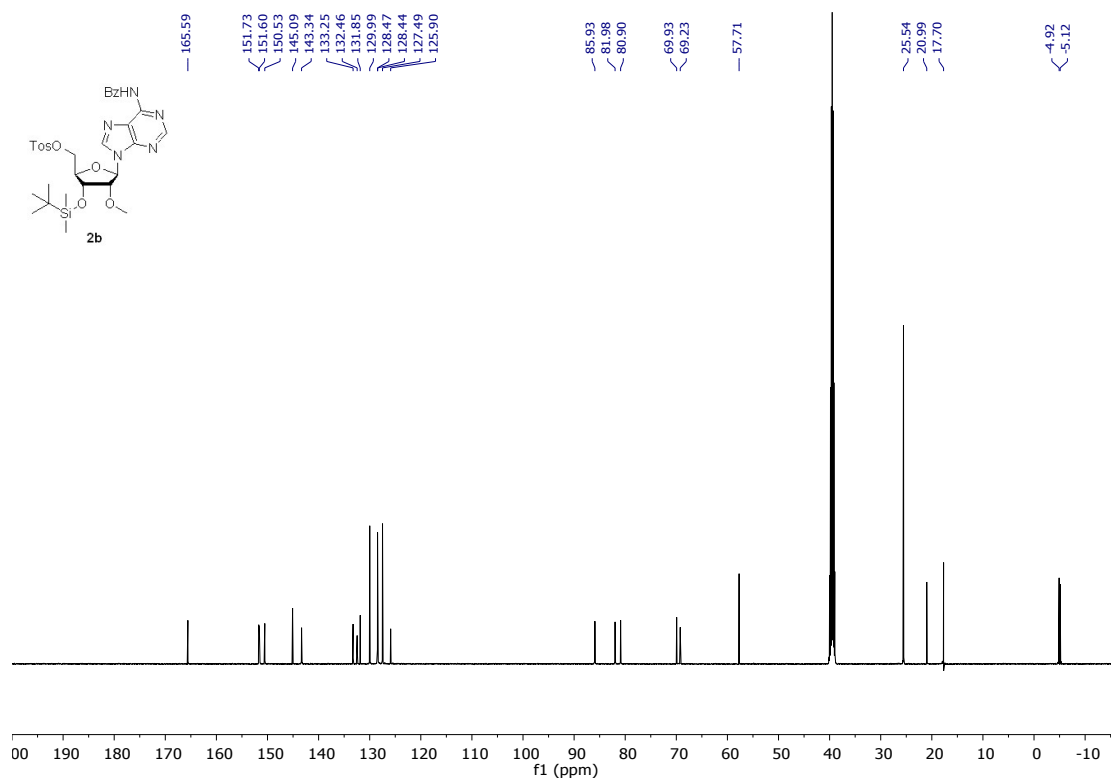
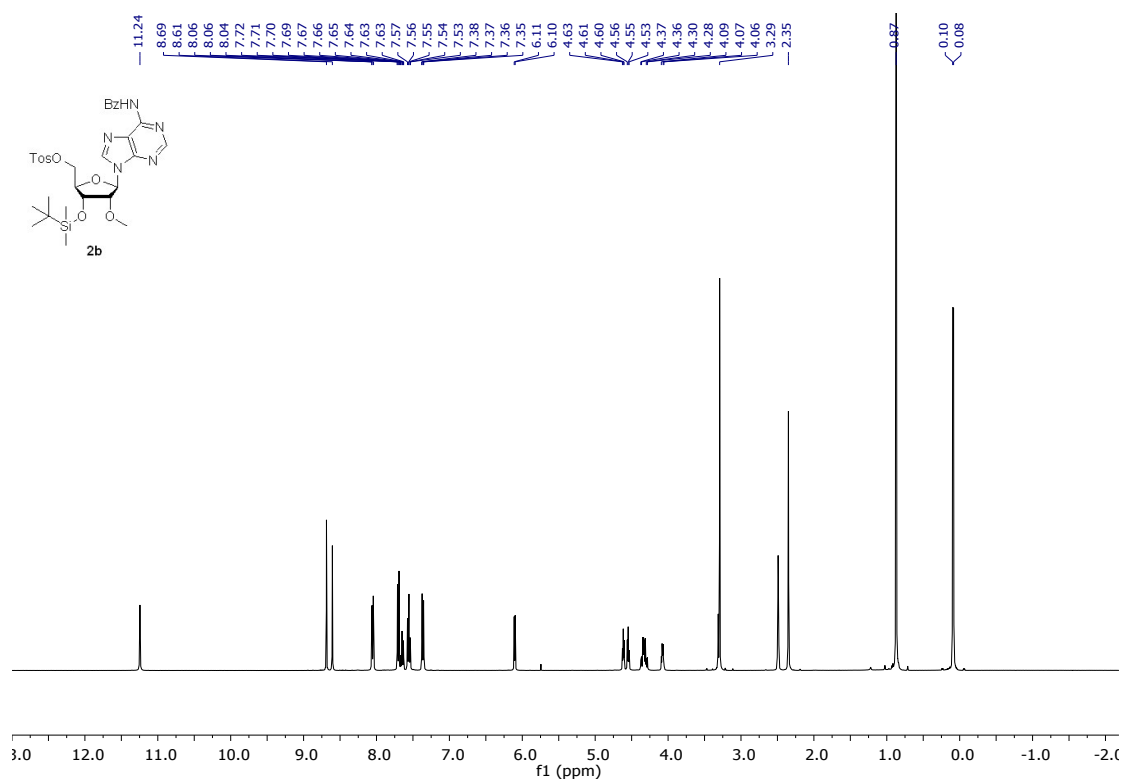


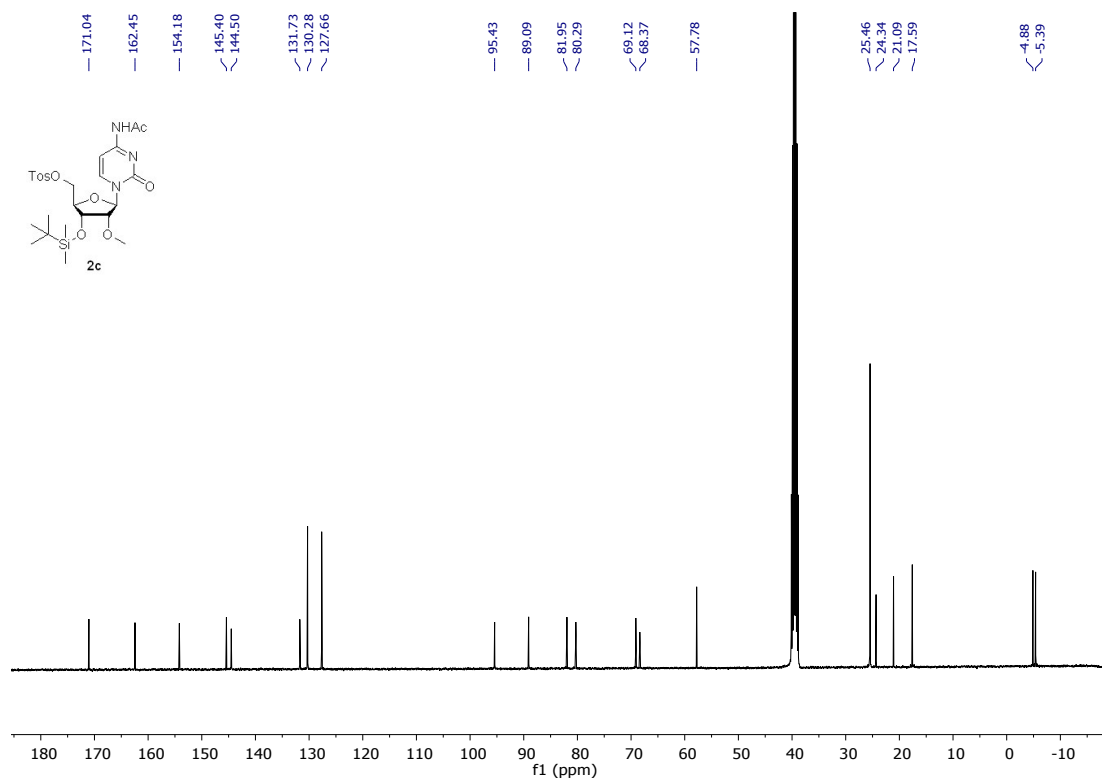
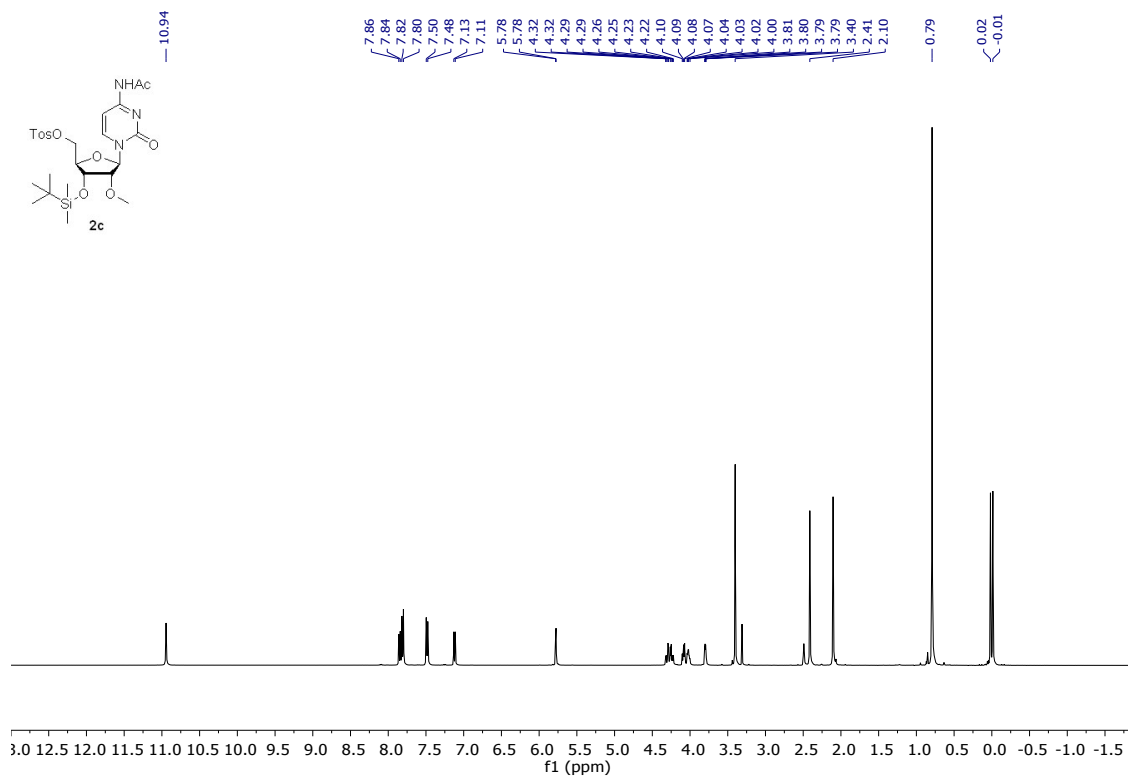


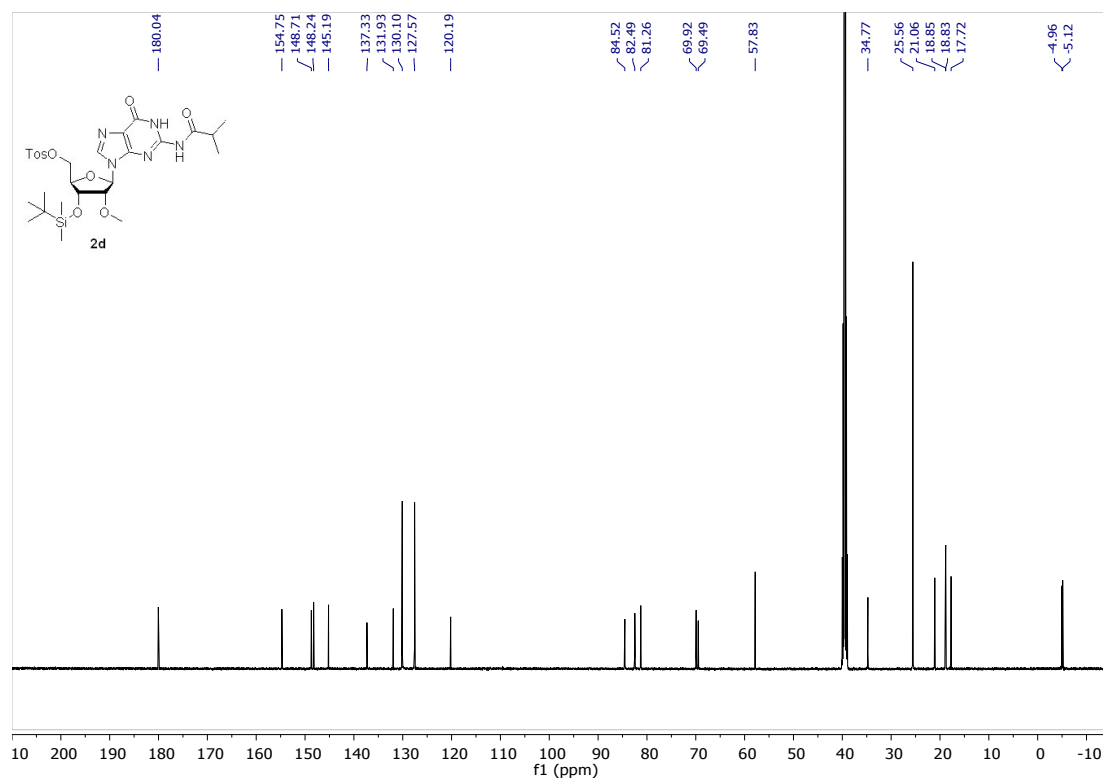
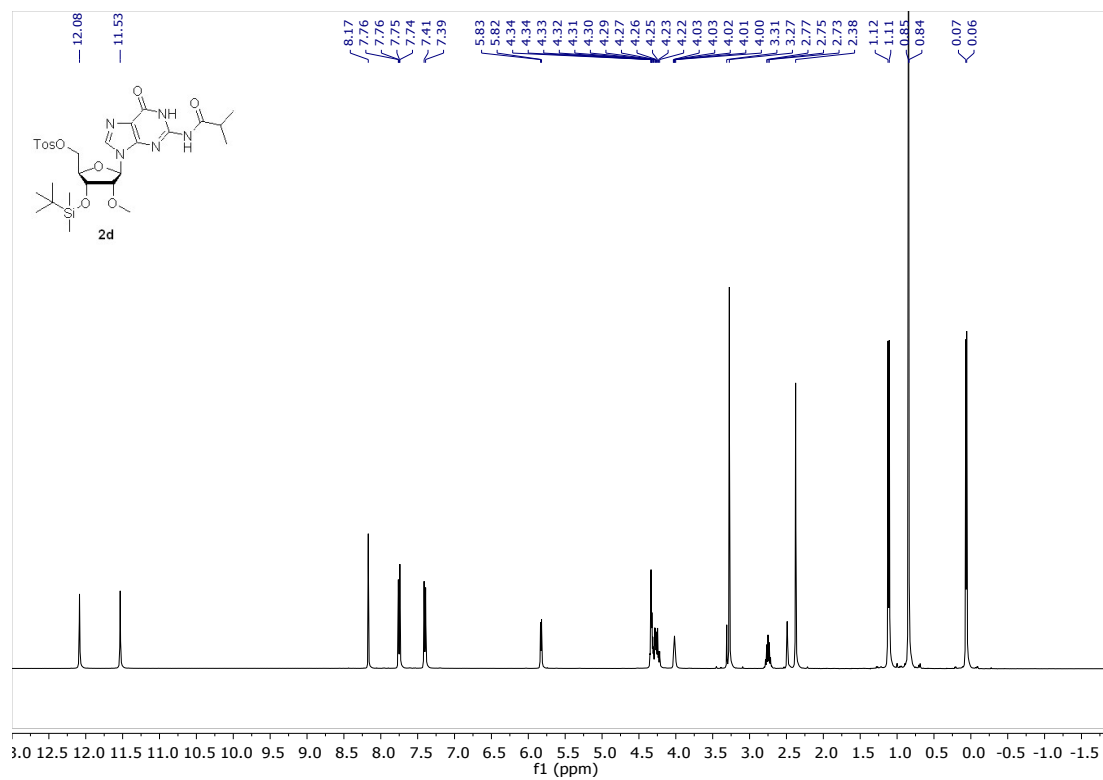


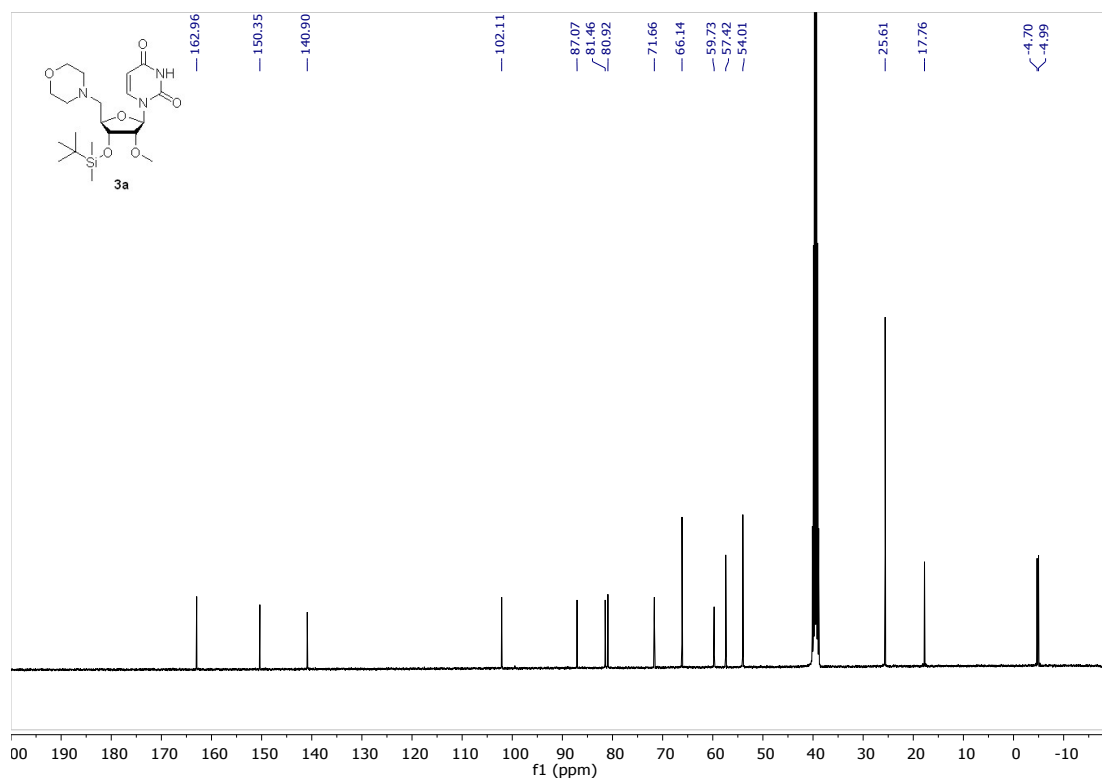
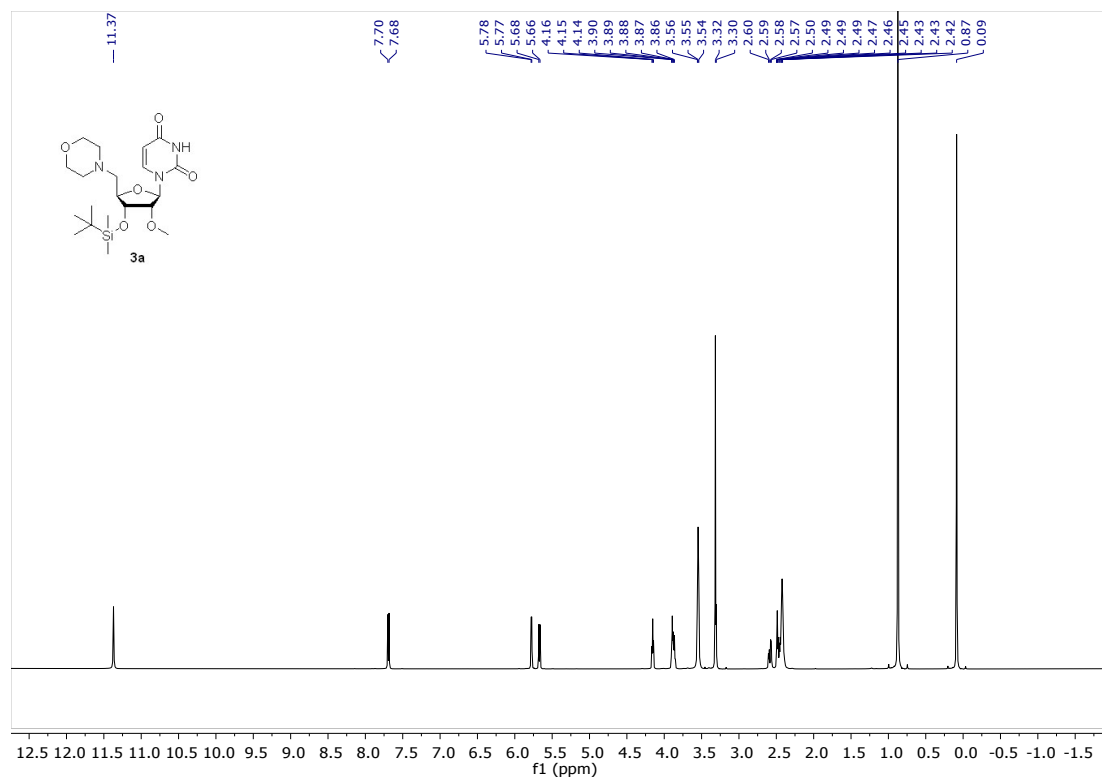


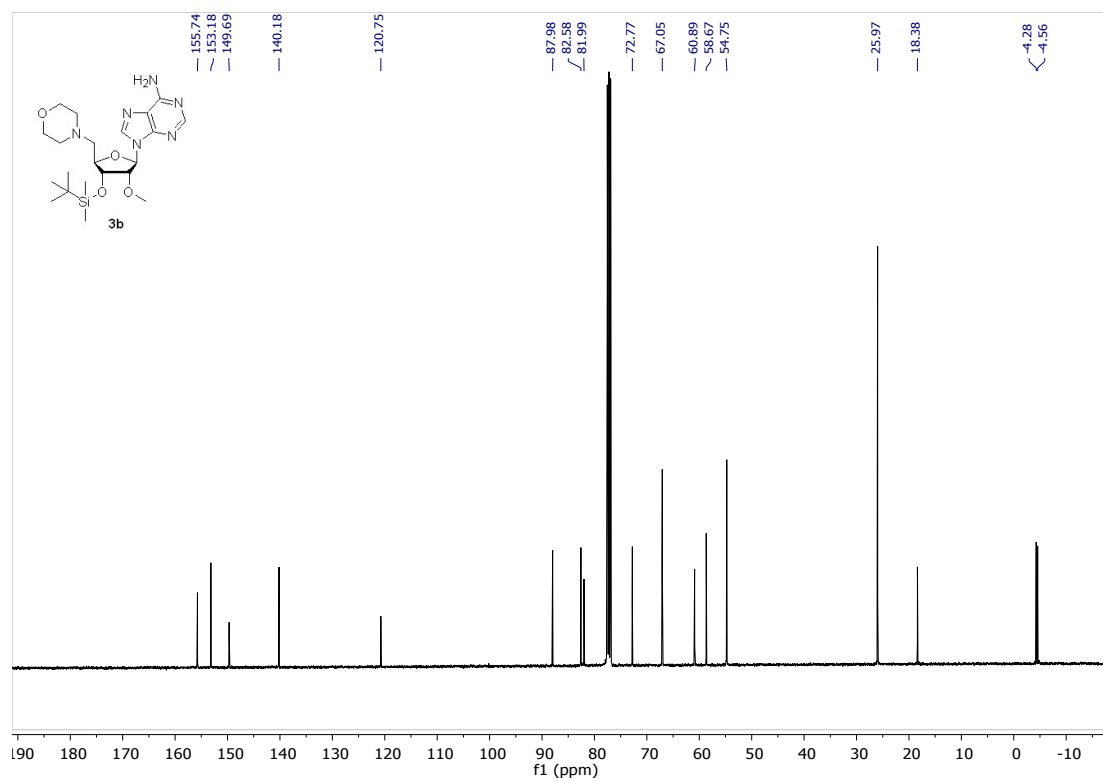
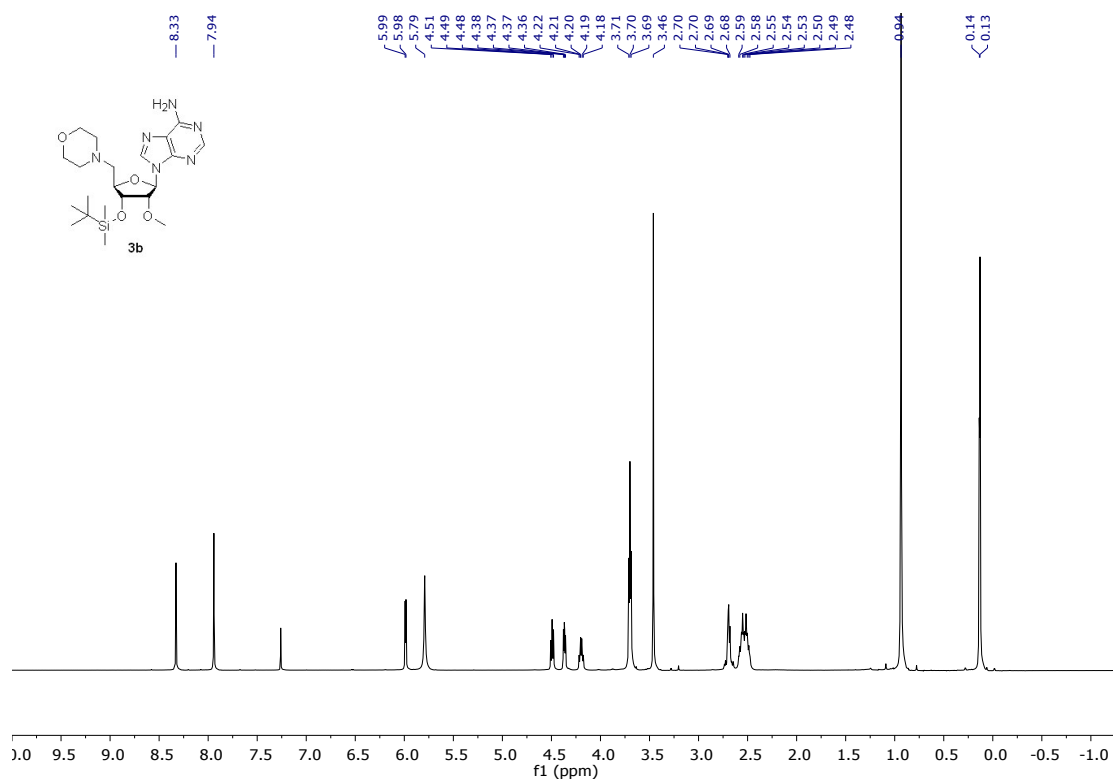


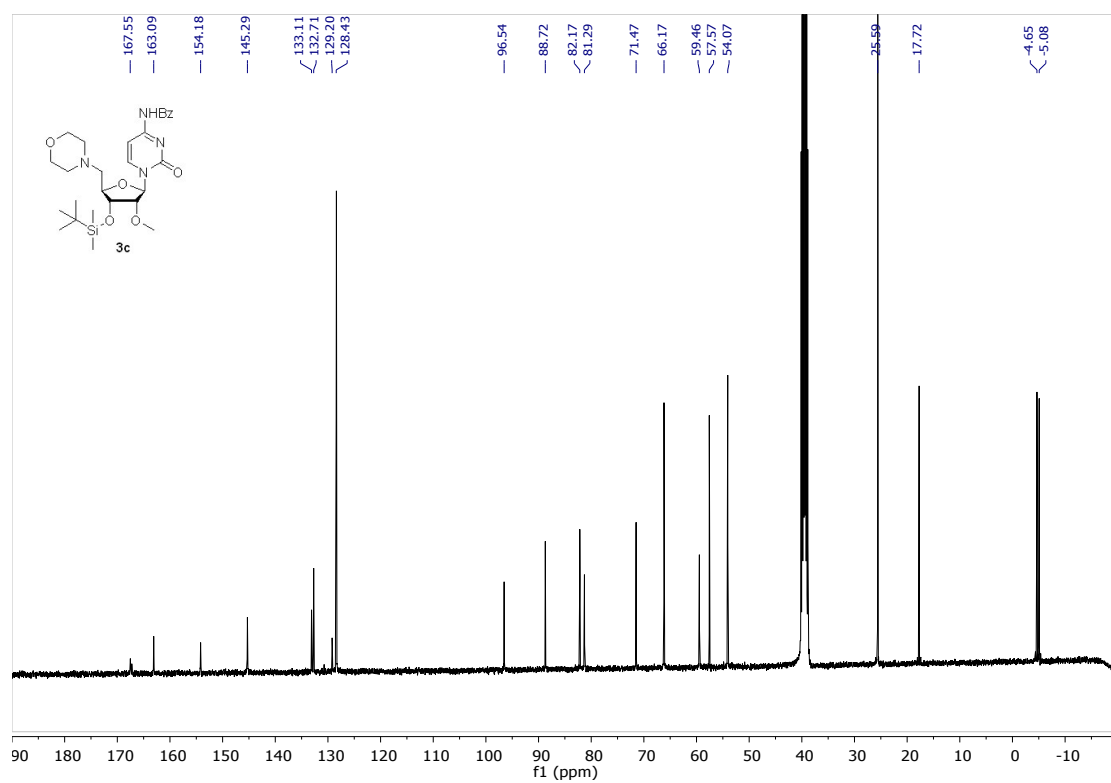
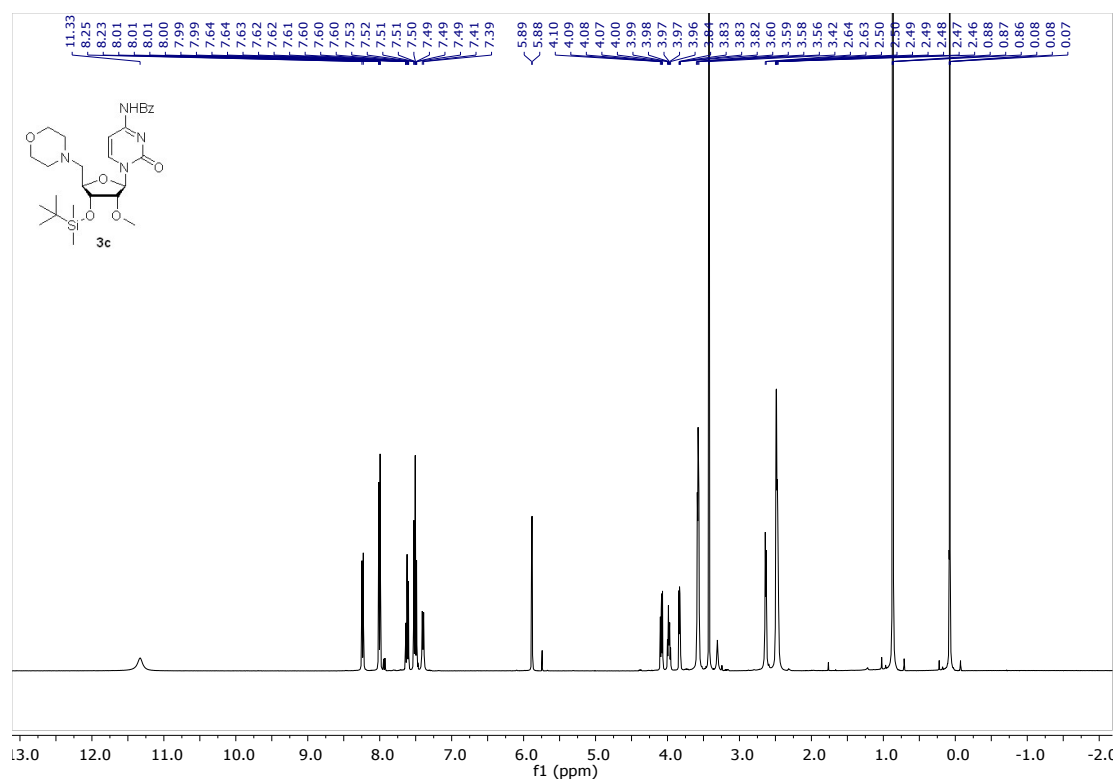


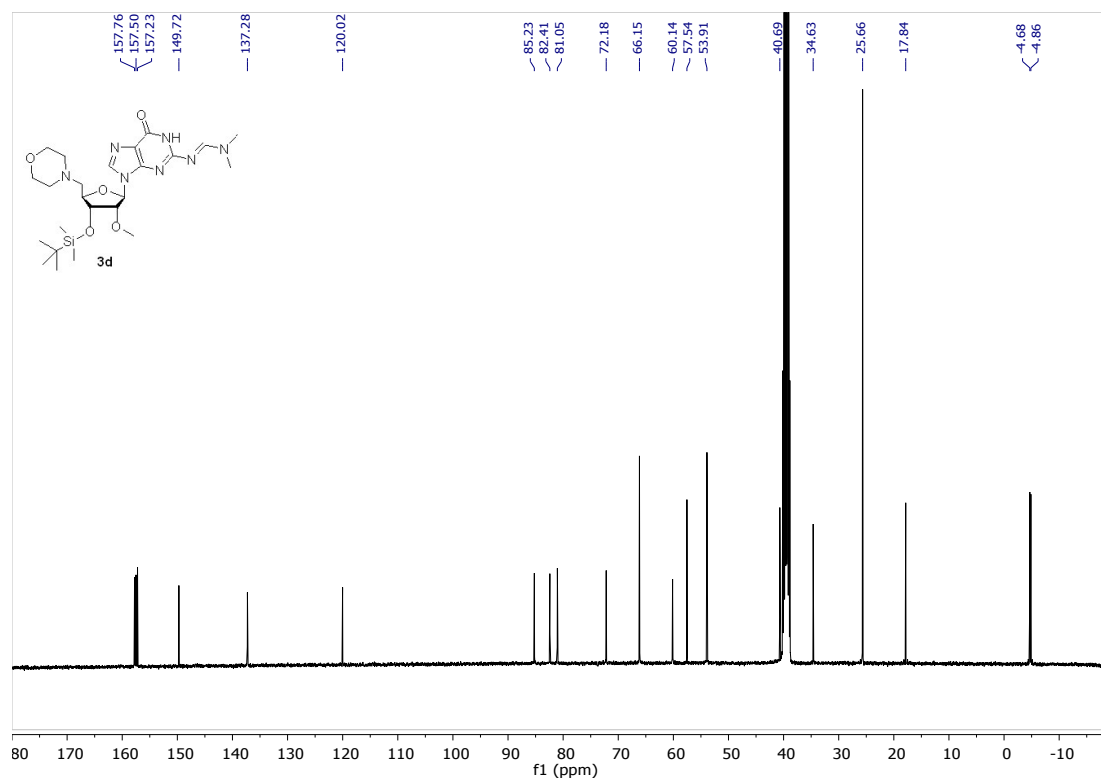
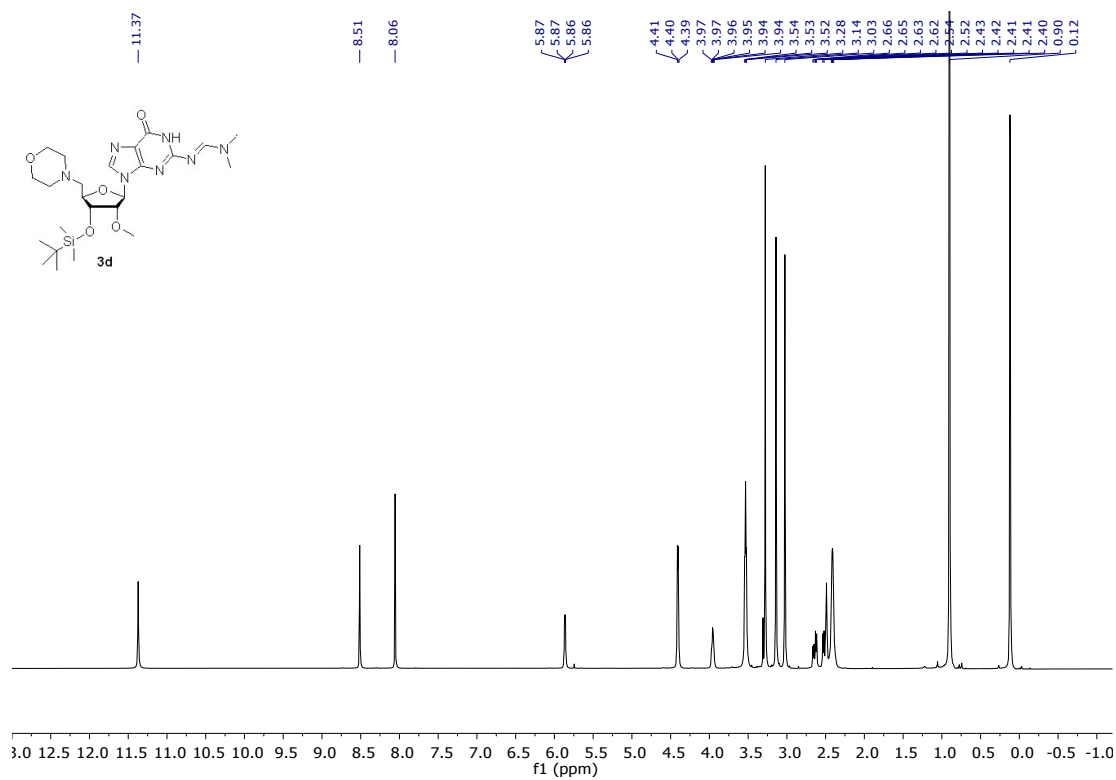


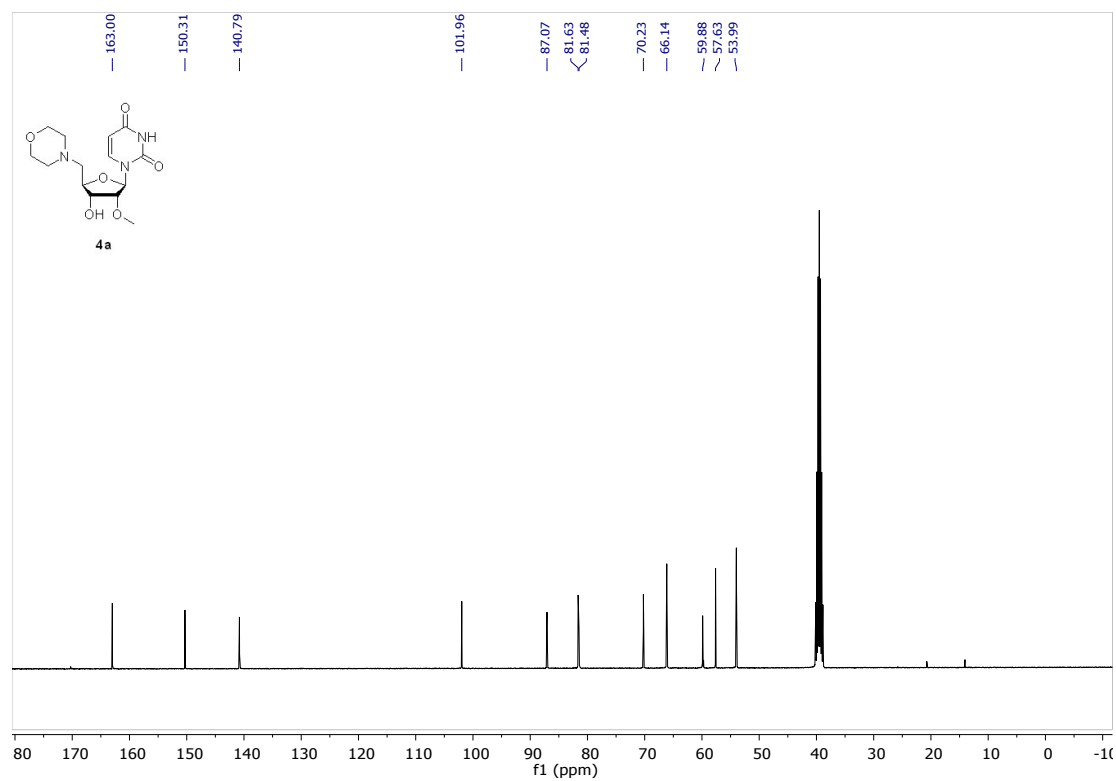
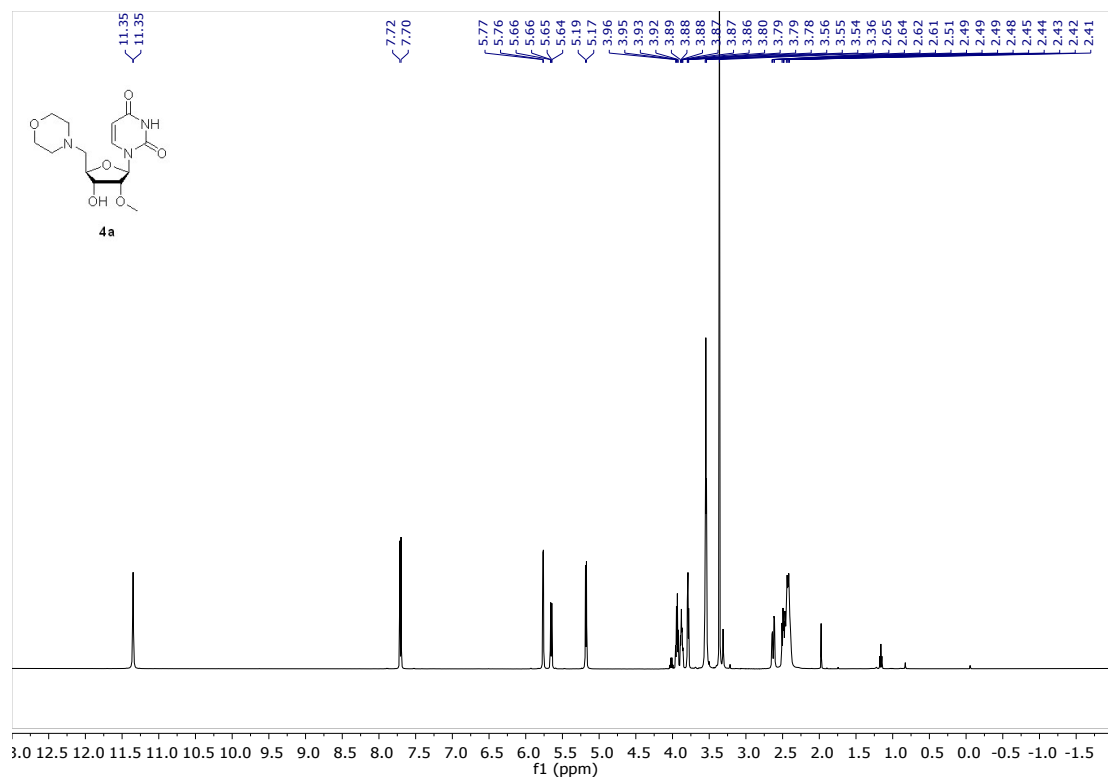


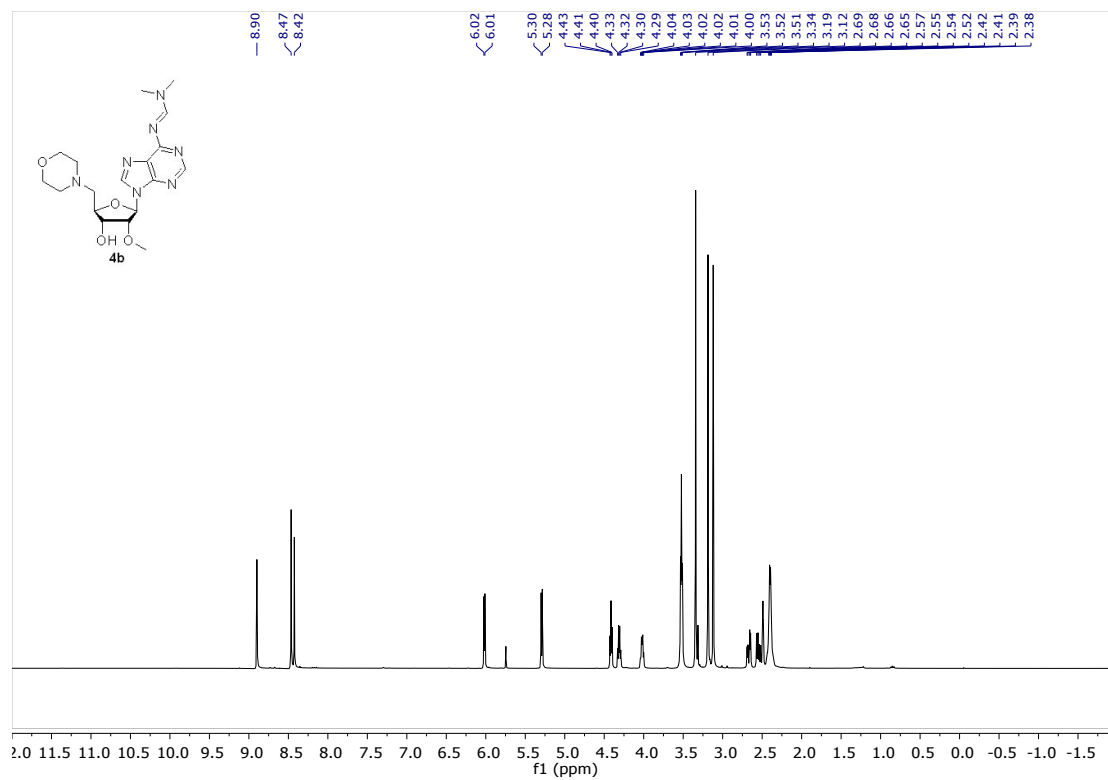


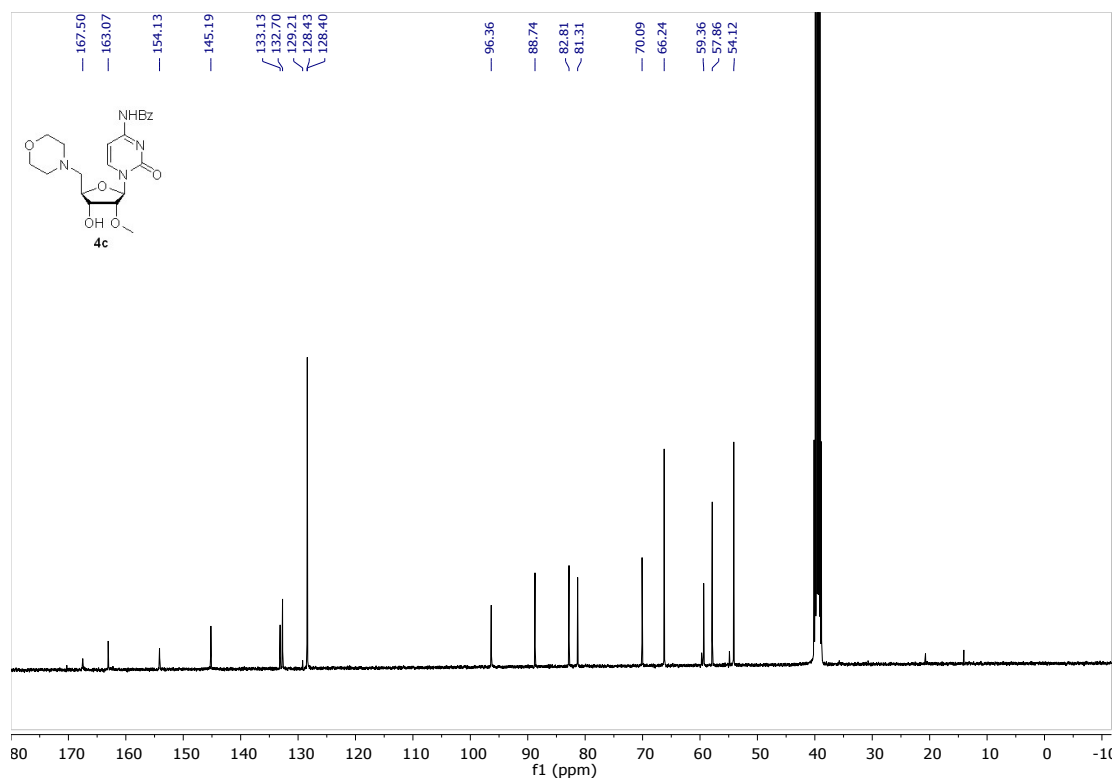
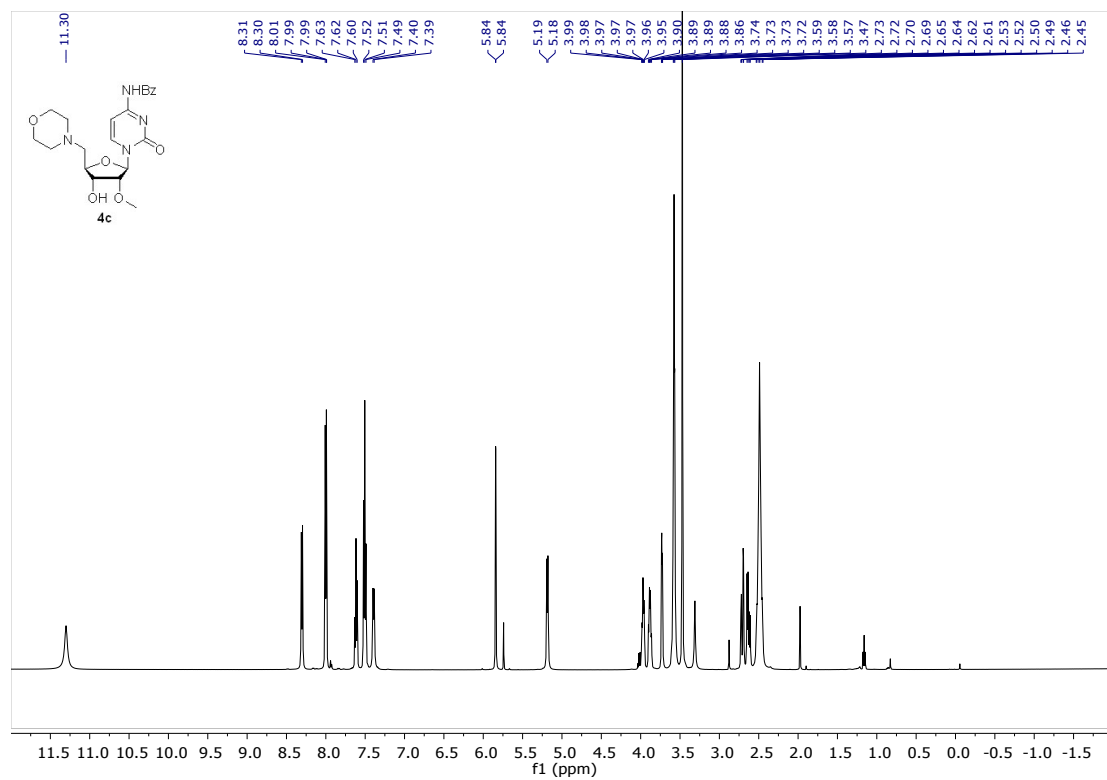


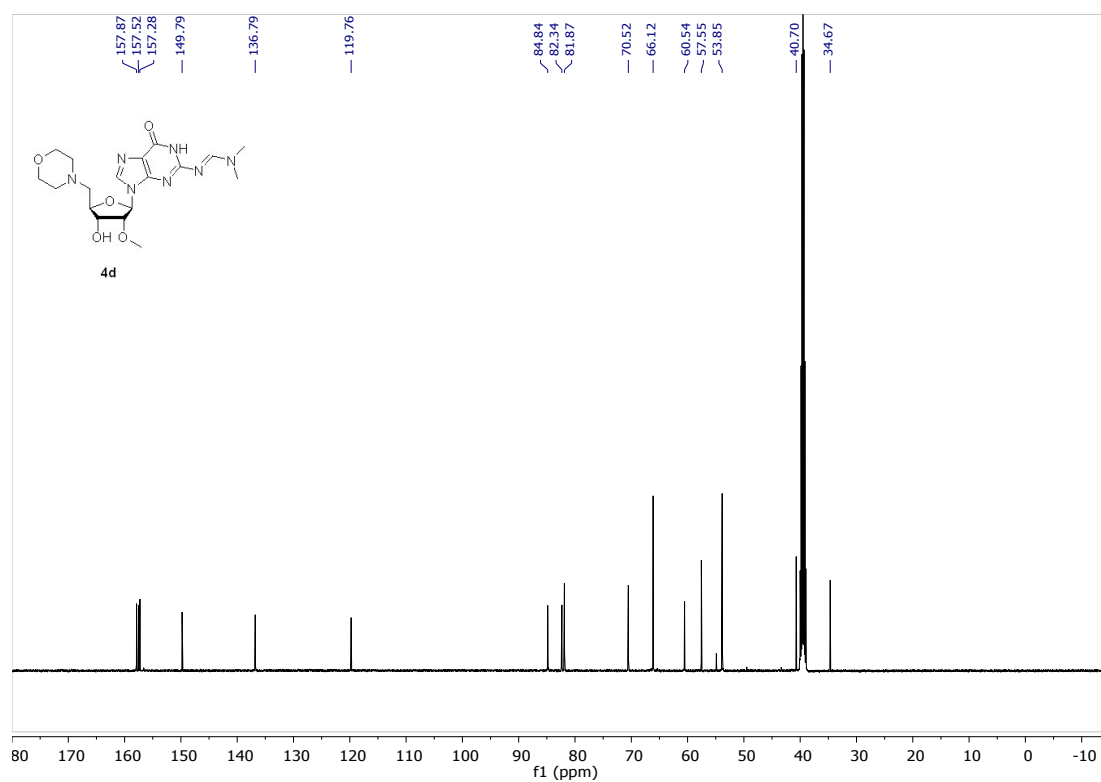
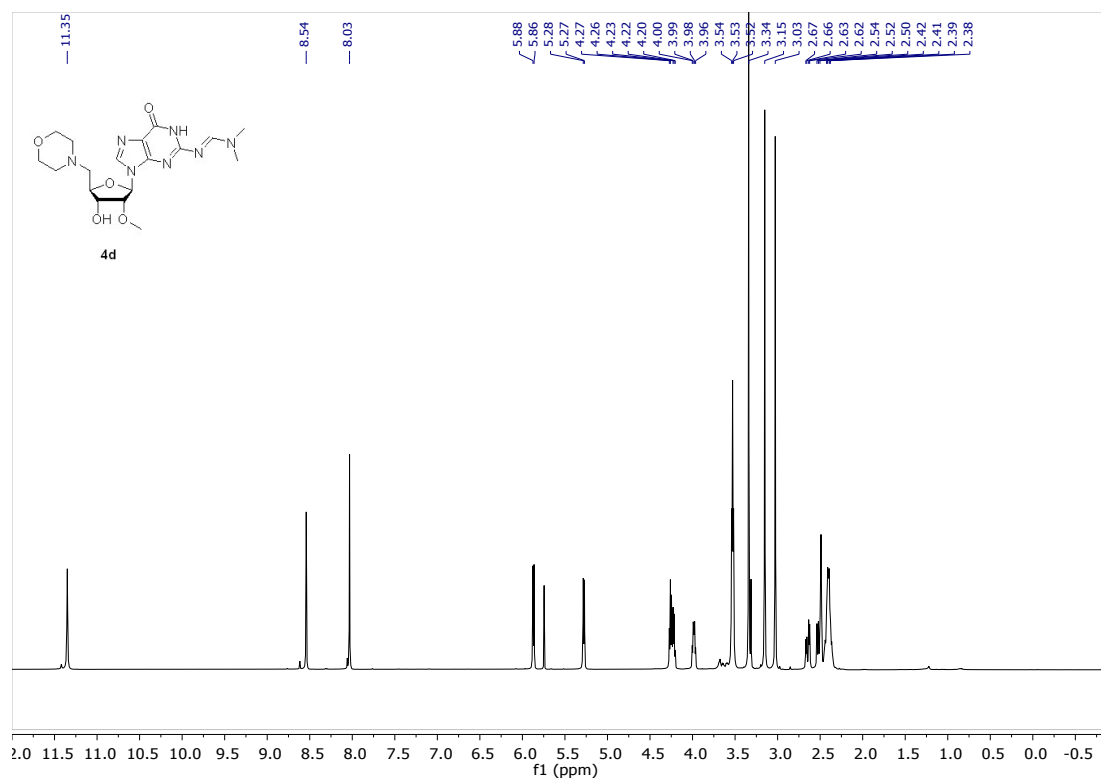


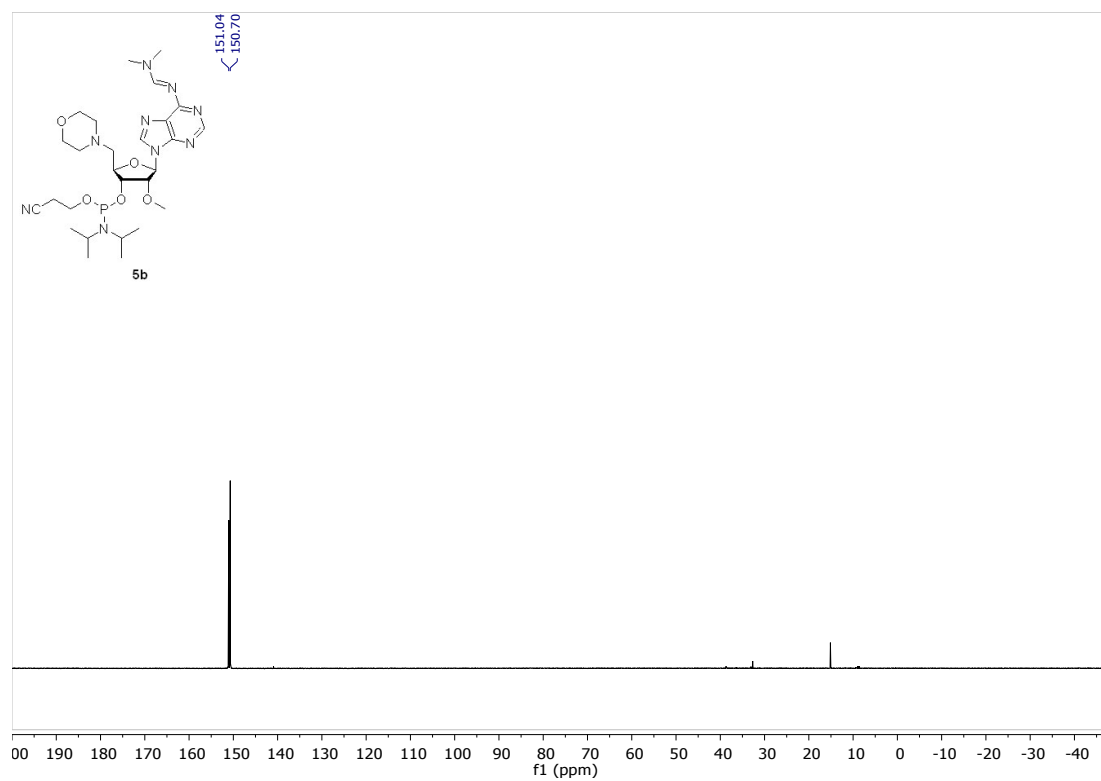
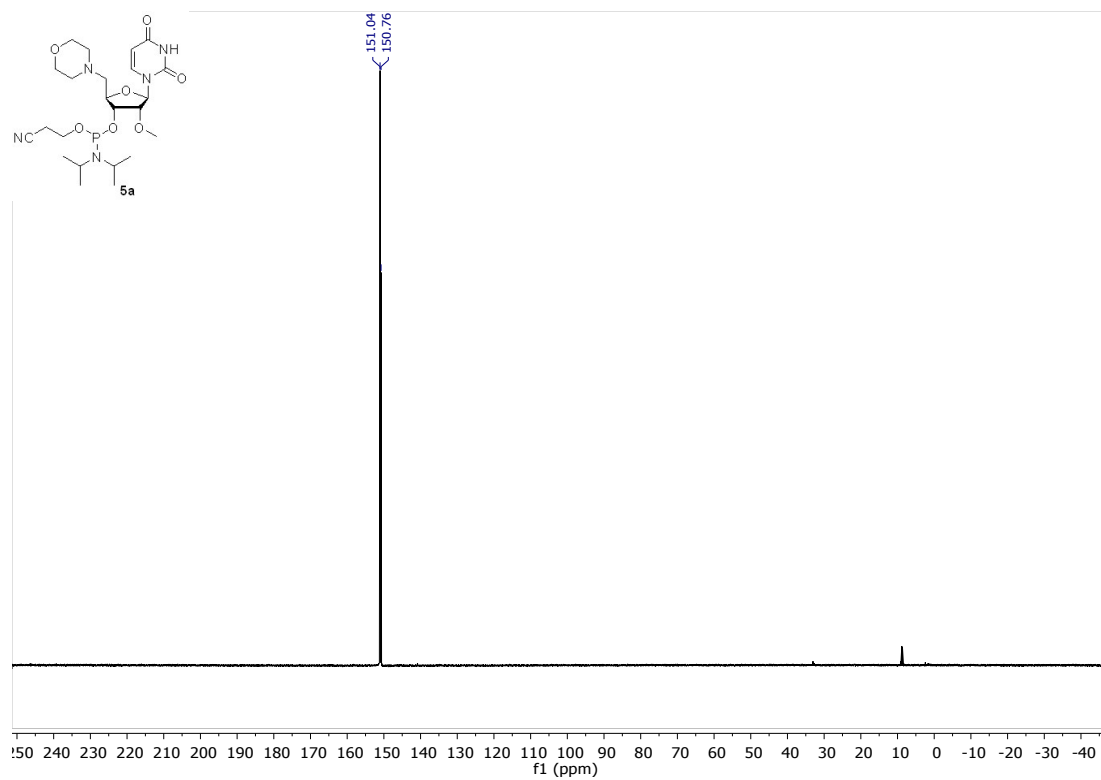


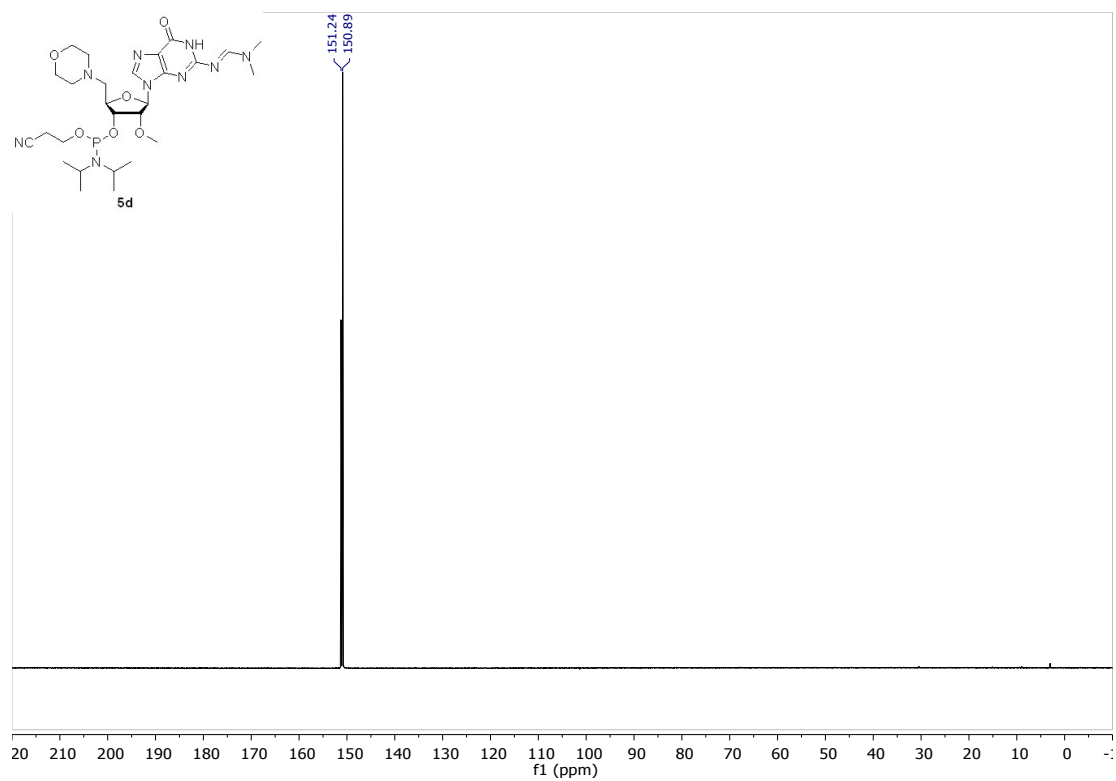
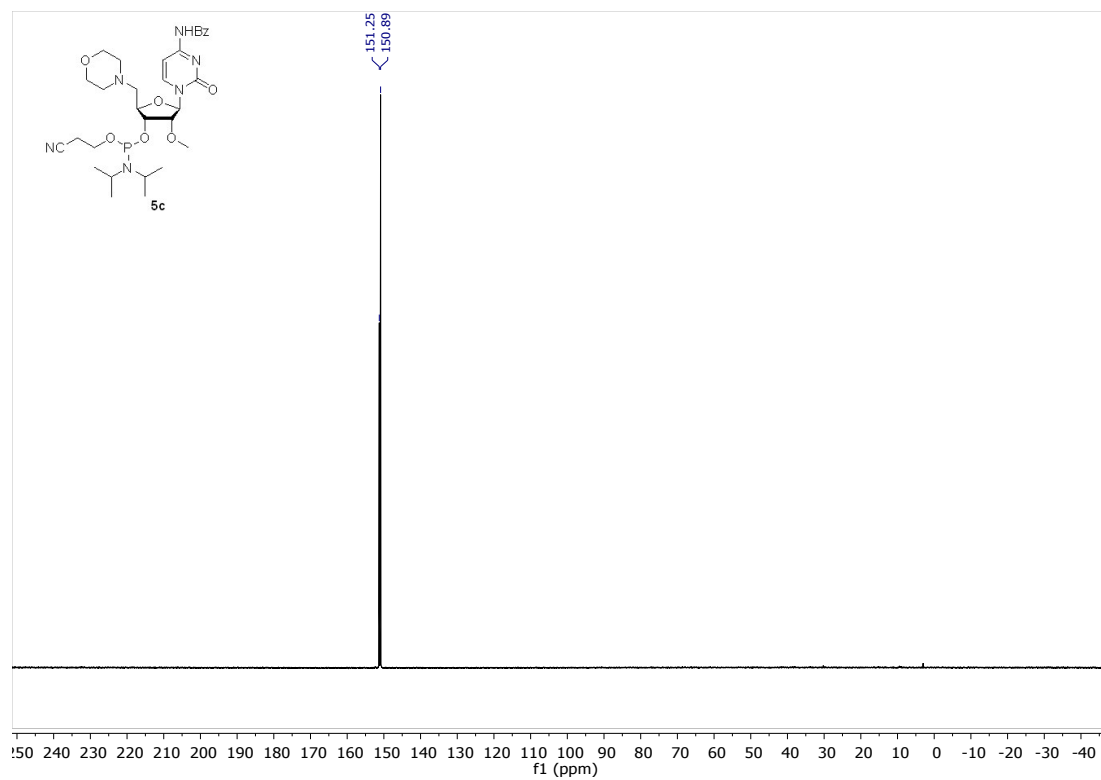


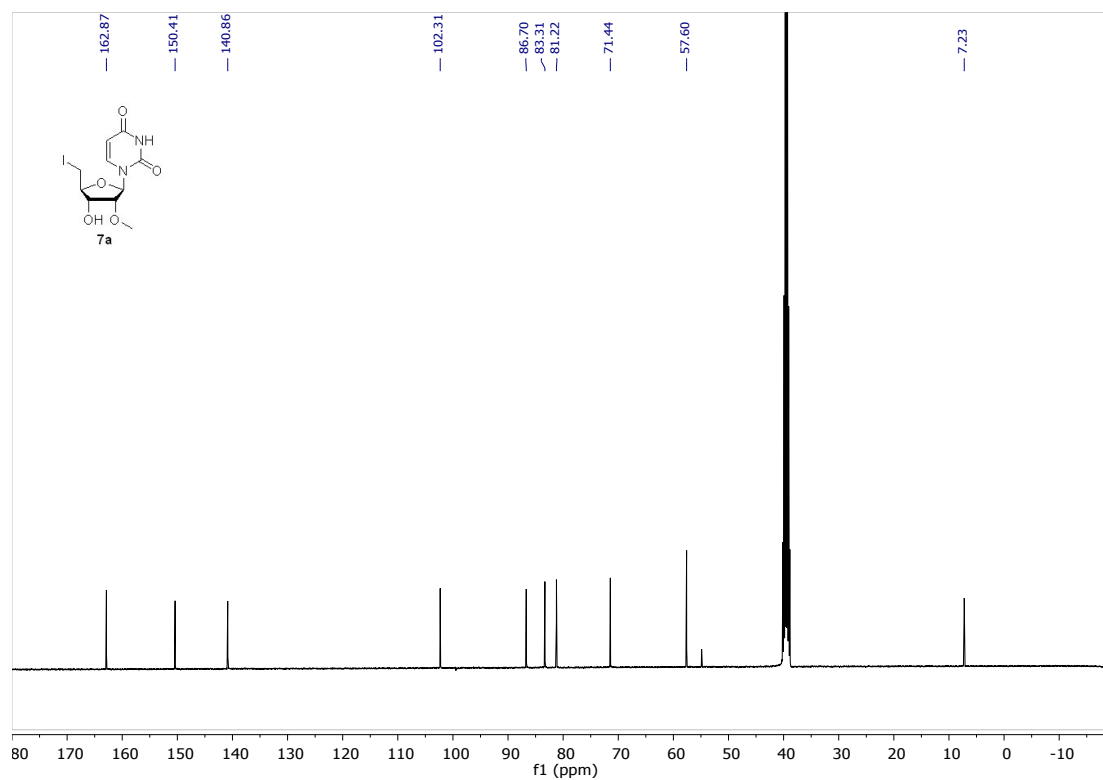
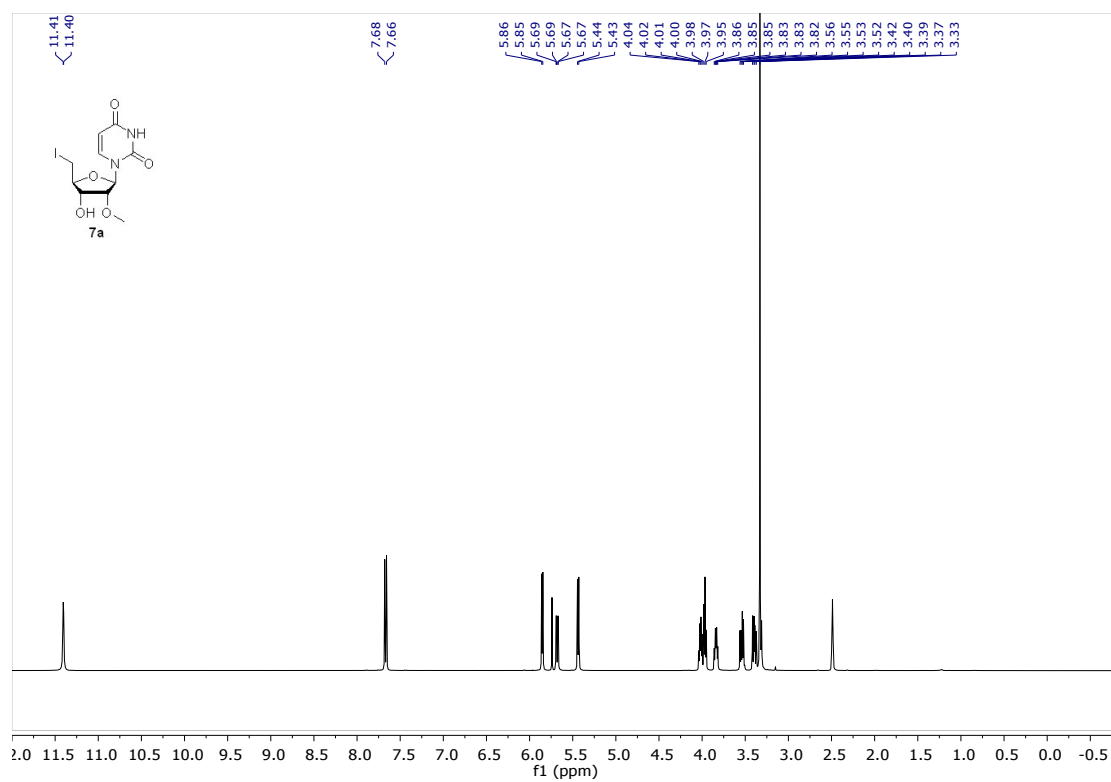


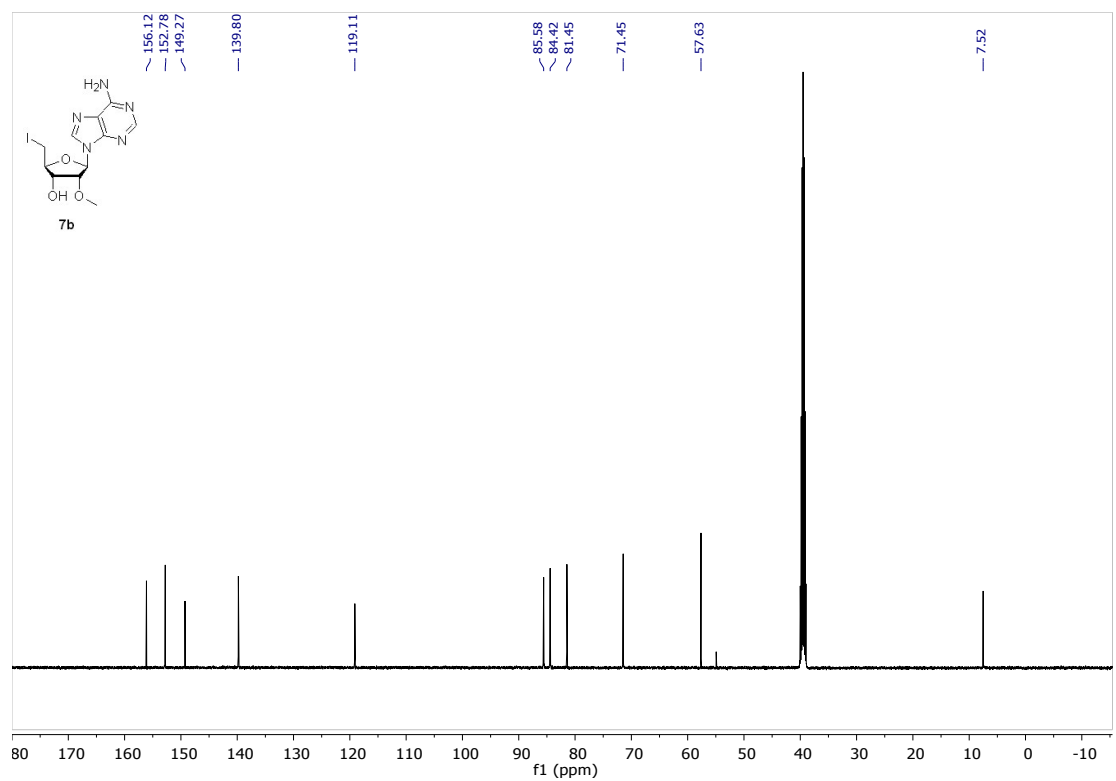
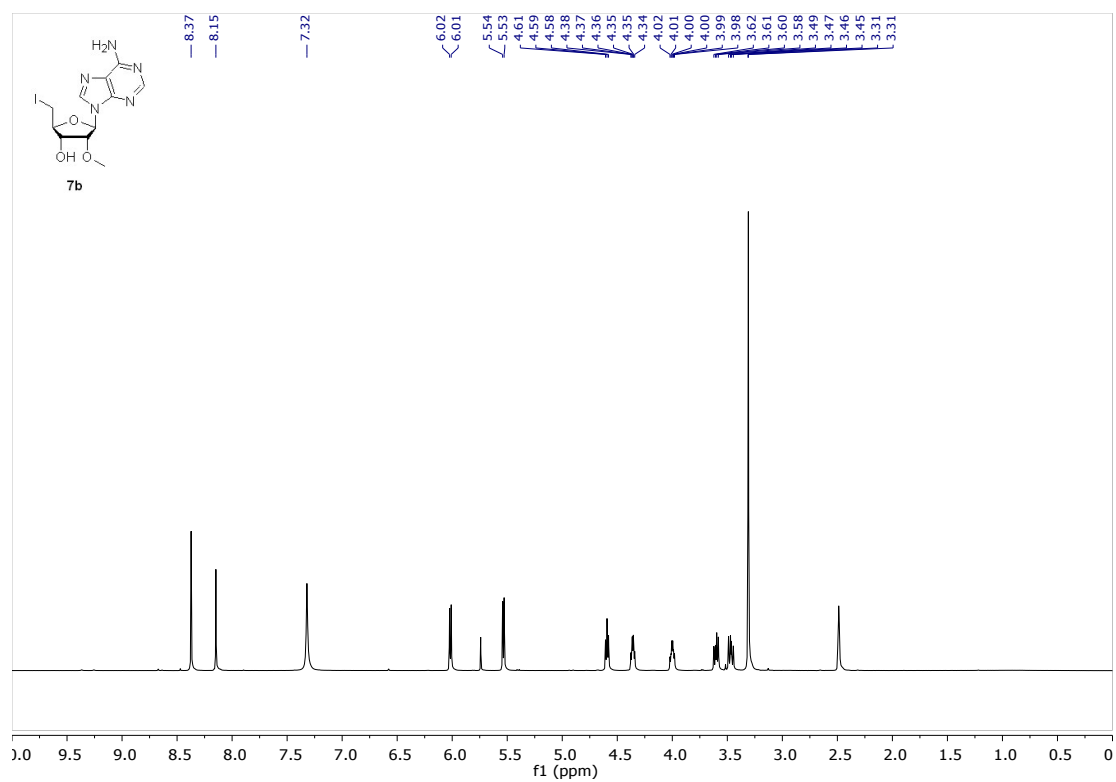




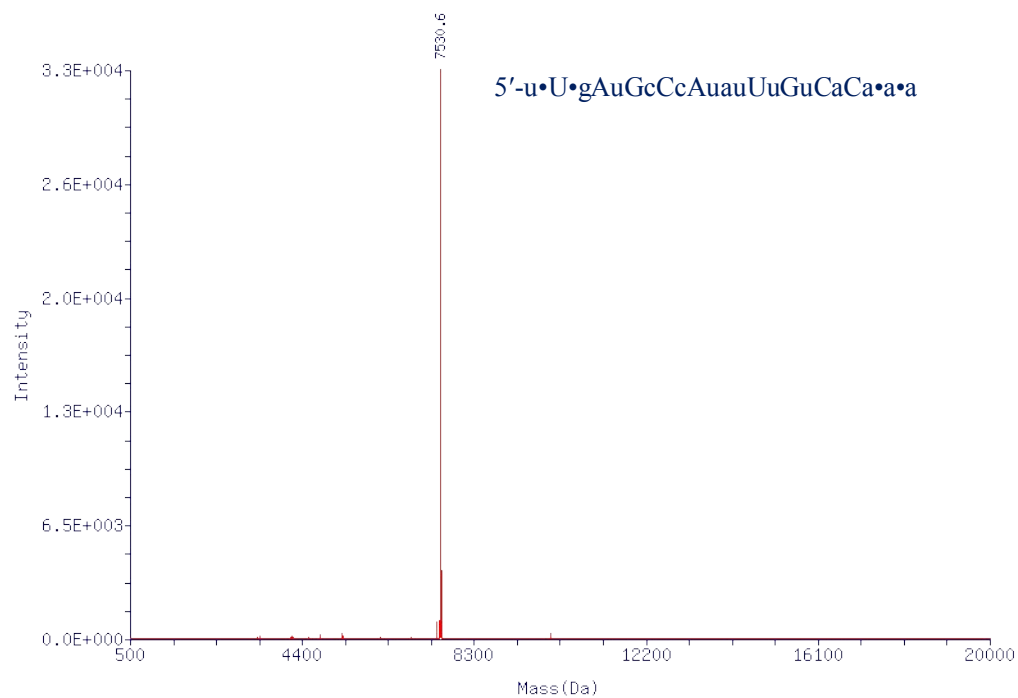
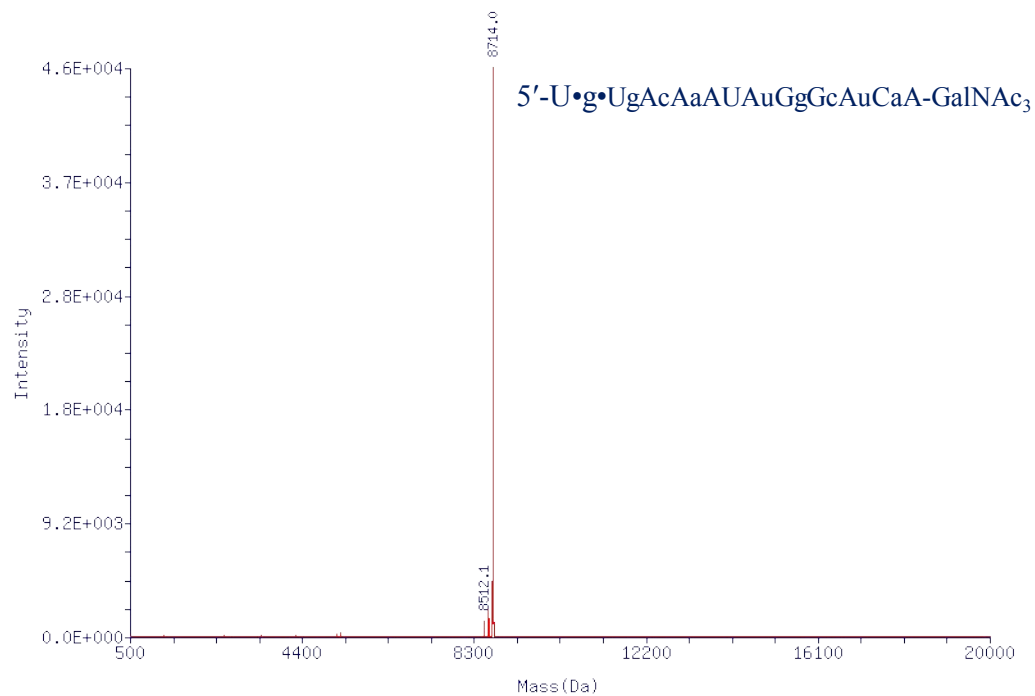


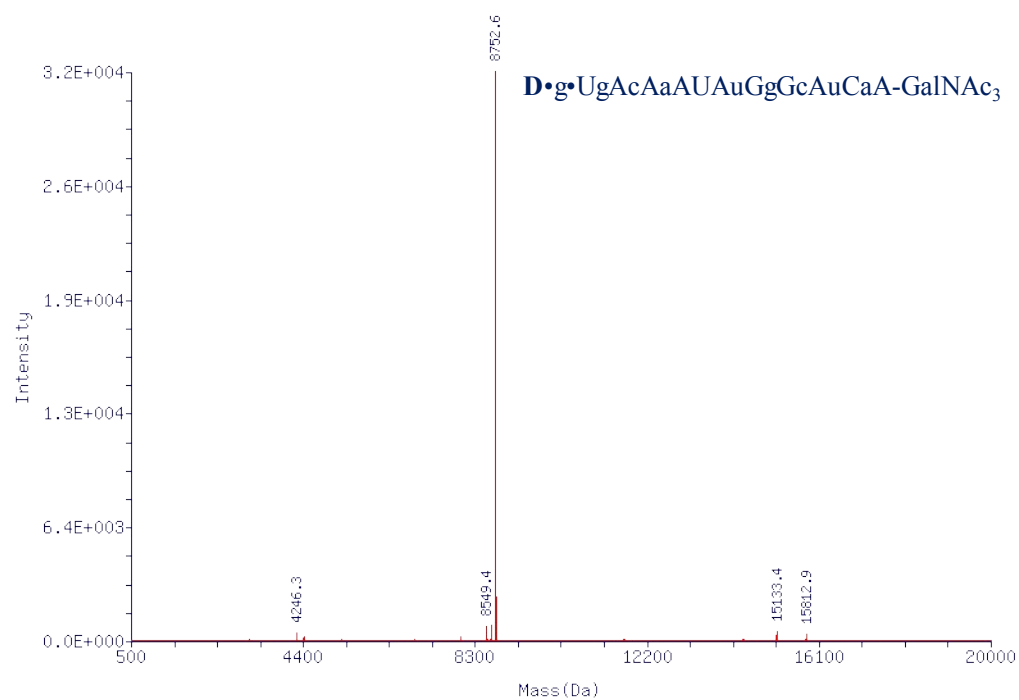
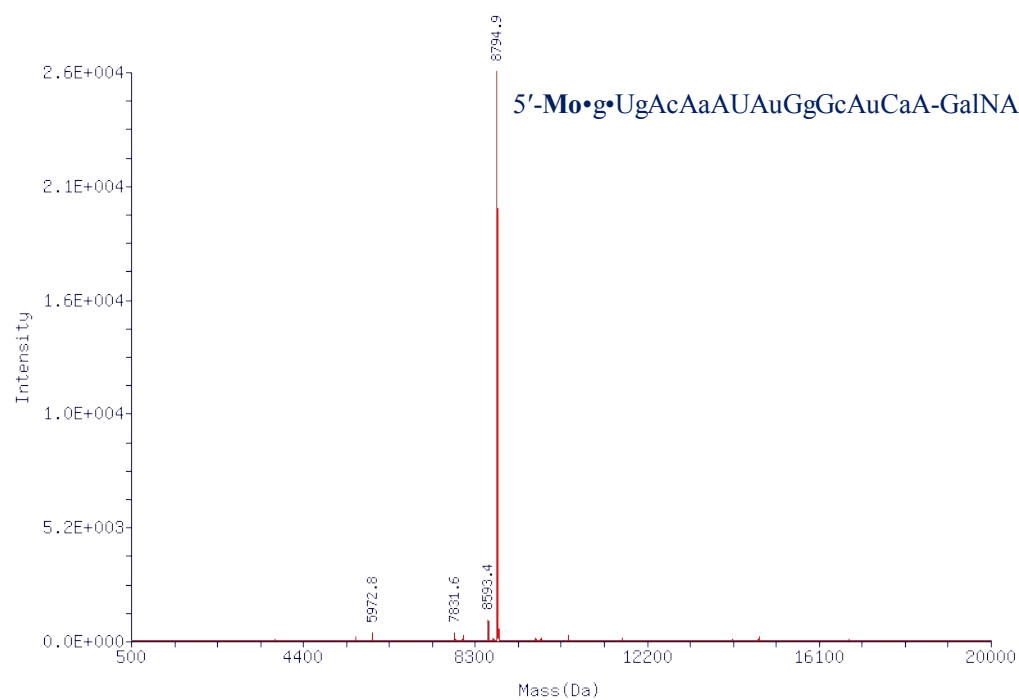


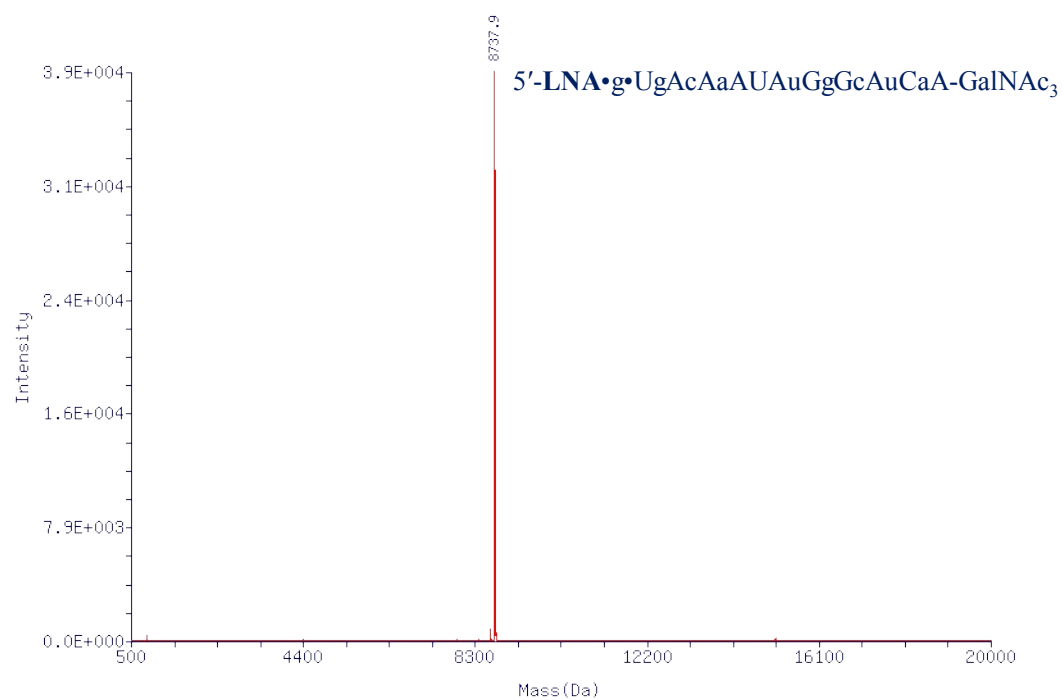
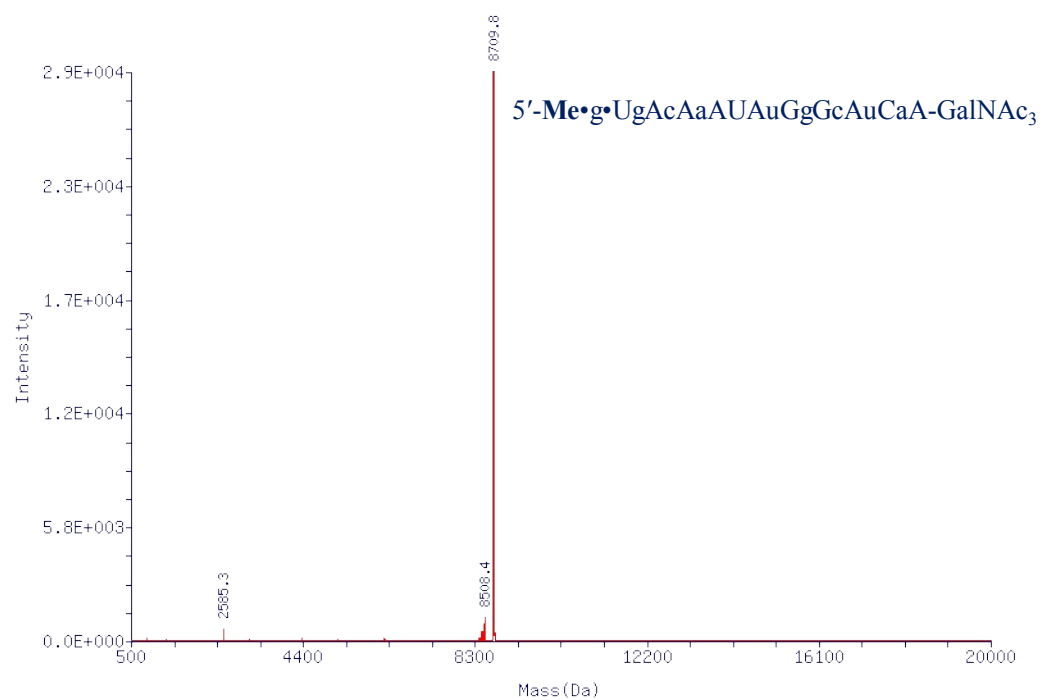


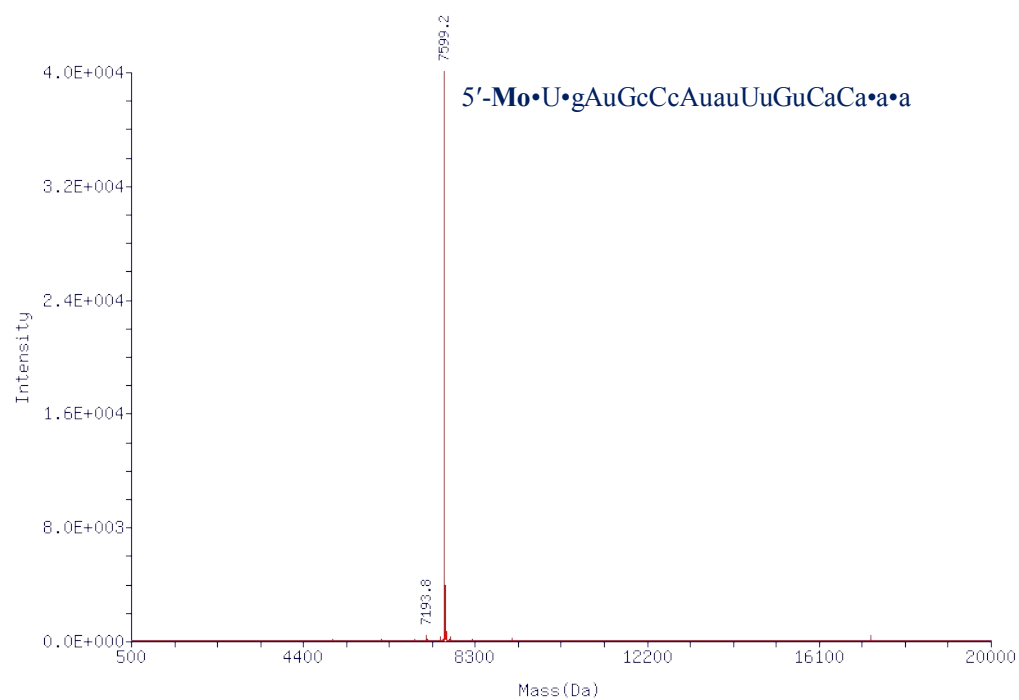
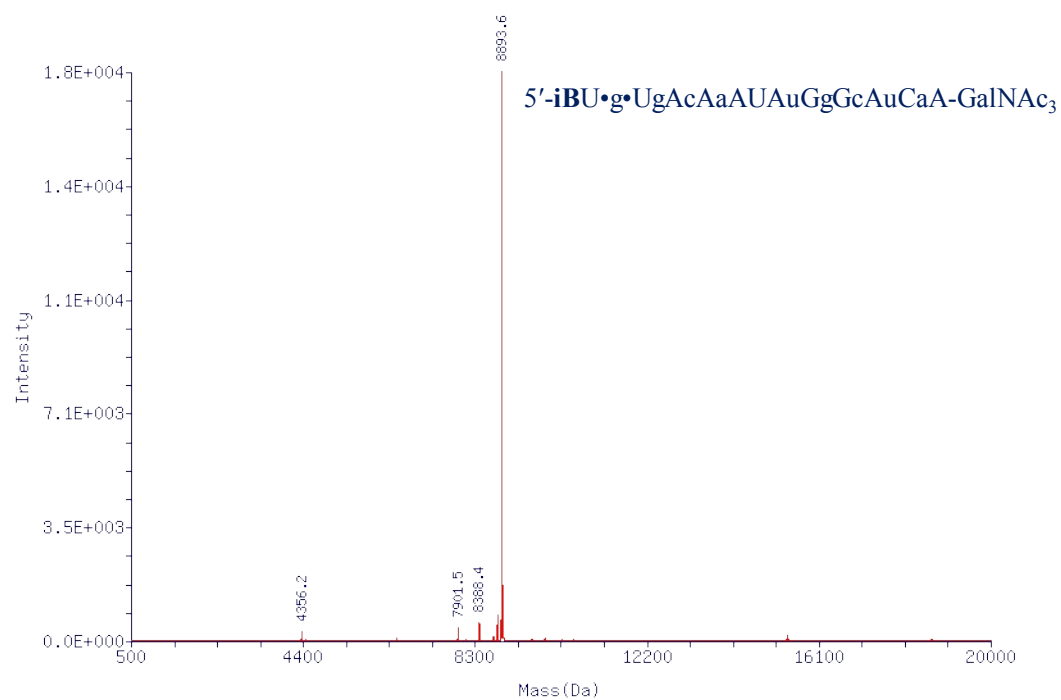


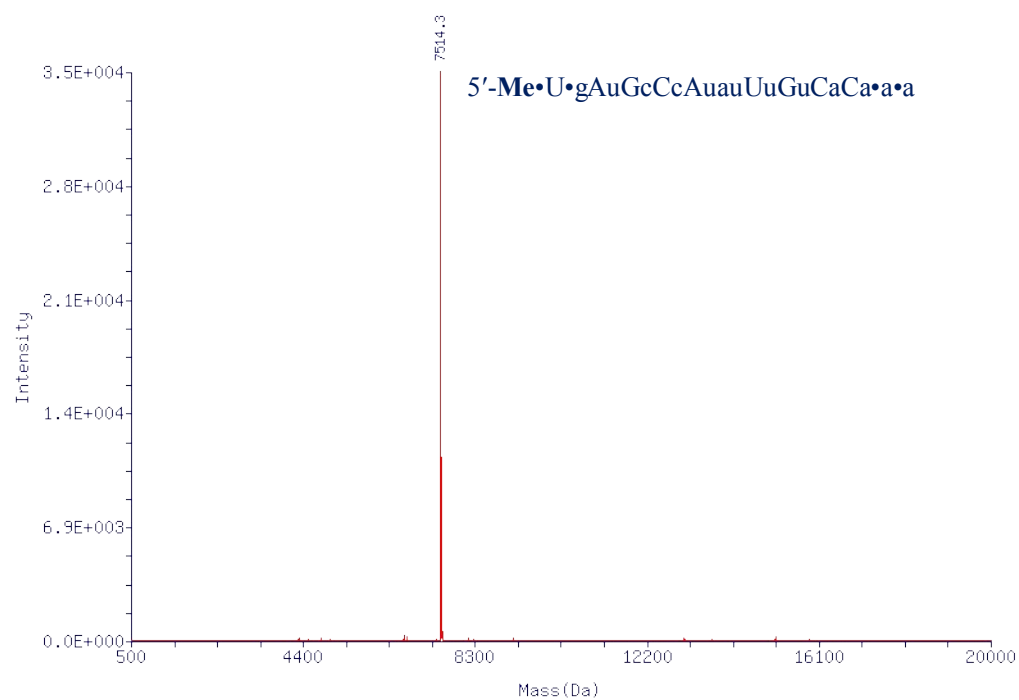
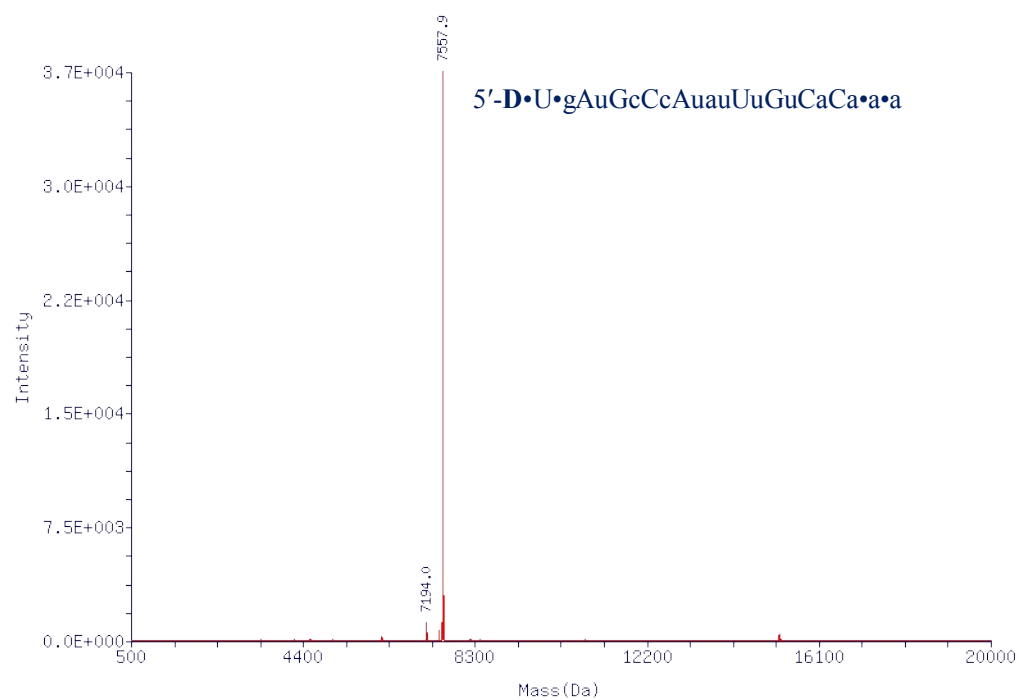
1.8 Representative MS spec of Oligonucleotides

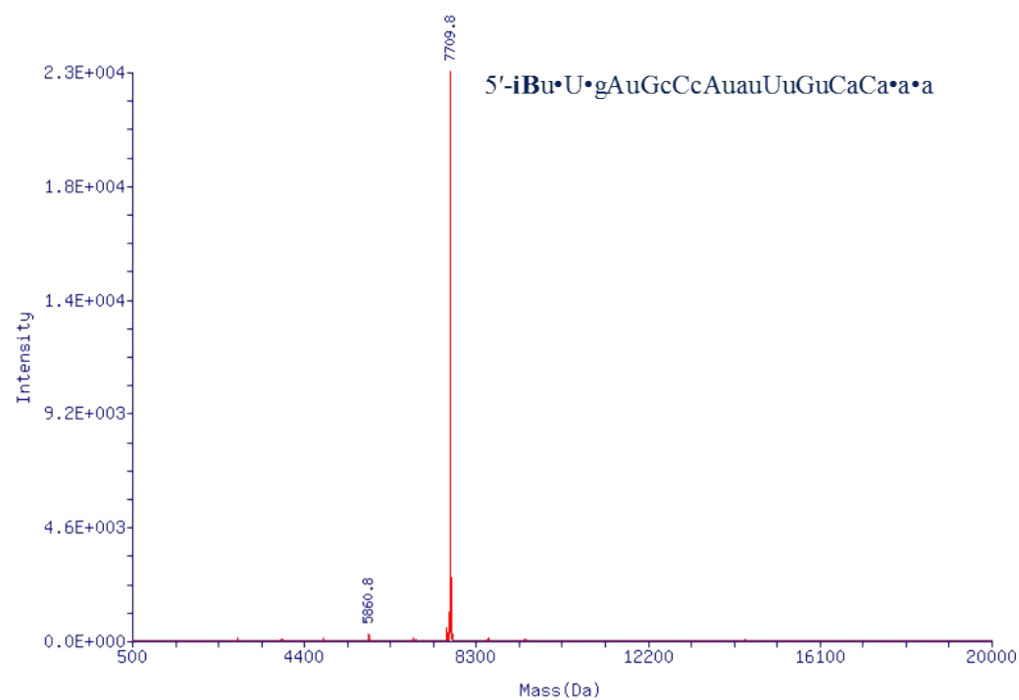
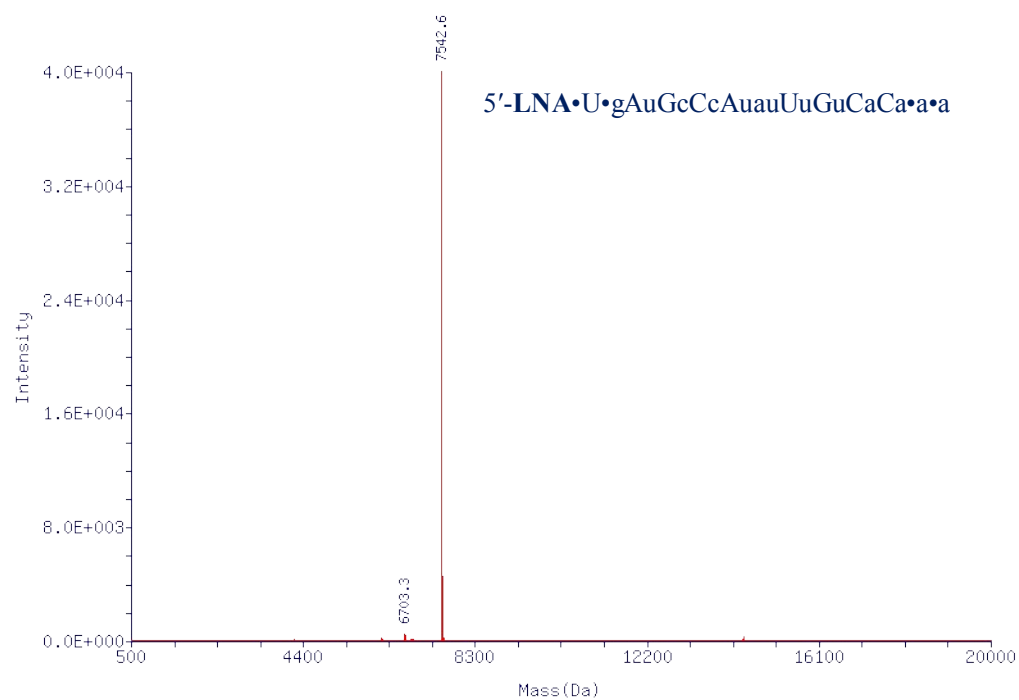


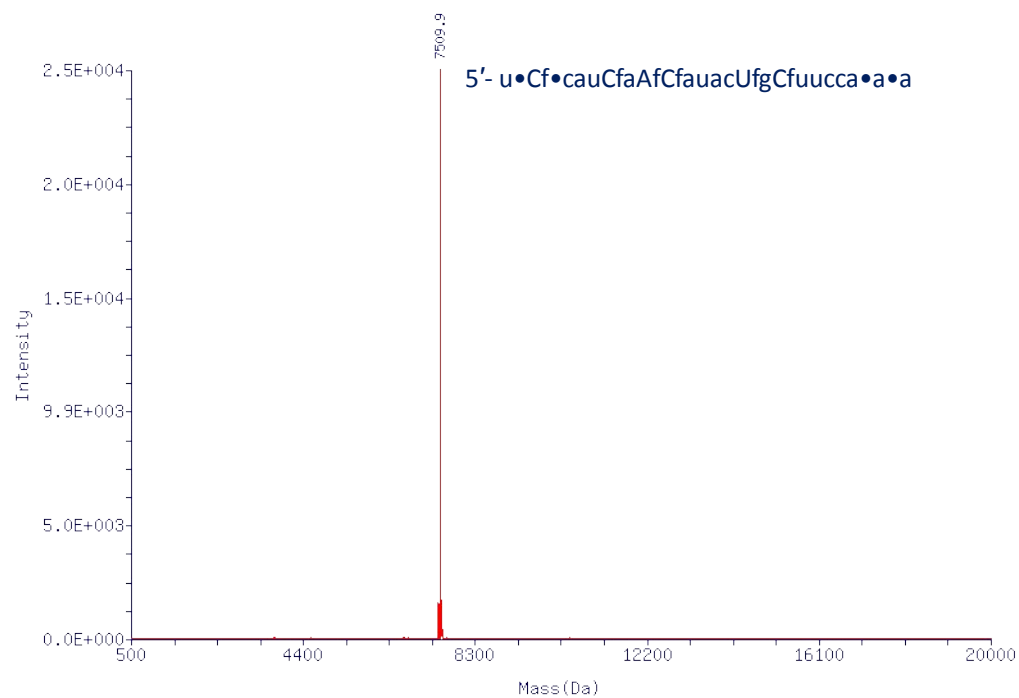
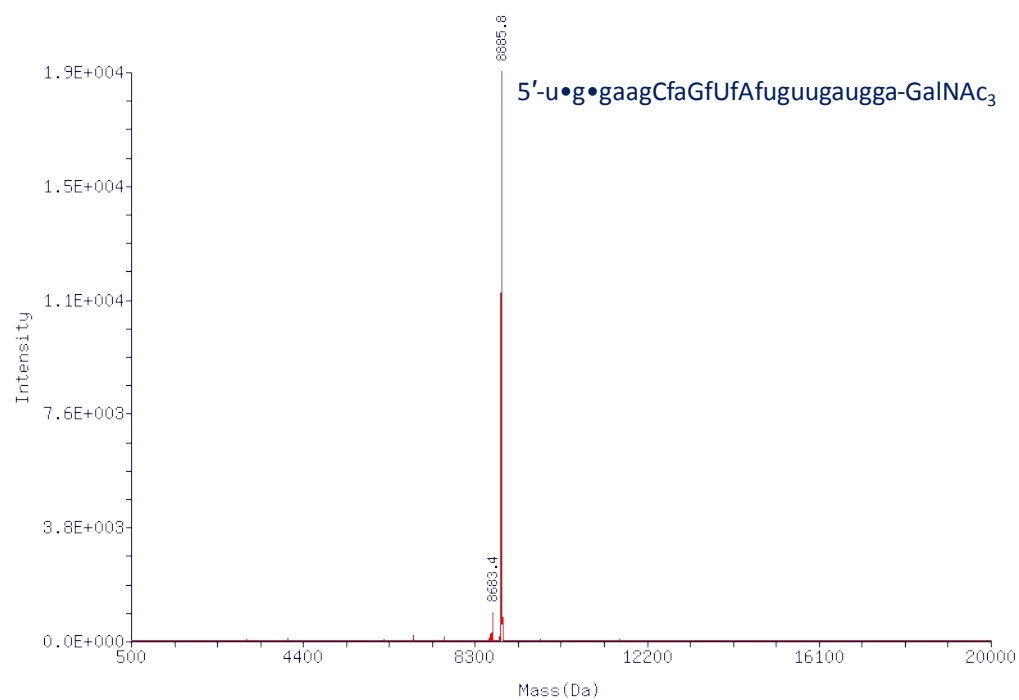


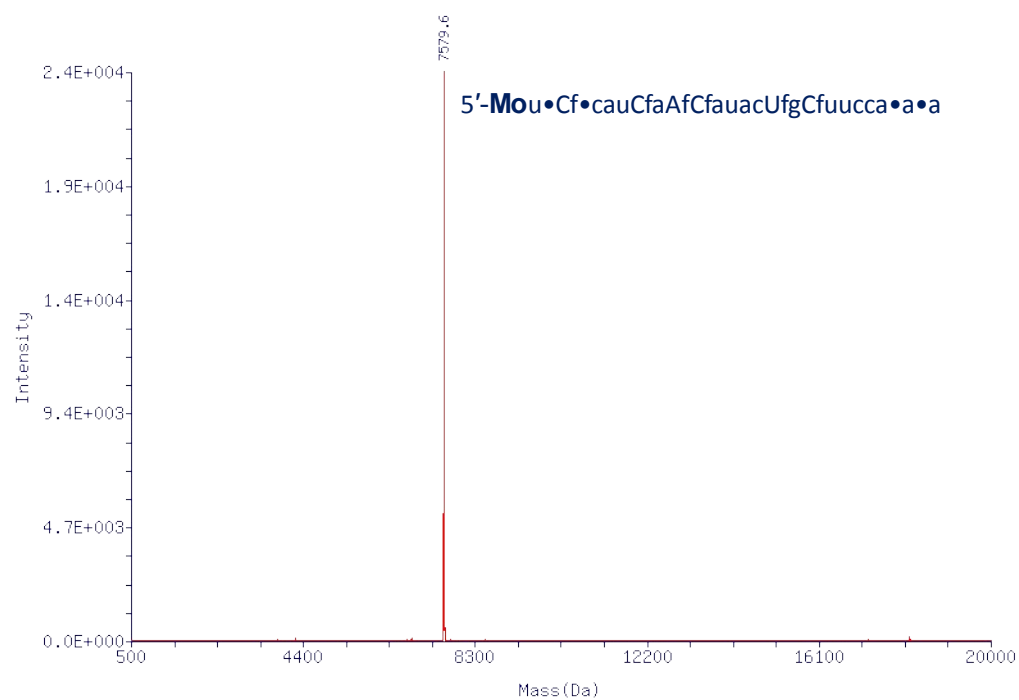
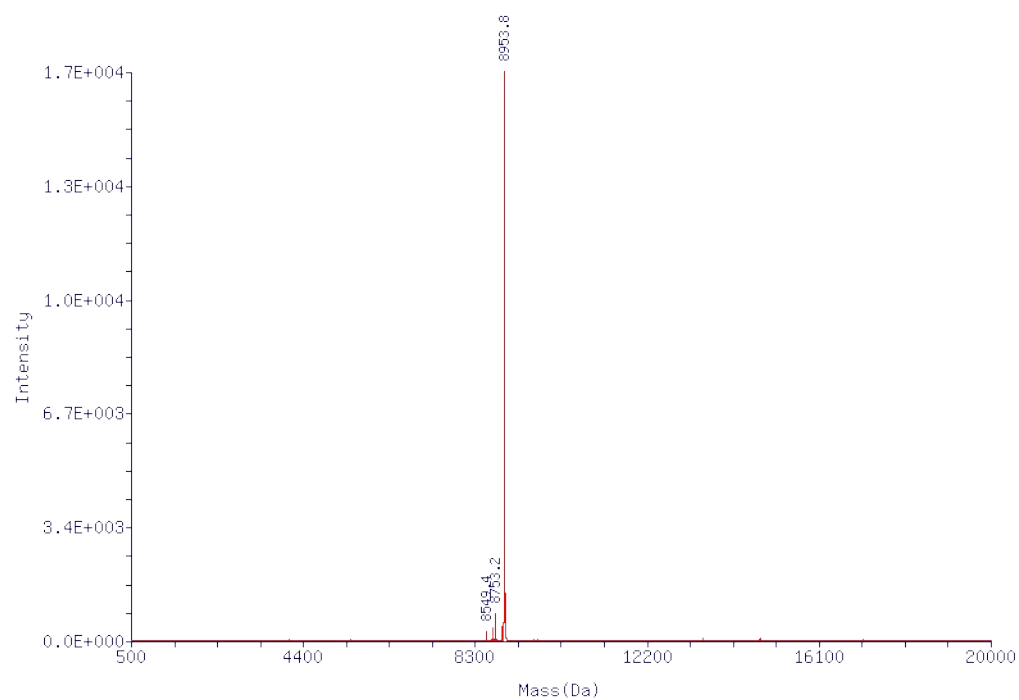












1. R. G. Parmar, C. R. Brown, S. Matsuda, J. L. S. Willoughby, C. S. Theile, K. Charisse, D. J. Foster, I. Zlatev, V. Jadhav, M. A. Maier, M. Egli, M. Manoharan and K. G. Rajeev, *J Med Chem*, 2018, **61**, 734-744.
2. M. K. Schlegel, D. J. Foster, A. V. Kel'in, I. Zlatev, A. Bisbe, M. Jayaraman, J. G. Lackey, K. G. Rajeev, K. Charissé, J. Harp, P. S. Pallan, M. A. Maier, M. Egli and M. Manoharan, *Journal of the American Chemical Society*, 2017, **139**, 8537-8546.
3. R. Parmar, J. L. S. Willoughby, J. Liu, D. J. Foster, B. Brigham, C. S. Theile, K. Charisse, A. Akinc, E. Guidry, Y. Pei, W. Strapps, M. Cancilla, M. G. Stanton, K. G. Rajeev, L. Sepp-Lorenzino, M. Manoharan, R. Meyers, M. A. Maier and V. Jadhav, *ChemBioChem*, 2016, **17**, 985-989.